

國立臺灣大學生物資源暨農學院動物科學技術學系



碩士論文

Department of Animal Science and Technology

College of Bioresources and Agriculture

National Taiwan University

Master Thesis

臺灣水牛族群遺傳結構與毛色基因之研析

Analysis of population genetic structure and coat color gene of
Taiwan swamp buffalo

辛佩蓉

Pei-Jung Hsin

指導教授：王佩華 博士

Advisor: Pei-Hwa Wang, Ph.D.

共同指導教授：張啟聖 博士

Co-Advisor: Chi-Sheng Chang, Ph.D.

中華民國 112 年 7 月

July, 2023

國立臺灣大學碩士學位論文
口試委員會審定書
MASTER'S THESIS ACCEPTANCE CERTIFICATE
NATIONAL TAIWAN UNIVERSITY



臺灣水牛族群遺傳結構與毛色基因之研析

Analysis of population genetic structure and coat color gene of
Taiwan swamp buffalo

本論文係辛佩蓉 (R10626006) 在國立臺灣大學動物科學技術學系完成之碩士學位論文，於民國 112 年 7 月 21 日承下列考試委員審查通過及口試及格，特此證明。

The undersigned, appointed by the Department of Animal Science and Technology, National Taiwan University on July 21, 2023 have examined a Master's thesis entitled above presented by Pei-Jung Hsin (R10626006) candidate and hereby certify that it is worthy of acceptance.

口試委員 Oral examination committee:

王佩華

張白聖

(指導教授 Advisor) (共同指導教授 Co-Advisor)

梁永義

葉振文

林德奇

系主任/所長 Director:

陳逸飛

誌謝



誠摯感謝指導教授 王佩華博士與共同指導教授 張啟聖博士從我大二上加入實驗室以來的悉心教導，謝謝老師們給予我參與本實驗以及各個研討會的寶貴機會，並在過程中予我許多指點，讓我累積了珍貴的學術經驗，也謝謝老師們費心為我撰寫推薦信，讓我有幸能夠到美國修讀博士班。本論文亦承蒙口試委員 宋永義博士、 蕭振文博士與 林德育博士的悉心審閱，使內容更加完備。

我也要特別感謝同實驗室的 林思仲教授，幫助我建立良好的統計觀念，也為我撰寫推薦信並提供我許多出國留學的建議。也要感謝動科系上所有老師在我大學與碩士班期間的教導，使我有成長並獲益良多。同時也感謝系辦的 廖奕雯學姊與 游位育學長在行政生活上的協助與支持。

在動物採樣方面，我要感謝行政院農委會畜產試驗所花蓮種畜繁殖場的 莊璧華主任的協助，以及花蓮場同仁 陳沛君助研、 劉東原先生、 楊發光先生、 賴瑞龍先生與 賀志偉先生的幫忙，才使得試驗得以順利進行。另外，也感謝臺大醫院皮膚科的 朱家瑜醫師，在皮膚組織切片的試驗上提供我寶貴的意見。

謝謝實驗室的每一位成員伴我在這一路上一同成長、同甘共苦，感謝 賴芳裕博士在我剛加入時一步步教導我實驗的基本操作和微衛星標識的相關技術，以及平日的照顧和研究上不吝給予我建言，謝謝智郁學長、恩庭、雅艾和曉磊在實驗室給予我的協助與生活上的陪伴。也要感謝動科系的其他學長姐與同學們，謝謝楷翔學長、絮如和筱茵在我的研究上提供幫助，謝謝筱涵、舒涵與育祥時常邀請我參與實驗室聚會，帶給我許多歡樂的回憶。

最後要感謝我的家人、朋友與男友對我的支持與鼓勵，謝謝大家。


中文摘要



自臺灣農業機械化以來，臺灣水牛的數量急劇下降，目前只剩下約 2,002 頭。行政院農業委員會畜產試驗所花蓮種畜繁殖場（後簡稱花蓮場）是臺灣水牛的保種基地，飼養著一群灰水牛和白水牛。為了保持臺灣水牛的遺傳多樣性，了解其族群遺傳結構是十分重要的課題。另一方面，臺灣水牛屬於沼澤型水牛，而沼澤型水牛的毛色以灰色為主，偶爾出現全白色毛色個體。先前的一項研究表明，白色沼澤型水牛的 *ASIP* 基因中的一段 *LINE-1* 插入序列可能導致白色毛色；然而，臺灣水牛的白色毛色之確切形成原因尚不清楚。

在本研究中，採集了花蓮場的 78 頭灰色臺灣水牛和 16 頭白色臺灣水牛的血樣本，並利用 15 組微衛星標識和水牛高密度 SNP 位點基因晶片（90K Axiom® Buffalo Genotyping Array）進行族群遺傳結構分析。結果顯示，剔除不具有多態性和可能具有無效交替基因的微衛星標識後，以其餘 12 組微衛星標識檢測所得之平均交替基因數 (N_a) 為 4.4、有效交替基因數 (N_e) 為 2.678、觀測異質度 (H_o) 為 0.584、期望異質度 (H_e) 為 0.581、多態性訊息含量 (PIC) 為 0.521 及族群近親係數 (F_{IS}) 為 -0.008；利用基因晶片中的 14,456 個 SNPs 所得之所有 N_a 為 2，平均 N_e 為 1.616、 H_o 為 0.372、 H_e 為 0.360、PIC 為 0.282 及 F_{IS} 為 -0.029。以兩種方法繪製所得之類緣關係樹十分相似，但類緣關係樹節點上表示重覆取樣 1,000 次生成的百分比數值是以在 14,456 個 SNPs 所得的結果中明顯較高。以兩種方法所進行的群集分析結果中 ($K=3$)，均將所有的 16 頭白水牛與部分灰水牛分至一個次族群，而其餘的灰水牛還可以再分為兩個次族群。

本試驗針對臺灣水牛的 *ASIP* 基因進行基因分型以檢測 *LINE-1* 插入序列是



否存在，但試驗結果中並未發現此插入序列，應代表臺灣水牛白色毛色之成因與先前的研究不同。本研究亦利用水牛高密度 SNP 位點基因晶片中的 14,456 個 SNPs 針對臺灣水牛的灰色與白色毛色進行全基因組關聯分析 (GWAS)，結果顯示了與白色毛色相關的 17 個最具顯著性的 SNPs 位點 ($P < 1 \times 10^{-11}$)，並找出了 26 個相關的基因。此外，前兩個最具顯著性的 SNPs 位點 ($P < 1 \times 10^{-17}$) 位在 18 號染色體上，且其位置十分接近 *MC1R* 基因，而 *MC1R* 基因是已知的重要的色素調控基因。因此，本試驗針對臺灣水牛的 *MC1R* 基因之 exon 1 進行了定序，檢測到一個臺灣水牛獨有的錯義突變位點 (*MC1R* c.901C>T) 並導致氨基酸置換 (p.R301C)。接著針對 115 頭灰色和 18 頭白色臺灣水牛進一步進行 *MC1R* c.901C>T 基因分型。結果顯示，17 頭白水牛為突變型純合子，1 頭白水牛和 37 頭灰水牛為雜合子，78 頭灰水牛為野生型純合子 ($P < 1 \times 10^{-21}$)。用於預測 p.R301C 對 *MC1R* 結構或功能的潛在影響的所有八種工具均表明此變異是有害的。以 qPCR 進行的基因表達分析結果顯示，*MC1R*、*ASIP*、*MITF*、*TYR*、*TYRP1* 和 *DCT* 的基因表達在 1 頭白水牛幼年和 2 頭灰水牛幼年耳朵皮膚組織之間無顯著差異。本試驗亦利用組織化學染色 (Fontana-Masson) 觀察水牛皮膚組織中的黑色素沉積。結果顯示白水牛皮膚組織的黑色素沉積較少，但仍能產生黑色素。

綜上所述，本研究可以為臺灣水牛保種族群的保育及毛色性狀的選育提供參考資訊。本試驗所發現的 *MC1R* c.901C>T 是一個極有可能的候選變異基因，會損害 *MC1R* 蛋白質的功能並導致臺灣水牛的白色毛色形成。

關鍵詞：臺灣水牛、族群遺傳結構、毛色基因、微衛星標識、基因晶片、全基因組關聯分析。

ABSTRACT



The number of Taiwan swamp buffaloes has dropped sharply since the mechanization of agriculture. There were only 2,002 head left. Hualien Animal Propagation Station (HAPS) is the conservation field of the Taiwan swamp buffalo, raising both gray and white buffaloes. In order to maintain the genetic diversity of the Taiwan swamp buffalo, estimating their population genetic structure is important. On the other hand, the coat color of the swamp buffalo is mainly gray, but white individuals appear occasionally. A previous study indicated that the *LINE-1* insertion in the *ASIP* gene of the white swamp buffalo might cause the white coat color. However, the exact mechanism for the white coat color of the Taiwan swamp buffalo still remained unclear.

In this study, blood samples were collected from 78 gray and 16 white Taiwan swamp buffaloes in HAPS. Fifteen microsatellite markers and 90K Axiom® Buffalo Genotyping Array were used for population genetic structure analysis. The results showed that excluding the nonpolymorphic marker and the markers with high null allele frequency, the average number of observed alleles per locus (N_a) was 4.4, effective alleles per locus (N_e) was 2.678, observed heterozygosity (H_o) was 0.584, expected heterozygosity (H_e) was 0.581, polymorphic information content (PIC) was 0.521, and Wright's F-statistics (F_{IS}) was -0.008 among the 12 microsatellite markers. The results based on the 14,456 SNPs from the genotyping array showed that all SNPs had two observed alleles, and the average N_e was 1.616, H_o was 0.372, H_e was 0.360, PIC was 0.282, and F_{IS} was -0.029. The phylogenetic trees drawn by the two methods were similar, but the numbers on the nodes of the phylogenetic tree indicating the percentage bootstrap values generated from 1,000 resamplings were much higher in the results of the 14,456 SNPs. The genetic structure clustering results ($K = 3$) of the two methods

both clustered all of the 16 white buffaloes into one subpopulation with some gray buffaloes, and the other gray buffaloes could be divided into two subpopulations.

The *ASIP* gene of the Taiwan swamp buffalo was genotyped to detect the *LINE-1* insertion, but no such insertion was found. The cause for the white coat color of the Taiwan swamp buffalo should be different from the previous study. The 14,456 SNPs from the genotyping array were also used to conduct a genome-wide association study (GWAS) on the gray and white coat color of the Taiwan swamp buffalo. The results showed 17 most significant SNPs ($P < 1 \times 10^{-11}$) associated with the white coat color, and 26 related genes were identified. In addition, the two most significant SNPs ($P < 1 \times 10^{-17}$) were on the chromosome 18 and were found to be close to the *MC1R* gene, which is a well-known pigmentation-related gene. Therefore, the coding region of the *MC1R* gene of the Taiwan swamp buffalo was sequenced. A missense variant (*MC1R* c.901C>T) causing an amino acid substitution (p.R301C) was detected exclusively in the Taiwan swamp buffalo. *MC1R* c.901C>T genotyping was further performed on 115 gray and 18 white Taiwan swamp buffaloes. The results showed that 17 white buffaloes were homozygous for the variant, one white and 37 gray buffaloes were heterozygous, and 78 gray buffaloes were homozygous for the wild-type allele ($P < 1 \times 10^{-21}$). All of the eight tools used to predict potential effect of p.R301C on *MC1R* structure or function indicated the mutation to be deleterious. The gene expression analysis by qPCR showed that *MC1R*, *ASIP*, *MITF*, *TYR*, *TYRP1*, and *DCT* gene expression in the ear skin tissue between one white calf and two gray calves had no significant difference. Histochemical staining (Fontana-Masson) was used to observe deposition of melanin in the skin tissue of the Taiwan swamp buffalo. The results showed that the skin tissue of the white Taiwan swamp buffalo had less melanin deposition, but it could still produce

melanin.

In conclusion, this study provided information for breeding designation and coat color trait selection of the Taiwan swamp buffalo. The *MC1R* c.901C>T is a strong candidate that may damage the MC1R protein function and cause the white coat color of the Taiwan swamp buffalo.

Keywords: Taiwan swamp buffalo, Population genetic structure, Coat color gene, Microsatellite marker, Genotyping array, Genome-wide association study (GWAS)

CONTENTS



口試委員會審定書	i
誌謝	ii
中文摘要	iii
ABSTRACT	v
CONTENTS	viii
LIST OF FIGURES	xi
LIST OF TABLES	xv
Chapter 1 Literature Review	1
1.1 Taiwan swamp buffalo	1
1.2 Population genetic analysis of Taiwan swamp buffalo	8
1.3 Microsatellite markers used in buffalo population genetic analysis	11
1.4 High-density single nucleotide polymorphism genotyping array used in buffalo population genetic analysis and genome-wide association study	13
1.5 Coat color genes of the buffalo	16
1.5.1 The coat color of the buffalo	16
1.5.2 The albinism and the <i>TYR</i> gene of the buffalo	17
1.5.3 An early research of the white swamp buffalo	18
1.5.4 Analysis of the <i>MC1R</i> gene of the buffalo	19
1.5.5 Analysis of the <i>MITF</i> gene of the buffalo	22
1.5.6 Analysis of the <i>ASIP</i> gene of the buffalo	22
1.5.7 Analysis of other coat color genes of the buffalo	25
1.5.8 Coat color gene analysis of the Taiwan swamp buffalo	26

1.6	Histological analysis of the buffalo skin	28
1.7	Aims of this study	30
Chapter 2	Materials and Methods.....	31
2.1	Population genetic structure analysis of Taiwan swamp buffalo.....	31
2.1.1	Blood sample collection	31
2.1.2	Genomic DNA (gDNA) isolation.....	31
2.1.3	Microsatellite markers analysis	33
2.1.4	HD SNP genotyping array analysis.....	38
2.2	Coat color gene analysis of Taiwan swamp buffalo	41
2.2.1	Genome-wide association study (GWAS).....	41
2.2.2	<i>ASIP</i> genotyping.....	41
2.2.3	<i>MC1R</i> sequencing	42
2.2.4	TaqMan™ SNP Genotyping Assay	43
2.2.5	Amino acid substitution and protein function prediction.....	44
2.2.6	Relative gene expression analysis	44
2.2.7	Histological examination and staining of the buffalo skin.....	50
Chapter 3	Results	51
3.1	Population genetic structure analysis of Taiwan swamp buffalo.....	51
3.1.1	Microsatellite markers analysis results	51
3.1.2	HD SNP genotyping array analysis results	63
3.2	Coat color gene analysis of Taiwan swamp buffalo	71
3.2.1	Genome-wide association study (GWAS) results	71
3.2.2	<i>ASIP</i> genotyping results	78
3.2.3	<i>MC1R</i> sequencing results	82

3.2.4	<i>MC1R</i> c.901C>T genotyping using TaqMan™ SNP Genotyping Assay results	85
3.2.5	Amino acid substitution and protein function prediction results	88
3.2.6	Relative gene expression analysis results	90
3.2.7	Histological examination and staining results of the buffalo skin	94
Chapter 4	Discussion.....	97
4.1	Population genetic structure analysis of Taiwan swamp buffalo.....	97
4.1.1	Microsatellite markers analysis.....	97
4.1.2	HD SNP genotyping array analysis.....	100
4.1.3	Comparison between microsatellite markers and HD SNP genotyping array analysis.....	103
4.2	Coat color gene analysis of Taiwan swamp buffalo	107
Chapter 5	Conclusion	115
	REFERENCE	116
	APPENDIX	143

LIST OF FIGURES



Figure 1. Synteny analysis of the cattle, river buffalo, and swamp buffalo.	2
Figure 2. The distribution map of the Taiwan swamp buffalo.....	5
Figure 3. The Taiwan swamp buffaloes in Hualien Animal Propagation Station, Livestock Research Institute, Council of Agriculture, Executive Yuan.	7
Figure 4. Different coat color and eye color of the swamp buffalo.....	17
Figure 5. The skin and the hair of the adult (10 years old) white Taiwan swamp buffalo from HAPS.	45
Figure 6. The adult (10 years old) white Taiwan swamp buffalo from HAPS analyzed in this study.	45
Figure 7. The ear skin tissue of the gray (brown) and white Taiwan swamp buffalo calves (three weeks old) from HAPS.....	46
Figure 8. The two gray (brown) Taiwan swamp buffalo calves (the left and the right ones) and one white Taiwan swamp buffalo calf (the middle one) from HAPS analyzed in this study.....	46
Figure 9. The neighbor-joining tree (daylight method) based on the 14 microsatellite markers for the population of the 94 Taiwan buffaloes from HAPS in this study.....	59
Figure 10. The neighbor-joining tree (rectangular layout) based on the 14 microsatellite markers for the population of the 94 Taiwan buffaloes from HAPS in this study.....	60
Figure 11. STRUCTURE analysis based on the 14 microsatellite markers for the population of the 94 Taiwan buffaloes from HAPS in this study.	62
Figure 12. Distribution of the 14,456 SNPs for the genetic parameters among the 94	

Taiwan swamp buffaloes from HAPS.	65
Figure 13. The neighbor-joining tree (daylight method) based on the 14,456 SNPs for the population of the 94 Taiwan buffaloes from HAPS in this study.	67
Figure 14. The neighbor-joining tree (rectangular layout) based on the 14,456 SNPs for the population of the 94 Taiwan buffaloes from HAPS in this study.	68
Figure 15. The fastSTRUCTURE cluster analysis plot (K = 2 to 6) of the 94 Taiwan buffaloes based on the 14,456 SNPs.....	70
Figure 16. The Manhattan plot showing SNPs associated with the white coat color among 94 Taiwan swamp buffaloes (16 white and 78 gray) based on the 14,456 SNPs from the 90K Axiom® Buffalo Genotyping Array.	73
Figure 17. The location of the two most significant ($P < 1 \times 10^{-17}$) SNPs associated with the white coat color among 94 Taiwan swamp buffaloes (16 white and 78 gray) in the GWAS results and the <i>MC1R</i> gene on the buffalo chromosome 18.	76
Figure 18. Manhattan plot subset of the chromosome 18 showing SNPs associated with the white coat color among 94 Taiwan swamp buffaloes (16 white and 78 gray) based on the 14,456 SNPs from the 90K Axiom® Buffalo Genotyping Array.	77
Figure 19. The 1.5% agarose gel electrophoresis results of genotyping the <i>LINE-1</i> insertion in the <i>ASIP</i> gene using the allele-specific PCR.	79
Figure 20. The Sanger sequencing results of genotyping the <i>LINE-1</i> insertion in the <i>ASIP</i> gene using the allele-specific PCR.	81
Figure 21. Alignment of <i>MC1R</i> nucleotide sequences of the river buffalo and swamp buffalo from NCBI database, and gray and white Taiwan swamp buffaloes	

in this study.....	83
Figure 22. Sanger sequencing of gDNA in gray and white Taiwan swamp buffaloes revealed a mutation (c.901C>T) in the <i>MC1R</i> gene.	84
Figure 23 Allelic discrimination plots obtained for genotyping of <i>MC1R</i> c.901C>T in gray and white Taiwan swamp buffaloes using TaqMan™ SNP Genotyping Assay with qPCR.....	87
Figure 24. Alignment of the <i>MC1R</i> amino acid sequences of the river buffalo and swamp buffalo from NCBI database, and gray and white Taiwan swamp buffaloes in this study.	89
Figure 25. Gene expression (<i>MC1R</i> , <i>ASIP</i> , <i>MITF</i> , <i>TYR</i> , <i>TYRP1</i> , and <i>DCT</i> gene) comparison of different parts of skin tissue (ventral side ear, dorsal side ear, back, and abdomen) of an adult white Taiwan swamp buffalo using qPCR analysis.	92
Figure 26. Gene expression (<i>MC1R</i> , <i>ASIP</i> , <i>MITF</i> , <i>TYR</i> , <i>TYRP1</i> , and <i>DCT</i> gene) comparison of the ventral side and dorsal side ear skin tissue of two gray (brown) Taiwan swamp buffalo calves and one white Taiwan swamp buffalo calf using qPCR analysis.	93
Figure 27. Fontana-Masson staining of four parts of a white Taiwan swamp buffalo skin tissue.	95
Figure 28. Fontana-Masson staining of ear skin tissue of gray (brown) and white Taiwan swamp buffalo calves.	96
Figure 29. A white buffalo calf (gray ♀ x gray ♂) and its gray buffalo parents in HAPS.	108
Figure 30. The different degree of the darkness of the coat color among the Taiwan	

swamp buffaloes in HAPS.....109



LIST OF TABLES

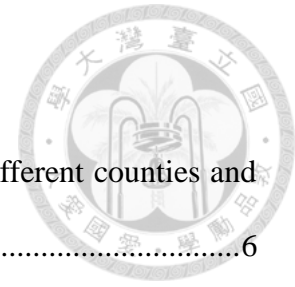
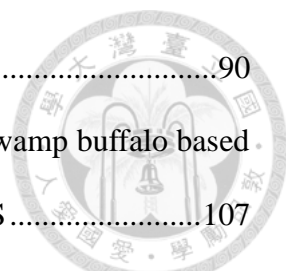


Table 1. The number of the Taiwan swamp buffalo distributed in different counties and cities in Taiwan	6
Table 2. The motifs, primer sequences, expected fragment sizes, and multiplex ID of the 15 microsatellite markers used in this study.....	35
Table 3. Primers designed for genotyping of the <i>LINE-1</i> insertion in the <i>ASIP</i> gene and for the <i>MC1R</i> gene sequencing of the Taiwan swamp buffalo	42
Table 4. Primers designed for gene expression analysis of the <i>MC1R</i> , <i>ASIP</i> , <i>MITF</i> , <i>TYR</i> , <i>TYRP1</i> , <i>DCT</i> , and <i>18s rRNA</i> gene by qPCR in this study	49
Table 5. Analysis of genetic polymorphism of 94 Taiwan swamp buffaloes based on 14 microsatellite markers in this study	56
Table 6. Analysis of the genetic polymorphism of the 94 Taiwan swamp buffaloes from HAPS based on the 14,456 SNPs from the 90K Axiom® Buffalo Genotyping Array	64
Table 7. The information of the top 17 SNPs and 26 related genes which are most significantly associated with coat color among Taiwan swamp buffaloes ...	74
Table 8. The location of the well-known pigmentation-related genes in the buffalo	75
Table 9. Genotype distribution and allele frequency of the mutation (c.901C>T) in the <i>MC1R</i> gene in 27 gray and 15 white Taiwan swamp buffaloes by Sanger sequencing	85
Table 10. Genotype distribution and allele frequency of the missense mutation (c.901C>T) in the <i>MC1R</i> gene in 115 gray and 18 white Taiwan swamp buffaloes by qPCR.....	88
Table 11. Potential effect of amino acid substitution (p.R301C) on MC1R structure or	

function by eight prediction tools	90
Table 12. Incidence of the gray and white coat color of the Taiwan swamp buffalo based on the pedigree record of 129 pair combinations in HAPS	107
Table 13. MC1R mutations at protein position 301 and their amino acid change, function significance, and its effect found in various species in past literature.....	111



Chapter 1 Literature Review

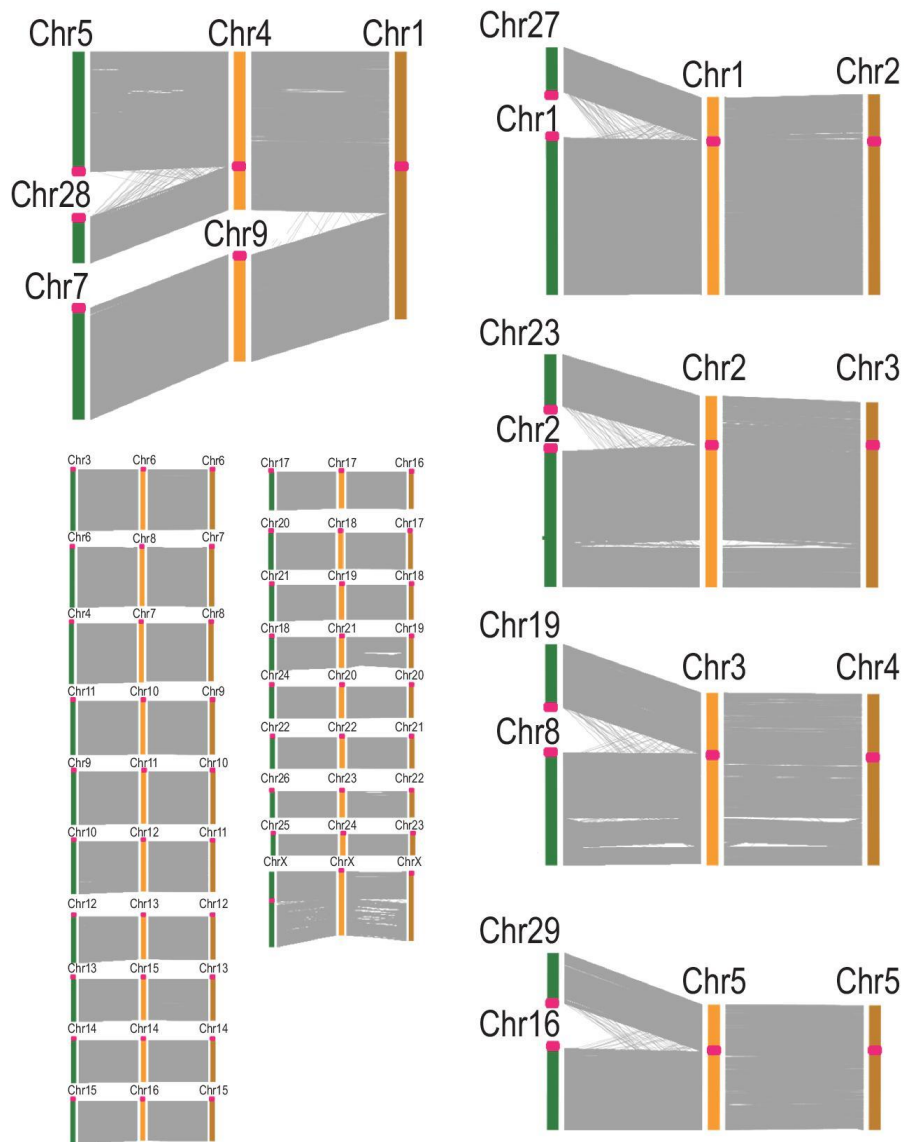
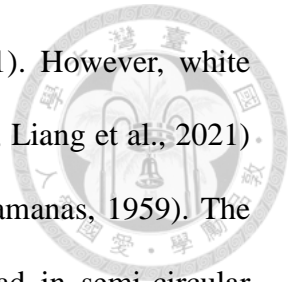


1.1 Taiwan swamp buffalo

There are about 204 million head of buffaloes in the world, with 198 million (97.1%) in Asia, 3.47 million (1.7%) in Africa, 1.98 million (1%) in South America, and 460,000 (0.2%) in Europe (FAOSTAT, 2019). The buffalo belongs to the Mammalia class, Artiodactyla order, and Bovidae family. The two main genera are the Asian buffalo (*Bubalus bubalus*) and the African buffalo (*Syncerus caffer*). The Asian buffalo comprises two subspecies, the river buffalo (*Bubalus bubalis bubalis*) and the swamp buffalo (*Bubalus bubalis carabanesis*) (Rife, 1962; Minervino et al., 2020; Rehman et al., 2021).

The river buffalo was domesticated in India around 2,500 BC and spread westward in the Balkans, Italy, Egypt, ...etc. (Cockrill, 1967; 1977; 1981; Sun et al., 2020). The river buffalo has 25 pairs of chromosomes ($2n = 50$) (Ulbrich and Fischer, 1966; Fischer and Ulbrich, 1967), and is mainly used as a dairy animal (Rife, 1962; Zhang et al., 2020). The river buffalo is usually black (Miao et al., 2010; Zhang et al., 2020), and the horns on its head are small and curly (Rife, 1962; Cockrill, 1981). The swamp buffalo was domesticated in China around 1,500 BC and distributed in Thailand, Indonesia, Malaysia, the Philippines, Taiwan, ...etc. (Cockrill, 1967; 1977; 1981; Sun et al., 2020). The swamp buffalo has 24 pairs of chromosomes ($2n = 48$) (Ulbrich and Fischer, 1966; Fischer and Ulbrich, 1967). The chromosome 4 and chromosome 9 of the river buffalo fused into chromosome 1 of the swamp buffalo (Figure 1) (Berardino and Iannuzzi, 1981; Luo et al., 2020). The swamp buffalo is mainly used as a draught animal (Rife, 1962; Zhang et al., 2020). The coat color of the swamp buffalo is usually gray with

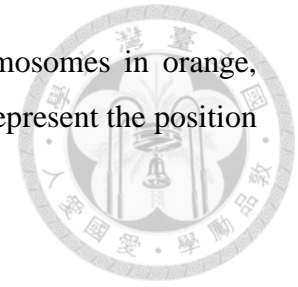
white chevrons and socks (Zhang et al., 2020; Liang et al., 2021). However, white swamp buffaloes appear occasionally (Rife, 1962; Miao et al., 2010; Liang et al., 2021) and are prevalent up to 10% of some populations (Rife and Buranamans, 1959). The swamp buffalo has massive horns growing outward from the head in semi-circular formation (Rife, 1962; Cockrill, 1981).



(Luo et al., 2020)

Figure 1. Synteny analysis of the cattle, river buffalo, and swamp buffalo. The cattle

chromosomes are presented in green, river buffalo chromosomes in orange, and swamp buffalo chromosomes in brown. The red dots represent the position of the centromere in the chromosome.



According to the characteristics mentioned above and the records in Taiwan Swamp Buffalo Breed Registration Application Document, buffaloes in Taiwan are swamp-type buffalo and named as Taiwan swamp buffalo (Animal Genetic Resources Information Network in Taiwan, 2010). Taiwan swamp buffaloes were introduced to Taiwan from Fujian and Guangdong in China with the migration of the ancestors in the 16th century and used as draught animals (Chuang, 2007; Animal Genetic Resources Information Network in Taiwan, 2010). In 1960, there were 318,162 head of Taiwan swamp buffaloes (Animal Genetic Resources Information Network in Taiwan, 2010). However, due to the mechanization of agriculture, the demand for draught animals dropped sharply, and there were only 2,002 head of Taiwan swamp buffaloes left at the end of 2021 (Statistic Office of C. O. A., 2022). Among all of the Taiwan swamp buffaloes, 789 head (39.41%) were in Hualien County, 472 head (23.58%) were in Pingtung County, and 250 head (12.49%) were in Taitung County (Statistic Office of C. O. A., 2022) (Figure 2; Table 1).

Due to the drastic reduction in the number of Taiwan swamp buffaloes in recent decades, Taiwan swamp buffaloes have been regarded as precious livestock resources. Hualien Animal Propagation Station (HAPS), Taiwan Livestock Research Institute, Council of Agriculture (TLRI, COA), Executive Yuan, has been the conservation field of Taiwan swamp buffaloes since 1981 (Animal Genetic Resources Information Network in Taiwan, 2010). HAPS introduced 39 cow buffaloes and two bull buffaloes from different places in Taiwan as the basic population, and after the last All Taiwan

Buffalo Show in Meilun, Hualien on January 1st, 1985 (Sung, 2003), the germplasm population of Taiwan swamp buffalo was officially established in 1987 (Animal Genetic Resources Information Network in Taiwan, 2010). Furthermore, the breed registration application of Taiwan swamp buffalo passed in 2010 (Animal Genetic Resources Information Network in Taiwan, 2010).

HAPS raises Taiwan swamp buffaloes with gray or white coat color (Figure 3). The first pair of the white Taiwan swamp buffaloes in HAPS were purchased from Taitung County in 1989. By natural group breeding, white buffaloes were bred with gray buffaloes. Until 2015, 43 white buffalo offspring have been bred (Animal Genetic Resources Information Network in Taiwan, 2015).

The buffalo has some advantages as a domestic animal. For example, it has strong environmental adaptability, it can be fed with low-quality roughage, it is disease resistant, and the content of cholesterol and fat in its meat is low (Animal Genetic Resources Information Network in Taiwan, 2010; Zhang et al., 2020; Rehman et al., 2021). However, Taiwan swamp buffalo is now underutilized. Furthermore, under the circumstance that the number of Taiwan swamp buffaloes is decreasing day by day, more attention should be paid to the conservation of Taiwan swamp buffalo.

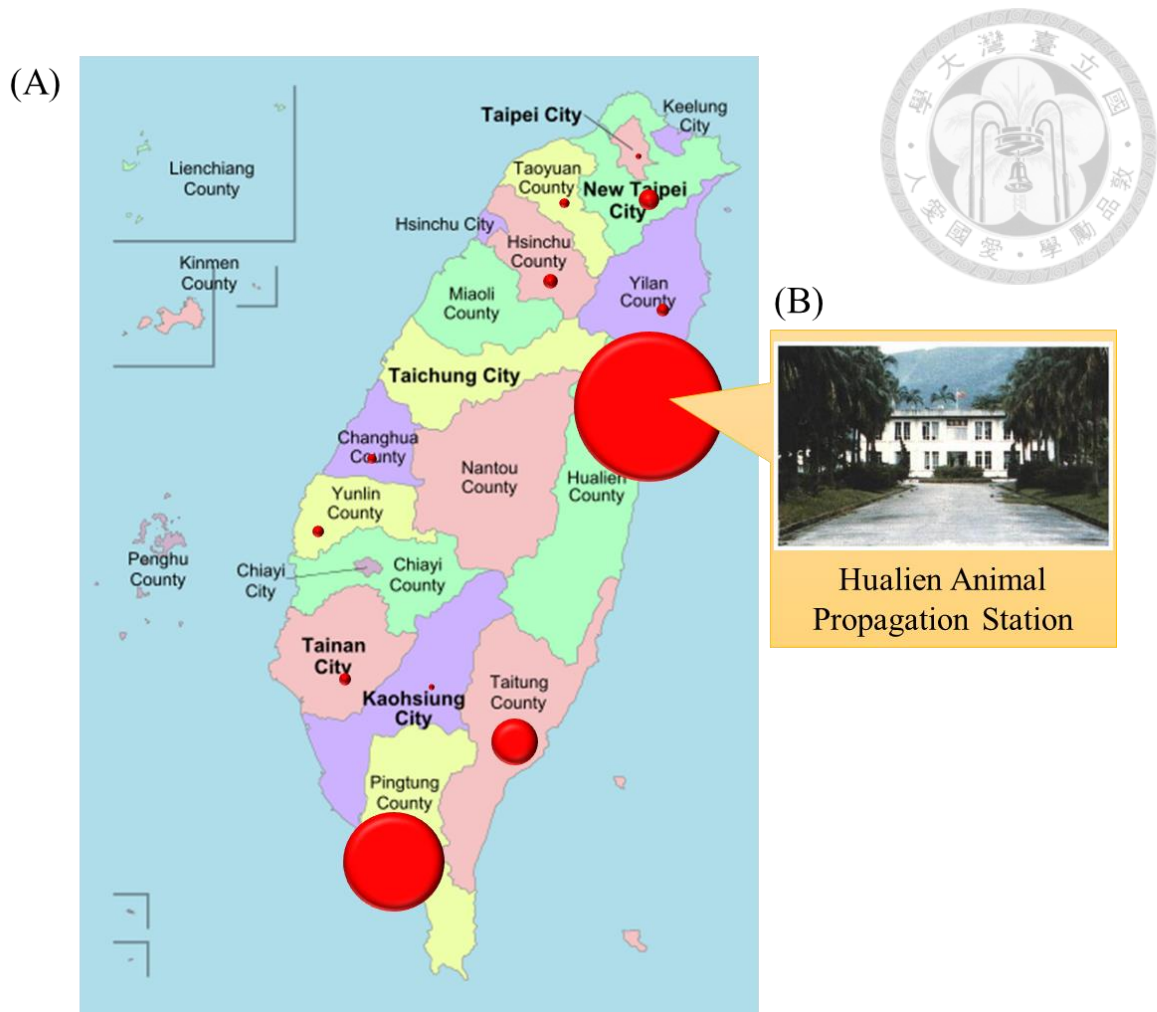
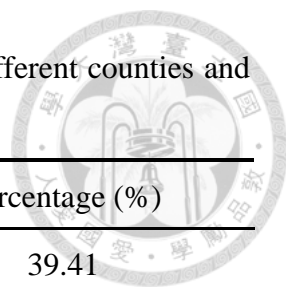


Figure 2. The distribution map of the Taiwan swamp buffalo. The number of Taiwan swamp buffaloes in different counties and cities was from Yearly Report of Taiwan's Agriculture 2021 (Statistic Office of C. O. A., 2022) (Table 1). The size of the red spots represents the proportion of the Taiwan swamp buffalo distributed in different places in Taiwan. (A) The map of Taiwan was from the website of Wikimedia Commons (2009). (B) The picture of Hualien Animal Propagation Station was from the website of Livestock Research Institute (2015).

Table 1. The number of the Taiwan swamp buffalo distributed in different counties and cities in Taiwan



City/County	Head*	Percentage (%)
Hualien County	789	39.41
Pingtung County	472	23.58
Taitung County	250	12.49
New Taipei City	136	6.79
Hsinchu County	74	3.70
Changhua County	33	1.65
Yilan County	47	2.35
Tainan City	40	2.00
Yunlin County	51	2.55
Taoyuan City	38	1.90
Kaohsiung City	30	1.50
Chiayi County	11	0.55
Miaoli County	4	0.20
Kinmen County	4	0.20
Taipei City	21	1.05
Taichung City	1	0.05
Nantou County	1	0.05
Sum	2,002	100.00

*The number of Taiwan swamp buffaloes in different counties and cities was from Yearly Report of Taiwan's Agriculture 2021 (Statistic Office of C. O. A., 2022).



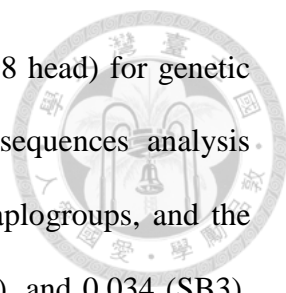
Figure 3. The Taiwan swamp buffaloes in Hualien Animal Propagation Station, Livestock Research Institute, Council of Agriculture, Executive Yuan. There were white (left) and gray (right) two different coat colors of Taiwan swamp buffaloes.

1.2 Population genetic analysis of Taiwan swamp buffalo

In order to understand the genetic characteristics of the Taiwan swamp buffalo, Huang (2000) carried out a blood type study on 122 Taiwan swamp buffaloes from HAPS and one Taiwan swamp buffalo from Taipei Zoo. The results showed that the proportion of polymorphic loci of Taiwan swamp buffalo was 0.67, the number of effective loci was 1.237, and the mean of heterozygosity was 0.144. Due to the rather high genetic polymorphism, it was inferred that the Taiwan swamp buffalo in the study did not undergo a strict selection process and was a random bred stock.

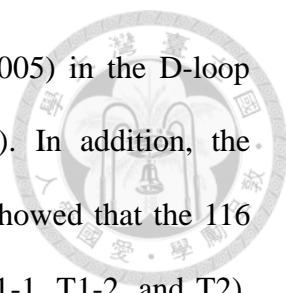
Lin et al. (2013) used 12 microsatellite markers to analyze the population genetic structure of 114 Taiwan swamp buffaloes in HAPS. The results showed that among the 12 microsatellite markers, the average number of observed alleles (N_a) was 4.3, the average number of effective alleles (N_e) was 2.5, the average observed heterozygosity (H_o) was 0.505, the average expected heterozygosity (H_e) was 0.532, the average polymorphic information content (PIC) was 0.48, and the Wright's inbreeding coefficient (F_{IS}) was 0.043. Based on the analysis of STRUCTURE 2.3 (Pritchard et al., 2000) and the UPGMA (unweighted pair group method with arithmetic mean) phylogenetic tree drawn with PHYLIP 3.6 (Felsenstein, 2002) using D_A genetic distances (Saitou and Nei, 1987), Taiwan swamp buffaloes in the study of Lin et al. (2013) could be clustered into three subpopulations. It was confirmed that the degree of inbreeding ($F_{IS} = 0.043$) was low in the Taiwan swamp buffaloes, and there was minor differentiation in the population.

Zhang et al. (2016) sequenced the mitochondrial DNA (mtDNA) *Cytochrome b* gene and control region and the Y-chromosomal *ZFY*, *SRY* and *DBY* sequences of 1,100 buffaloes from China (681 head), Taiwan (29 head), Vietnam (100 head), Laos



(96 head), Thailand (54 head), Nepal (42 head), and Bangladesh (98 head) for genetic and geographic differentiation analysis. The results of mtDNA sequences analysis showed that Taiwan swamp buffalo could be divided into three haplogroups, and the frequencies of mtDNA haplogroups were 0.897 (SA1), 0.069 (SA2), and 0.034 (SB3). There were three *Cytochrome b* haplotypes found in Taiwan swamp buffalo, and the heterozygosity was 0.197. Only one haplotype (YS3A) was found in the seven male Taiwan swamp buffaloes in the study. In addition, the study pointed out that the swamp buffalo had higher maternal and paternal lineage diversity than the river buffalo, and the area with the highest genetic diversity of the swamp buffalo was at the junction of southern China and northern Indochina Peninsula.

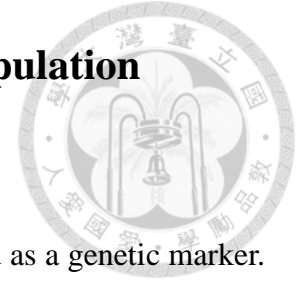
Chen et al. (2019) conducted a genetic diversity analysis on the mitochondrial D-loop region, *Cytochrome b* gene, and *12S rRNA* gene of 116 Taiwan swamp buffaloes at HAPS. The results showed that there were 25 single-nucleotide polymorphisms (SNPs) and seven haplotypes in the D-loop sequence, with the nucleotide diversity 0.0044 and the haplotype diversity 0.783. There were 11 SNPs and three haplotypes in the *Cytochrome b* gene, with the nucleotide diversity 0.0009 and the haplotype diversity 0.192. There were two SNPs and three haplotypes in the *12S rRNA* gene, with the nucleotide diversity 0.0006 and the haplotype diversity 0.192. Because of the low haplotype diversity and nucleotide diversity observed in the *Cytochrome b* gene and the *12S rRNA* gene of the Taiwan swamp buffalo, the author indicated that the genetic diversity of the Taiwan swamp buffalo population at HAPS might have gradually declined due to the closed breeding. Other possible reasons were that Taiwan was not the origin of the Taiwan swamp buffalo, and there might be a founder effect because the initial buffaloes in HAPS were introduced from few places in Taiwan. Besides, the high



haplotype diversity (> 0.5) and the low nucleotide diversity (< 0.005) in the D-loop sequence might indicate a bottleneck effect (Nei and Li, 1979). In addition, the neighbor-joining phylogenetic tree based on the D-loop sequence showed that the 116 Taiwan swamp buffaloes could be divided into three subgroups (T1-1, T1-2, and T2), and the proportions were 90, 6 and 4%, respectively.

In summary, the population genetic structure of the Taiwan swamp buffalo in HAPS had been estimated by blood type (Huang, 2000), microsatellite markers (Lin et al., 2013), mitochondrial *Cytochrome b* gene, D-loop region, and *12S rRNA* gene (Zhang et al., 2016; Chen et al., 2019). The results showed that the Taiwan swamp buffalo could be clustered into three subgroups. The genetic polymorphism of the Taiwan swamp buffalo was moderate to high (Huang, 2000; Lin et al., 2013) and the degree of inbreeding was low (Lin et al., 2013). However, it seemed that the genetic diversity of the Taiwan swamp buffalo had gradually declined because of the closed breeding at HAPS (Chen et al., 2019).

1.3 Microsatellite markers used in buffalo population genetic analysis



Microsatellite is a repetitive sequence on DNA and can be used as a genetic marker. By detecting the different sizes of the repeating sequence fragments, multiple genotypes of the microsatellite can be distinguished, which means microsatellite is a multiallelic genetic marker (Tautz, 1989; Bruford and Wayne, 1993; Barker, 2002).

Lots of studies have used the polymorphisms of microsatellites to conduct genetic analysis on the buffalo. Of all, there was the most research in India, including studies on various breeds of river buffaloes (Navani et al., 2002; Arora et al., 2004; Kumar et al., 2006; Sukla et al., 2006; Tantia et al., 2006; Mishra et al., 2008; Vijn et al., 2008; Kataria et al., 2009; Nagarajan et al., 2009; Mishra et al., 2010; Mishra et al., 2015; Vohra et al., 2021b) and swamp buffaloes (Mishra et al., 2015; Singh et al., 2022).

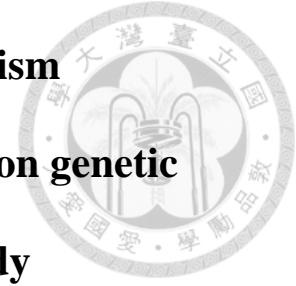
In other countries, some studies used microsatellite markers to estimate the population genetic structure of the river buffalo in Pakistan (Babar et al., 2009; Saif et al., 2012; Hussain et al., 2017), Turkey (Gargani et al., 2010; Özkan Ünal et al., 2014; Ünal et al., 2021), Iran (Shokrollahi et al., 2009; Yousefi et al., 2019), Colombia (Ángel-Marín et al., 2010), Egypt (Hassanane et al., 2000; El-Kholy et al., 2007; Hassanane et al., 2007; Abo Bakr et al., 2012; Attia et al., 2014; Merdan et al., 2020), and Brazil (Rogberg Muñoz et al., 2011). Elbeltagy et al. (2008) analyzed genetic diversity of both Egyptian and Italian river buffalo, and Moioli et al. (2001) compared the genetic differences between river buffaloes in Italian, Greek and Egyptian.

On the other hand, for the swamp buffalo, research using microsatellite markers to analyze the population genetic structure were in Indonesia (Saputra et al., 2020),

Thailand (Triwitayakorn et al., 2006; Sraphet et al., 2008), Vietnam (Berthouly et al., 2010), and Taiwan (Lin et al., 2013).

Scientists in China conducted genetic structure analysis on swamp and river buffaloes of different regions and breeds (Zhang et al., 2007; Zhang et al., 2008a; Zhang et al., 2008b; Yang et al., 2011; Zhang et al., 2011). In Cuba, there were studies on mixed breeds of river buffaloes and swamp buffaloes (Acosta et al., 2014; Uffo et al., 2017). There were even studies estimating swamp buffaloes from Thailand, Malaysia, Indonesia, Philippines, and Australia and river buffaloes from Sri Lanka and Malaysia at the same time (Moore et al., 1995; Barker et al., 1997). As for the African buffalo, there were fewer population genetic studies based on microsatellites (Simonsen et al., 1998; Van Hooft et al., 1999; Greyling et al., 2008).

1.4 High-density single nucleotide polymorphism genotyping array used in buffalo population genetic analysis and genome-wide association study



The microarray technology utilized in the high-density single nucleotide polymorphism genotyping array (HD SNP genotyping array) allows a large number of SNPs in DNA samples be analyzed at one time. There may be thousands to millions of nucleic acid probes complementary to SNP sequences on a chip. Affymetrix (Santa Clara, CA) developed the first SNP array which was designed to genotype 1,494 SNPs in 1996 (Balagué-Dobón et al., 2022). Since then, many manufacturers have developed SNP arrays, including Affymetrix (Santa Clara, CA), Agilent (Santa Clara, CA), Illumina (San Diego, CA), and Nimblegen (Madison, WI) (Lamy et al., 2011). There were studies comparing arrays of different content released by Affymetrix and Illumina (Anderson et al., 2008; Ha et al., 2014; Verlouw et al., 2021), which are the most commonly used platforms (Lamy et al., 2011).

Since the technology for analyzing a large number of SNPs was not mature in the past, SNPs were rarely used in population genetic analysis. A SNP is a biallelic genetic marker in one locus, so its polymorphism is lower than that of a microsatellite marker in a locus. However, it was indicated that about 100 SNP markers were equivalent to 10-20 microsatellite markers (Kalinowski, 2002; Glaubitz et al., 2003), and when sufficient SNPs were available, they could perform better than microsatellites (Liu et al., 2005; Helyar et al., 2011; Sturm et al., 2020). Nevertheless, even if a large amount of genotype information of SNP markers is obtained, it is still necessary to overcome the high cost and the huge amount of data when conducting a population genetic analysis

because it may not be applicable to the past methods and software (Vignal et al., 2002; Fan et al., 2010; Helyar et al., 2011; Nicolazzi et al., 2015; Laoun et al., 2020).

In recent years, the first SNP genotyping array (Axiom® Buffalo Genotyping Array; 90K Affymetrix; Thermo Fisher Scientific, Wilmington, DE) designed specifically for buffaloes has been developed (Iamartino et al., 2017). Some scientists have begun to use this array to analyze the genetic structure of different buffalo populations. With the 90K Axiom® Buffalo Genotyping Array, Colli et al. (2018) and Macciotta et al. (2021) estimated genomic diversity and described population structure of river buffaloes from India, Pakistan, Iran, Turkey, Egypt, Italy, Bulgaria, Romania, Mozambique, Colombia, Brazil and swamp buffaloes from China, Philippines, Thailand, Indonesia, Brazil. Scientists in Iran investigated genetic diversity and genomic structure of river buffaloes in Iran (Mokhber et al., 2018; Mokhber et al., 2019; Davoudi et al., 2020; Ghoreishifar et al., 2020) and performed a genome-wide scan of copy number variants (Strillacci et al., 2021) in Iranian river buffaloes using the 90K Axiom® Buffalo Genotyping Array. Lu et al. (2020) analyzed the genetic diversity, linkage disequilibrium pattern, and signature of selection of river buffaloes, crossbred buffaloes, and swamp buffaloes in China with the 90K Axiom® Buffalo Genotyping Array. Thakor et al. (2021) analyzed genetic variability and population structure of seven Indian river buffalo breeds, Rahimadar et al. (2021) analyzed linkage disequilibrium and effective population size of river buffaloes in Iran, Turkey, Pakistan, and Egypt, and Noce et al. (2021) explored the genetic diversity and population structure of river buffaloes in Germany, Bulgaria, Romania, and Hungary and compared their potential relations to buffaloes worldwide with the 90K Axiom® Buffalo Genotyping Array. There is not yet a study conducting a genetic analysis on the Taiwan swamp buffalo

using such HD SNP genotyping array.

In addition, scientists also used the 90K Axiom® Buffalo Genotyping Array for genome-wide association study (GWAS) to find genetic variants associated with a specific trait or disease. Uffelmann et al. (2021) described the workflow of a GWAS, including collection of DNA and phenotypic information from the samples, genotyping of each sample with available arrays or other sequencing strategies, quality control of the genotyping results, performing a statistical analysis for association, and interpreting the results by conducting multiple post-GWAS analyses. PLINK (Purcell et al., 2007) is a free and open-source whole genome association analysis toolset, which is designed to perform many of the quality control steps in genetic data and to conduct genetic association analysis. The output of a GWAS analysis is a list of *P*-values generated from the association tests of all tested genetic variants with a target phenotype. The results are visualized as a Manhattan plot to show the genomic positions and the strength of association of the genetic variants.

With the 90K Axiom® Buffalo Genotyping Array, SNPs related to milk production (de Camargo et al., 2015; El-Halawany et al., 2017; Iamartino et al., 2017; da Costa Barros et al., 2018; Liu et al., 2018; Deng et al., 2019; Abdel-Shafy et al., 2020; Gonzalez Guzman et al., 2020), reproductive traits (de Camargo et al., 2015; Li et al., 2018; de Araujo Neto et al., 2020; Vohra et al., 2021a), and mammary gland morphology (Li et al., 2020) in buffaloes had been identified. Before the 90K Axiom® Buffalo Genotyping Array was available, milk production traits of buffalo were studied through GWAS using the bovine SNP chip: Illumina BovineSNP50 BeadChip (Wu et al., 2013) and Illumina Infinium® BovineHD BeadChip (Venturini et al., 2014).

1.5 Coat color genes of the buffalo

1.5.1 The coat color of the buffalo

The Asian buffalo is divided into the river buffalo and the swamp buffalo. The coat color of the river buffalo is usually dark black, sometimes with brown or white spots or patches (Rife, 1962; Miao et al., 2010; Gurao et al., 2022), and all-white or all-brown individuals also exist (Rife, 1962; da Cruz et al., 2020; Ali et al., 2022). For example, Nili Ravi, a breed of river buffalo in India, has black coat color with white patches and pink skin underneath (Gurao et al., 2022). Based on the degree and the distribution of the white markings, the Nili Ravi buffalo could be subclassified as “typical”, “over-white” and “under-white” (Dhandapani et al., 2021).

The coat color of the swamp buffalo is usually gray with dark skin, white stripes on the neck, and white hair below the hocks (Zhang et al., 2020; Liang et al., 2021). On the other hand, some of the swamp buffaloes have white coat color, pink skin, and the same pigmented eyes as the gray swamp buffaloes (Rife, 1962; Liang et al., 2021). White swamp buffaloes are commonly found in Laos and Thailand, and about 10% of the swamp buffaloes in Thailand are white (Rife and Buranamas, 1959). In addition, white-spotted swamp buffaloes are found in Indonesia, which have been preserved by the local people due to the cultural traditions. Compared with the diluted color of the white swamp buffalo, the white color of the white-spotted swamp buffalo seems to be more extreme. According to the appearance of the spots and the color of the iris (white or black), white-spotted swamp buffalo can be divided into four subclasses, for example: *Saleko* type, *Lotong Boko* type, *Bonga* type, and *Toddi*' type (Yusnizar et al., 2015) (Figure 4).





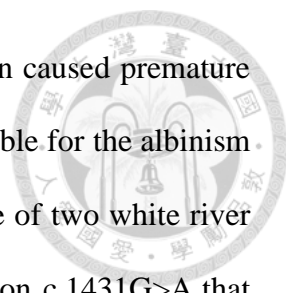
(Yusnizar et al., 2015)

Figure 4. Different coat color and eye color of the swamp buffalo. (A) Gray coat color with black eyes. (B) White coat color with black eyes. (C) White-spotted coat color with white eyes (*Saleko* type). (D) White-spotted coat color with black eyes (*Lotong Boko* type). (E) White-spotted coat color with white eyes (*Bonga* type). (F) White-spotted coat color with black eyes (*Toddi'* type).

1.5.2 The albinism and the *TYR* gene of the buffalo

The phenotype of oculocutaneous albinism (OCA) is the lack of melanin in the hair, skin, and eyes of an animal (Grønskov et al., 2007). It is usually caused by the impairment of pigment production in melanocytes, resulting in complete lack of pigment in various body parts of an animal (Cieslak et al., 2011). Genetic variants in *TYR* gene were known to result in albinism in a variety of animals, including the human (Oetting, 2000), mouse (Yokoyama et al., 1990), rabbit (Aigner et al., 2000), cattle (Schmutz et al., 2004), cat (Imes et al., 2006), ...etc.

Damé et al. (2012) conducted a study on four normal black river buffaloes and six river buffaloes diagnosed with albinism, and they found that the albino river buffaloes



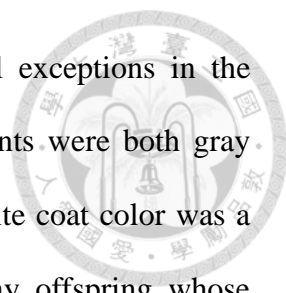
had a mutation c.1431G>A in the *TYR* gene. This missense mutation caused premature translation termination (p.W477*), which was thought to be responsible for the albinism of the river buffaloes. da Cruz et al. (2020) sequenced the *TYR* gene of two white river buffaloes, and the results showed that they did not carry the variation c.1431G>A that caused albinism in the buffalo found by Damé et al. (2012). Besides, the eyes of the white river buffaloes in the study of da Cruz et al. (2020) were pigmented. Therefore, it was inferred that the two white river buffaloes were not albinos. Forty river buffaloes suffering from skin and hair depigmentation in the Brazilian Amazon biome were also genotyped (Barbosa et al., 2023) for the mutation c.1431G>A in the *TYR* gene causing albinism described by Damé et al. (2012). The results showed that none of the buffaloes with leucoderma had a mutation in the *TYR* gene (Barbosa et al., 2023).

The albino buffaloes were lack of pigment in the eyelashes, conjunctiva, and iris, and they showed signs of photophobia (Damé et al., 2012). Since the white swamp buffalo had pigmented eyes (Rife and Buranamanas, 1959; Rife, 1962; Yusnizar et al., 2015; Liang et al., 2021) and could adapt to the outdoor environment (Chuang, 2007), it is generally believed that the white swamp buffalo is not albino.

Liang et al. (2021) examined the expression levels of the *TYR* gene among three white and three gray swamp buffaloes with the RNA-seq data, and the results showed that in the ear skin tissue, the *TYR* gene expression levels were lower in the white swamp buffaloes than in the gray swamp buffaloes ($P < 0.01$).

1.5.3 An early research of the white swamp buffalo

Rife and Buranamanas (1959) and Rife (1962) speculated that the gene for white coat color of the swamp buffalo should be dominant to the gray coat color from the trait

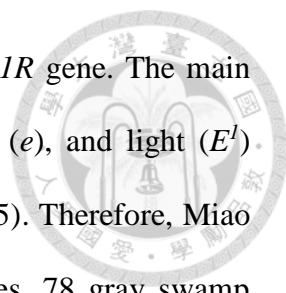


records of swamp buffalo in Thailand. However, there were still exceptions in the pedigree. For example, there was one white offspring whose parents were both gray (Rife, 1962), which did not conform to the assumption that the white coat color was a Mendelian dominant inheritance. Conversely, there were two gray offspring whose parents were both white (Rife, 1962), so it could not be determined that the gray coat color was dominant to the white coat color. The author only made inferences based on the probability of errors in pedigree records, as well as the calculation and assumptions of gene frequencies. However, the P -values of the chi-square tests were not significant ($P > 0.1$).

1.5.4 Analysis of the *MC1R* gene of the buffalo

MC1R (Melanocortin 1 receptor) protein is a G protein-coupled receptor, made up of seven α -helical transmembrane domains, on the plasma membrane of melanocytes (García-Borrón et al., 2005). MC1R protein is activated by melanocortins, in particular α -melanocyte stimulating hormone (α -MSH), and suppressed by Agouti signal protein (ASIP) (Rees, 2003). The activation of *MC1R* pathway enhances transcription of microphthalmia transcription factor (*MITF*) (Abdel-Malek et al., 2008). Increased *MITF* further stimulates transcription of genes such as tyrosinase (*TYR*), tyrosinase-related protein 1 (*TYRP1*), and tyrosinase-related protein 2 (*TYRP2*) (also known as dopachrome tautomerase, *DCT*) which are necessary for the eumelanogenesis pathway, and thus induces a switch from pheomelanin to eumelanin synthesis and increases the number, size and transport of the melanosome (Schiaffino, 2010).

It is well-known that the *MC1R* gene involves in the regulation of pigmentation in mammals (Rees, 2003; Switonski et al., 2013; Hashimoto et al., 2021). For example, the



different coat color of the cattle is affected by the variation of *MC1R* gene. The main alleles are the wild-type (E^+), dominant black (E^D), recessive red (e), and light (E^l) (Klungland et al., 1995; Klungland et al., 2000; Rouzaud et al., 2005). Therefore, Miao et al. (2010) analyzed the *MC1R* genes of 49 black river buffaloes, 78 gray swamp buffaloes, and 58 white swamp buffaloes, and the results showed that the *MC1R* gene fragment of those buffalo was 954 bp and translated into 317 amino acids, which was the same length as the cattle *MC1R* gene fragment. The *MC1R* gene of the buffalo and the cattle had 97% similarity, but no variants found in the cattle *MC1R* gene were observed in the buffalo. Therefore, the variation in coat color in the buffalo should not be explained by the *MC1R* genotype of the cattle.

Miao et al. (2010) found that there were two variants, c.310G>A and c.384G>T, in the *MC1R* gene between the river buffalo and the swamp buffalo. Both of the variants were missense mutations, resulting in amino acid changes p.G104S and p.M128I, respectively. All of the river buffaloes in the experiment were c.310A and c.384T genotypes, which was defined as the E^{BR} allele, so the *MC1R* genotype of the river buffalo was E^{BR}/E^{BR} . All of the swamp buffaloes in the experiment were c.310G and c.384G genotypes, which was defined as the E^{BS} allele, so the *MC1R* genotype of the swamp buffalo was E^{BS}/E^{BS} . The PANTHER software (Thomas et al., 2006) was used to predict that the mutation of the E^{BR} allele might affect the function of MC1R, resulting in the lighter coat color.

In addition, the black river buffaloes were crossed with the gray swamp buffaloes in the study (Miao et al., 2010). The F1 offspring had brown coat color with E^{BR}/E^{BS} genotype, so it was deduced that E^{BR} was related to the black coat color of the buffalo and was important for maintaining the normal function of MC1R. On the other hand,

the gray and white swamp buffaloes in the study were all E^{BS}/E^{BS} genotypes, so it was concluded that the *MC1R* gene was not associated with the gray and white coat color of the swamp buffalo.

However, da Cruz et al. (2020) put forward a different argument. In their study, the *MC1R* gene of nine black river buffaloes, eight brown river buffaloes and two white river buffaloes were sequenced. The results showed that there were black river buffaloes not E^{BR}/E^{BR} genotypes, and there were brown and white river buffaloes with E^{BR}/E^{BR} genotypes. Therefore, da Cruz et al. (2020) indicated that the E^{BR}/E^{BR} genotypes was not the reason for the black coat color of the buffalo, and the *MC1R* gene did not affect the coat color of the river buffalo.

Liang et al. (2021) examined the expression levels of the *MC1R* gene among three white and three gray swamp buffaloes with the RNA-seq data, and the results showed that in the ear skin tissue, the *MC1R* gene expression levels were not significantly different between the white and gray swamp buffaloes ($P > 0.05$).

Azakheli buffalo is a breed of river buffalo in Pakistan. Azakheli buffalo had color variation ranging from complete albino, brown, piebald, and to black (Ali et al., 2022). Ali et al. (2022) sequenced the *MC1R* gene of 68 Azakheli buffaloes, and further combined the results with the Chinese and Indian buffaloes *MC1R* haplotype sequences retrieved from GenBank. The results showed 22 haplotypes from 68, 198, and 142 sequences of Azakheli, Indian and Chinese buffaloes, respectively. High mutations in the albino Azakheli buffaloes were observed, and all the black Azakheli buffaloes shared haplotypes with Chinese and Indian black buffaloes, indicating signs and possibilities that the black coat color of Azakheli buffalo was due to the variation of the *MC1R* gene (Ali et al., 2022).

1.5.5 Analysis of the *MITF* gene of the buffalo

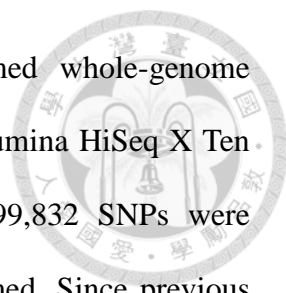
Yusnizar et al. (2015) Sanger-sequenced the *MITF* gene, which is known to affect both coat color and iris color (Pingault et al., 2010), of 32 gray swamp buffaloes, 23 white swamp buffaloes and 38 white-spotted swamp buffaloes. The results showed that two SNPs on the *MITF* gene were highly correlated with the white-spotted color, namely c.328C>T on *MITF* exon 3 ($P = 1.3 \times 10^{-7}$) and c.840+2T>A on *MITF* intron 8 ($P = 0.05$). The former was a missense mutation leading to a premature translation termination (p.R110*), and the latter was a donor splice-site mutation leading to the amino acid change p.E281_L282Ins8.

However, none of the white-spotted buffaloes carrying the variants were homozygous, and no individuals carried both of the two variants at the same time. Furthermore, gray swamp buffaloes with the variants and white-spotted buffaloes without any variants were still observed in the experiment. Therefore, it was speculated that there were still other unknown genetic variants affecting the white-spotted coat color of the swamp buffalo. In addition, the white swamp buffalo had no variation in these two loci, so it was deduced that the cause of the white coat color and the white-spotted coat color of the swamp buffalo should be different.

Liang et al. (2021) examined the expression levels of the *MITF* gene among three white and three gray swamp buffaloes with the RNA-seq data, and the results showed that in the ear skin tissue, the *MITF* gene expression levels were not significantly different between the white and gray swamp buffaloes ($P > 0.05$).

1.5.6 Analysis of the *ASIP* gene of the buffalo

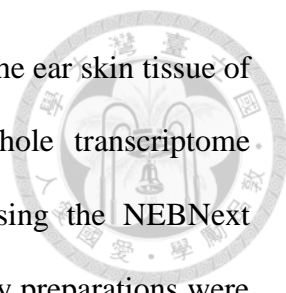
Liang et al. (2021) attempted to figure out the gene regulation mechanism of the



white coat color of the swamp buffalo. Firstly, they performed whole-genome sequencing on 22 white and 41 gray swamp buffaloes using the Illumina HiSeq X Ten system (Illumina, San Diego, CA). After quality control, 10,999,832 SNPs were identified. A genome-wide association study (GWAS) was performed. Since previous literature pointed out that the white coat color of swamp buffalo should be dominant (Rife and Buranamas, 1959; Rife, 1962), the author used the Fisher's exact test and the dominance gene effect model in the PLINK software v1.07 (Purcell et al., 2007) for GWAS analysis. The results showed that there was a significant peak on chromosome 14, which contained 407 SNPs associated with the white coat color ($P < 1 \times 10^{-8}$). The significant region spanned 1.07 Mb, covering 5 pseudogenes and 23 genes, containing the *ASIP* gene which is known to be related to the pigmentation.

In order to verify the GWAS results, Liang et al. (2021) genotyped a panel of 19 SNPs and one indel that showed significant associations with the white color in the target genomic region on 80 white and 122 gray swamp buffaloes from Thailand, Bangladesh and China with the Kompetitive allele specific PCR (KASP) method. The results showed that as the number of samples increased, the correlation between the variants and the white coat color increased ($P < 1 \times 10^{-18}$). The four most significant SNPs were located at the first intron and the upstream of the *ASIP* gene. Besides, in the linkage disequilibrium (LD) analysis, 13 SNPs were found to form an LD block covering the *ASIP* gene. Therefore, the *ASIP* gene was considered as a candidate gene for the white coat color.

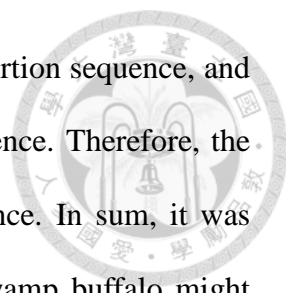
In the GWAS analysis, 51 SNPs on the *ASIP* gene were highly correlated with the white coat color. However, none of these variants was predicted to affect the function of the *ASIP* protein. Therefore, Liang et al. (2021) turned to focus on the gene expression



of the 23 most significantly correlated genes in the GWAS results. The ear skin tissue of three white and three gray swamp buffaloes was used for whole transcriptome sequencing (RNA-seq). Sequencing libraries were constructed using the NEBNext Ultra™ RNA Library Prep Kit (NEB, Ipswich, MA), and the library preparations were sequenced using the Illumina HiSeq X Ten system. The results showed that the *ASIP* gene transcription level is 10.3 times that of the gray buffalo, which was further verified by real-time qPCR analysis ($P < 0.001$). Therefore, it was inferred that the white coat color of the swamp buffalo may be due to the increase expression level of the *ASIP* gene in the skin.

Liang et al. (2021) then used RACE-PCR to obtain the full-length transcripts of the *ASIP* genes in one gray and one white swamp buffalo. The results showed there was an unknown 165 bp sequence in the *ASIP* gene of the white swamp buffalo. The unknown sequence had 98% similarity as the bovine long interspersed nuclear element-1 (*LINE-1*) transposon element. Subsequent analysis of soft-clipped reads mapped this insertion at BBU14:19996791-19996806. The Nanopore long-read sequencing technology was used to determine that the insertion sequence was 2,809 bp in full length. It was further confirmed that the insertion sequence located at 44 kb upstream of the first coding exon of the *ASIP* gene, and a 165 bp fragment was spliced into the first coding exon of the *ASIP* gene during transcription. It was speculated that the *LINE-1* insertion might act as a powerful alternative promoter for the *ASIP* gene to increase the expression of the *ASIP* gene.

In order to validate the correlation between the *LINE-1* insertion in the *ASIP* gene and the white coat color, Liang et al. (2021) genotyped 91 white and 194 gray swamp buffaloes. The results showed that none of the gray buffaloes had the *LINE-1* insertion

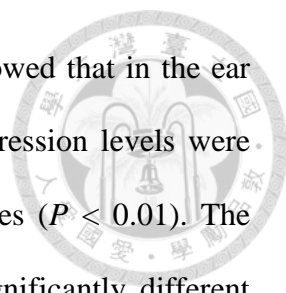


sequence, 88 white buffaloes were heterozygous for the *LINE-1* insertion sequence, and three white buffaloes were homozygous for *LINE-1* insertion sequence. Therefore, the white coat color was identified as a Mendelian dominant inheritance. In sum, it was deduced that the overexpression of the *ASIP* gene in the white swamp buffalo might prevent melanocyte differentiation and thus led to the white coat color of the white swamp buffalo.

On the other hand, Kumari et al. (2023) found four SNPs (c.292C>T, c.391C>A, c.393C>T, c.396C>A) in the *ASIP* gene of 21 river buffaloes by sequencing the coding exons 2, 3, and 4 of the *ASIP* gene with the dideoxy chain termination method. The c.292C>T SNP in exon 3 was a non-synonymous SNP that resulted in an arginine to cysteine amino acid change at protein position 98. Tetra-Primer Amplification Refractory Mutation System-Polymerase Chain Reaction (Tetra-ARMS PCR) was used to further genotype 268 river and swamp buffaloes from 10 different populations for the SNP (c.292C>T). The mutant TT genotype occurred at a higher rate in Murrah and Nili Ravi buffaloes (42.63% vs. 19.30%), giving them darker coat color, while the swamp buffalo with grayish-black coat color and other river breeds with brownish black coat colors have less or no occurrence of the “T” allele. It was implied that there might be association of the black coat color of the Murrah buffalo with the *ASIP* gene TT genotype and the light coat color phenotype in other breeds with the CC genotype at the c.292C>T locus. In addition, the ‘T’ allele encoding for the p.R98C of the *ASIP* protein was also reported in the alpaca for the black fiber color (Feeley et al., 2011).

1.5.7 Analysis of other coat color genes of the buffalo

Liang et al. (2021) also examined the expression levels of other

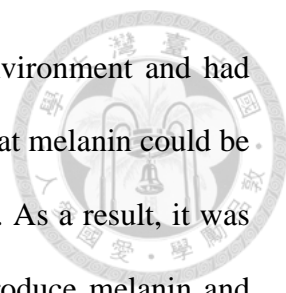


skin-color-associated genes with the RNA-seq data. The results showed that in the ear skin tissue, the *DCT/TYRP2*, *TYRP1*, *PMEL*, and *OCA2* gene expression levels were lower in the white swamp buffaloes than the gray swamp buffaloes ($P < 0.01$). The *KITLG*, *EDNRB*, and *SOX10* gene expression levels were not significantly different between the white and gray swamp buffaloes ($P > 0.05$). Only the gene expression level of the *KIT* gene was slightly higher in the ear skin of the white swamp buffaloes ($P < 0.05$). Among all, it was emphasized that the *TYRP1* gene did not express in the ear skin tissue of the white swamp buffaloes.

Gurao et al. (2022) identified the differential methylome signatures of white pigmented skin patches in the Nili Ravi buffalo. The DNA was isolated from the skin tissues of the forehead of three over-white Nili Ravi buffaloes, three under-white Nili Ravi buffaloes and black Murrah buffaloes in India, and the sample was subjected to reduced representation bisulfite sequencing. The DNA methylation analysis revealed 68.44, 63.39, and 47.94% of the promoter regions were hypermethylated in over-white Nili Ravi buffaloes versus Murrah buffaloes, under-white Nili Ravi buffaloes versus Murrah buffaloes, and under-white Nili Ravi buffaloes versus over-white Nili Ravi buffaloes, respectively. The *TBX2*, *SNAI2*, *HERC2*, and *CITED1* genes were identified to be differentially methylated among over-white and under-white Nili Ravi buffaloes.

1.5.8 Coat color gene analysis of the Taiwan swamp buffalo

In order to understand the reason for the white coat color of Taiwan swamp buffalo, Chuang (2007) analyzed the melanin content of the skin and hair of the gray and white Taiwan swamp buffaloes in HAPS and compared six genes (*MC1R*, *KIT*, *KITLG*, *TYR*, *TYRP1*, and *DCT*) between the gray and white Taiwan swamp buffaloes. In the study,



the white Taiwan swamp buffaloes could adapt to the sunshine environment and had black eyes and brown to gray skin. In addition, the results showed that melanin could be observed in the skin and hair of the white Taiwan swamp buffaloes. As a result, it was inferred that the white Taiwan swamp buffalo had the ability to produce melanin and was not albinism.

In addition, it was found that the sequences of the three coat color genes, *MC1R*, *KIT* (exon 11-18) and *KITLG* (exon 2-9), of gray and white Taiwan swamp buffaloes were completely identical, and no genetic variation was found (Chuang, 2007). In the analysis of gene expression, it was found that the gene expression of *TYRP2* (*DCT*) in white Taiwan swamp buffaloes was significantly lower than that in gray Taiwan swamp buffaloes ($P < 0.05$), and there was no significant difference between *TYR* and *TYRP1* gene expression (Chuang, 2007). It was indicated that the expression of the *TYR* family genes might affect the synthesis of melanin and thus led to the white coat color of Taiwan swamp buffalo. However, the exact gene regulation mechanism of the white coat color of Taiwan swamp buffalo was not fully clarified.

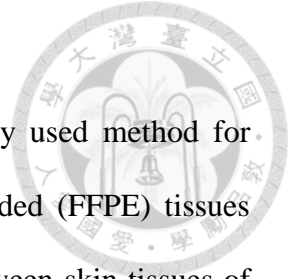
1.6 Histological analysis of the buffalo skin

Mohammed et al. (2022) identify histological features of the skin of various animals including buffalo, cow, camel, sheep, goat, dog, and donkey. The skin specimens were collected from the neck region and stained with hematoxylin and eosin (H&E), Periodic acid-Schiff (PAS), Alcian blue, and Crossman's trichrome stain. It was indicated that the epidermis layer of the buffalo skin was very thick, and the papillomatous epidermis was very frequent in buffalo. Ibrahim and Hussin (2018) made a histological comparison between the skin (muzzle, neck, thorax, dorsum, abdomen, and perineum) of buffaloes and cows. The samples were stained by H&E stain, PAS reagents, and Van Gieson stain. The results revealed that the skin of the buffalo was thicker and stronger than that of the cow in all regions of the body. There were also histological examinations by H&E stain of skin of the African buffalo infected with *Trypanosoma congolense* (Grootenhuis et al., 1990) and scrotal skin of the buffalo bull (Ahmed et al., 2023).

With the rabbit polyclonal antibody anti-TRP1 (ab83774, Abcam, Cambridge, MA), immunohistochemical staining was performed on the ear skin tissue of the gray and white swamp buffalo in the study of Liang et al. (2021). The results showed that no TYRP1 expression was found in the ear skin tissue of the white swamp buffaloes, and no melanin was observed around melanocytes in the white swamp buffaloes in H&E staining. However, using the H&E stain, it was reported that melanin could be observed in the skin of the white Taiwan swamp buffaloes (Chuang, 2007). On the other hand, with H&E stain and toluidine blue, leucoderma in the skin of river buffaloes within the Brazilian Amazon biome was observed (Barbosa et al., 2023). The results showed that there was a disruption in the presence of melanin, as well as mild dermal fibrosis,

perivasculitis, mononuclear perianexitis, and pigment incontinence.

The Fontana-Masson (FM) stain has become the most widely used method for identifying the melanin granules in formalin-fixed paraffin embedded (FFPE) tissues (Barbosa et al., 1984; Joly-Tonetti et al., 2016). The difference between skin tissues of the black and white fur sheep in China was compared by the FM stain (Shi et al., 2021). Singh et al. (2016) utilized the FM stain to observe the melanin content in the skin of healthy Indian river buffaloes and Indian river buffaloes with vitiligo. However, the FM stain has not been used to observe melanin pigments in the skin of the gray and white swamp buffalo.



1.7 Aims of this study

There were two main aims in this study. One was to analyze the population genetic structure of the Taiwan swamp buffalo in HAPS. The other was to investigate the coat color genes associated with the white coat color of the Taiwan swamp buffalo.

In order to maintain the genetic diversity of Taiwan swamp buffaloes in HAPS, estimating their population genetic structure is important. By providing information for breeding designation, this study could help improve the conservation of the Taiwan swamp buffalo. Moreover, this study would be the first study using a HD SNP genotyping array to conduct a genetic analysis of the Taiwan swamp buffalo in HAPS. What's more, by using microsatellite markers and SNP genotyping array at the same time, this study could compare two methods of estimating population genetic structure.

Although Liang et al. (2021) has discovered a potential genetic cause of the white coat color of the swamp buffalo, the exact reason for the white coat color of the Taiwan swamp buffalo remained unclear. This study could help the trait selection of the coat color of the Taiwan swamp buffalo by confirming the genes that were associated with the coat color. In addition, research on buffalo coat color genes is still limited and incomplete. Looking at the existing related literature, there are still some contradictions between the research results and some questions that need to be further clarified. As a result, the academic value of this research on the coat color gene of the Taiwan swamp buffalo should not be overlooked.

Chapter 2 Materials and Methods



2.1 Population genetic structure analysis of Taiwan swamp buffalo

2.1.1 Blood sample collection

Blood samples were collected from 94 Taiwan swamp buffaloes (78 gray Taiwan swamp buffaloes and 16 white Taiwan swamp buffaloes) in Hualien Animal Propagation Station (HAPS). The samples were collected by the veterinarians at the farm when conducting health checks for the Taiwan swamp buffaloes. The blood sample was collected from the tail veins of the buffaloes and was collected into a 10 mL tube containing K₂EDTA (BD biosciences, Franklin Lakes, NJ, USA) to prevent clot formation. The animal experiments involved in this study, the use, feeding and test content of the animals were carried out in accordance with the test guidelines approved by the Institutional Animal Care and Use Committee (IACUC) of Hualien Animal Propagation Station. The approval number of the IACUC was HUA IACUC10603.

2.1.2 Genomic DNA (gDNA) isolation

Whole blood sample (300 µL) was added into a 1.5 mL microcentrifuge tube, and then 900 µL of 1X RBC lysis buffer (Genepure Tech. Co., LTD., Taichung, Taiwan) was added into the tube. After mixing thoroughly, the sample was incubated for 10 minutes at room temperature. Next, the sample was centrifuged at 11,000 × g for 30 seconds with a centrifuge (Labnet PRISM microcentrifuge, Edison, NJ, USA). The supernatant was discarded, and the white blood cell was remained. The tube was tapped to break up

the precipitate. 1X RBC lysis buffer (900 μ L) (Genepure Tech. Co., LTD., Taichung, Taiwan) was added into the tube. The sample was mixed well and then incubated for 10 minutes at room temperature. After centrifuging the sample at $11,000 \times g$ for 30 seconds, the supernatant was removed, and the white blood cell was remained. The tube was tapped to break up the precipitate. Genomic DNA Isolation Reagent (1 mL) (Genepure Tech. Co., LTD, Taichung, Taiwan) was added, and the sample was mixed slowly with a pipette.

After incubating the sample for 15 minutes at room temperature, 500 μ L of chloroform (Sigma-Aldrich Co., St. Louis, MO, USA) was added. The tube was inverted several times to gently mix the sample, and the sample was incubated for 20 minutes at room temperature. After centrifuged at $11,000 \times g$ for 15 minutes, the supernatant was transferred into a new 1.5 mL microcentrifuge tube, and the steps mentioned above were repeated. Chloroform (500 μ L) (Sigma-Aldrich Co., St. Louis, MO, USA) was added, the tube was slowly inverted several times, the sample was incubated for 10 minutes at room temperature, the sample was centrifuged at $11,000 \times g$ for 15 minutes, and the supernatant was transferred into a new 1.5 mL microcentrifuge tube.

Next, cold isopropanol (Sigma-Aldrich Co., St. Louis, MO, USA) was added at a volume of 0.7 times that of the supernatant. The tube was inverted several times to mix well until white filaments appeared. After centrifuging the sample at $11,000 \times g$ for 20 seconds, the supernatant was removed. The DNA pellet was washed with 1 mL of 75% ethanol, and the tube was inverted several times. The ethanol was discarded, and the DNA pellet was remained. The washing step was repeated once again. After the remaining ethanol was removed, the pellet was dried with the tube inverted at room

temperature for about 3 hours.

The air-dried gDNA pellet was resuspended in about 50 μL of distilled water (ddH₂O). The DNA sample was incubated at room temperature overnight until it dissolved thoroughly. The DNA solution (1.0 μL) was used to evaluate DNA quality and quantity with NanoDrop® ND-1000 (Thermo Fisher Scientific, Waltham, MD, USA) by detecting the absorbance at 230, 260, and 280 nm. The 260/280 ratio should be about 2.0 and the 260/230 ratio should be in the range of 1.8-2.2 to ensure the purity for DNA (Desjardins and Conklin, 2010). The DNA samples were stored at 4°C or -20°C for downstream applications.

2.1.3 Microsatellite markers analysis

2.1.3.1 Selection of microsatellite markers

Microsatellite markers were selected based on previous literature using microsatellite markers to estimate genetic information of Indian river buffaloes (Tantia et al., 2006), African buffaloes and cattle (Greyling et al., 2008), river and swamp buffaloes in China (Zhang et al., 2008b), and river buffaloes in Pakistan (Hussain et al., 2017). Fifteen microsatellite markers (loci) with similar ligation temperature were selected, and their product fragment sizes were suitable for designing a multiplex PCR system. According to the product fragment sizes recorded in the literature, the microsatellite markers with non-overlapping sizes were classified into the same group and marked with different fluorescent lights. The 15 microsatellite markers were divided into four multiplex PCR systems as follows. Group I: *ILSTS058*, *INRA128*, and *CSSM022*; Group II: *INRA005*, *ILSTS059*, *ETH152*, and *BM1818*; Group III: *ILSTS033*,

ILSTS029, *BM1824*, and *ETH10*; Group IV: *CSSM061*, *CSSM046*, *CSSM008*, and *TGLA159* (Table 2).

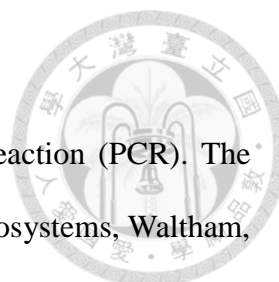
CSSM022, *ILSTS033*, *CSSM061*, *CSSM046*, and *CSSM008* were Food and Agriculture Organization (FAO, 2011) recommended buffalo microsatellite markers; *INRA005*, *ETH152*, *BM1818*, *BM1824*, and *ETH10* were FAO recommended cattle microsatellite markers (FAO, 2011). The repeated motifs, primer sequences, expected product fragment sizes, and multiplex system grouping of the 15 microsatellite markers were shown in Table 2.

Table 2. The motifs, primer sequences, expected fragment sizes, and multiplex ID of the 15 microsatellite markers used in this study

Locus	Motif	Primer sequence (5' → 3')*	Expected fragment size (bp)	Multiplex ID
<i>ILSTS058</i> ³	GT	F: GCCTTACTACCATTTCCAGC R: CATCCTGACTTTGGCTGTGG	122-152	I
<i>INRA128</i> ¹	GT	F: TAAGCACCGCACAGCAGATGC R: AGACTAGTCAGGCTTCCTAC	166-182	I
<i>CSSM022</i> ^{4,5}	CA	F: TCTCTCTAATGGAGTTGGTTTTTG R: ATATCCCACTGAGGATAAGAATTC	203-213	I
<i>INRA005</i> ^{2,5}	CA	F: TTCAGGCATACCCTACACCACATG R: AAATATTAGCCAACCTGAAAACCTGGG	110-149	II
<i>ILSTS059</i> ³	GT	F: AGTATGGTAAGGCCAAAGGG R: CGACTTGTGTTGTTCAAAGC	154-176	II
<i>ETH152</i> ^{3,5}	CA	F: ACTCGTAGGGCAGGCTGCCTG R: GAGACCTCAGGGTTGGTGATCAG	181-216	II
<i>BM1818</i> ^{3,5}	TG	F: AGCTGGGAATATAACCAAAGG R: AGTGCTTTCAAGGTCATGC	248-278	II
<i>ILSTS033</i> ^{2,4,5}	CA	F: TATTAGAGTGGCTCAGTGCC R: ATGCAGACAGTTTTAGAGGG	126-172	III
<i>ILSTS029</i> ^{2,3}	AC	F: TGTTTTGATGGAACACAGCC R: TGGATTTAGACCAGGGTTGG	138-168	III
<i>BM1824</i> ^{1,5}	TG	F: GAGCAAGGTGTTTTTCCAATC R: CATTCTCCAACCTGCTTCCTTG	169-199	III
<i>ETH10</i> ^{1,5}	AC	F: GTTCAGGACTGGCCCTGCTAACA R: CCTCCAGCCCCTTTCTCTTCTC	207-231	III
<i>CSSM061</i> ^{4,5}	-	F: AGGCCATATAGGAGGCAAGCTTAC R: TTCAGAAGAGGGCAGAGAATACAC	100-126	IV
<i>CSSM046</i> ^{4,5}	AC	F: GGCTATTAAGTGTCTTAGGAAT R: TGCACAATCGGAACCTAGAATATT	152-160	IV
<i>CSSM008</i> ^{3,4,5}	TG	F: CTTGGTGTACTAGCCCTGGG R: GATATATTTGCCAGAGATTCTGCA	179-196	IV
<i>TGLA159</i> ¹	TG	F: GCATCCAGGGAACAAATTACAAAC R: TTTATTTCTGAATCTCTTGAGTACAG	208-242	IV

*F: forward primer; R: reverse primer.

¹Greyling et al. (2008). ²Hussain et al. (2017). ³Tantia et al. (2006). ⁴Zhang et al. (2008b). ⁵FAO (2011).



2.1.3.2 Amplification of microsatellite markers

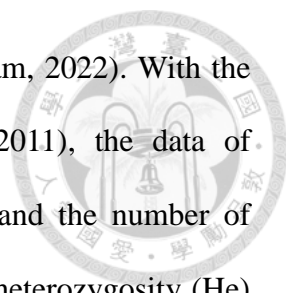
Microsatellite markers were amplified by polymerase chain reaction (PCR). The PCR was performed on Veriti® 96-well Thermal Cycler (Applied Biosystems, Waltham, Massachusetts, USA) using reaction mixture of 15 μ L containing 50-100 ng of gDNA, 2 μ M forward primer, 2 μ M reverse primer, 2 μ M CAGtag, 10x PCR buffer, 0.25 mM MgCl₂, 0.2 mM dNTP, ddH₂O, and 0.025 U *Taq* DNA polymerase (final concentrations). PCR conditions were: 95°C for 5 minutes followed by 35 cycles of 95°C for 30 seconds, 57°C for 40 seconds, and 72°C for 50 seconds, and the final extension for 10 minutes at 72°C. Electrophoresis in 1.5% agarose gel was used to make sure that PCR products were well amplified. The gel was stained in ethidium bromide for 15 minutes, soaked in ddH₂O for 15 minutes, and then the bands on the gel were visualized upon illumination with UV light.

2.1.3.3 Genotyping of microsatellite markers

Highly deionized (Hi-Di) formamide (Applied Biosystems, CA, USA) and 600 Liz size standard (GeneScan Size Standard GeneScan-600 LIZ) (Applied Biosystems, Foster City, CA, USA) were mixed at a ratio of 120:1. The mixture (10 μ L) was added to a 96-well sample plate, and then the diluted (30 to 40X) PCR product (1 μ L) was added in the mixture. The separation and detection of amplicons of different sizes were done by the ABI 3730 DNA Analyzer (Applied Biosystems, Foster City, CA, USA). The allele size determination in comparison with size standard was performed by Peak Scanner software 1.0 (Applied Biosystems, Halle, Belgium).

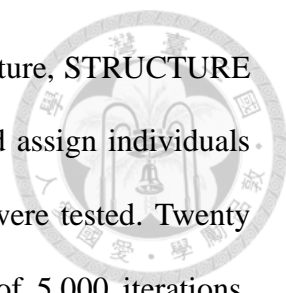
2.1.3.4 Statistical analysis

The statistical analysis of the 15 microsatellite markers was performed using R



4.1.3 (R Core Team, 2022) and RStudio 2022.2.0.443 (RStudio Team, 2022). With the *adegenet* package 2.1.8 (Jombart, 2008; Jombart and Ahmed, 2011), the data of microsatellite genotypes was exported into “genind” file format, and the number of observed alleles (N_a), observed heterozygosity (H_o), and expected heterozygosity (H_e) were calculated using the “df2genind” function. Next, the H_e values were used to calculate the number of effective alleles (N_e). After calculating gene frequency with the “makefreq” function in the *adegenet* package 2.1.8 (Jombart, 2008; Jombart and Ahmed, 2011), polymorphic information content (PIC) was calculated using the “PIC” function in the *polysat* package 1.7-7 (Clark and Jasieniuk, 2011; Clark and Schreier, 2017). The Wright’s inbreeding coefficient (F_{IS}) was calculated using the “basic.stats” function in the *hierfstat* package 0.5-11 (Goudet, 2005). The Hardy-Weinberg equilibrium (HWE) test was performed with the “hw.test” function in the *pegas* package 1.1 (Paradis, 2010). Finally, the null allele frequency was calculated using the “null.all” function in the *PopGenReport* package 3.0.7 (Adamack and Gruber, 2014; Gruber and Adamack, 2015), and the results from “summary1” using the formula proposed by Chakraborty et al. (1994) was adopted.

The “about” function in the *poppr* package 2.9.3 (Kamvar et al., 2014; Kamvar et al., 2015) was used to calculate Nei's genetic distance (Nei, 1972; 1978) and construct a neighbor-joining (NJ) (Saitou and Nei, 1987) tree with a bootstrap (Felsenstein, 1985) test of 1,000 replicates. The numbers indicating the percentage bootstrap values were represented on the nodes of the neighbor-joining (rectangular layout). In addition, the “as.treedata” function in the *treeio* package 1.16.2 (Wang et al., 2019) was used to convert the tree object to “treedata” object, and the *ggtree* package 3.0.4 (Yu et al., 2017; 2018; Yu, 2020) was used to draw another tree layout with the “daylight” method.

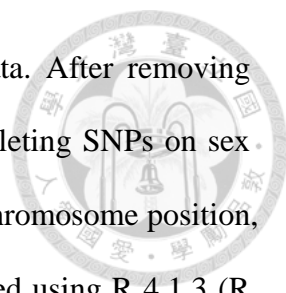


To investigate the population structure and the degree of admixture, STRUCTURE 2.3.4 software (Pritchard et al., 2000) was used. The program could assign individuals into pre-defined K clusters. Clusters (K) ranging from two to six were tested. Twenty replicate runs were calculated for each K with a burn-in period of 5,000 iterations, followed by 50,000 iterations of the Markov chain Monte Carlo (MCMC) algorithm. STRUCTURE HARVESTER 0.6.94 (Earl and vonHoldt, 2012) was used to determine the most likely cluster number (K), the number of genetic groups that best fit the data. CLUMPAK (Kopelman et al., 2015) was used to align the 20 repetitions and generate a master cluster of each K. Finally, the results were visualized with STRUCTURE PLOT V2.0 (Ramasamy et al., 2014).

2.1.4 HD SNP genotyping array analysis

2.1.4.1 Selection and data quality control of HD SNP genotyping array

The samples in this study were genotyped using the Axiom® Buffalo Genotyping Array (90K Affymetrix; Thermo Fisher Scientific, Wilmington, DE) (Iamartino et al., 2017), which provided about 90,000 common and rare markers. This array was the only commercially available high-density buffalo genotyping tool. The genome of one Mediterranean female buffalo was assembled at >100x genome sequence coverage. Sequence contigs and paired-end reads were aligned from 86 other buffaloes representing eight breeds (Italian Mediterranean, Murrah, NiliRavi, Jaffarabadi, Kundhi, Aza-Kheli, Egyptiana, and Swamp type from Philippines) and two subspecies, including river and swamp types. Iamartino et al. (2017) indicated that there were sufficient polymorphic loci (about 24K) in this array to explore the diversity of the swamp buffalo, but creation of a revised SNP set specific for the swamp buffalo was advised.



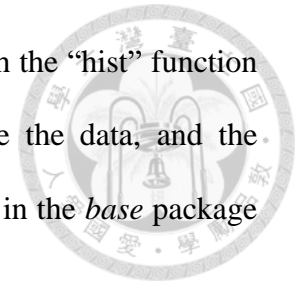
There were 75,079 SNPs with call rate >97% in the raw data. After removing monomorphic SNPs, there were 21,296 SNPs remained. Further deleting SNPs on sex chromosomes to avoid the effect of gender and SNPs on unknown chromosome position, there were 19,201 SNPs left. The quality of the data set was checked using R 4.1.3 (R Core Team, 2022) and RStudio 2022.2.0.443 (RStudio Team, 2022). The “new” function of the *adegenet* package 2.1.8 (Jombart, 2008; Jombart and Ahmed, 2011) was used to convert the raw data to a “genlight” object. With *dartR* package 2.0.4 (Gruber et al., 2018), the “gl.report.callrate” function was used to confirm individual call rate >96%, the “gl.filter.maf” function was used to delete SNPs with minor allele frequency <0.05, and the “gl.filter.hwe” function was used to remove SNPs that significantly deviated from Hardy-Weinberg equilibrium ($P < 10^{-6}$). At last, there were 14,456 SNPs remained for further analysis.

The annotation of the SNPs in this array was based on the genome assembly UOA_WB_1, which was for the Mediterranean river buffalo. As a result, it should be noticed that the actual chromosomal position of the SNPs in this array in the Taiwan swamp buffalo should be different. The chromosomal difference between river and swamp buffalo could be referred to Figure 1.

2.1.4.2 Statistical analysis

The statistical analysis of the 14,456 SNPs detected from the HD SNP genotyping array was performed using R 4.1.3 (R Core Team, 2022) and RStudio 2022.2.0.443 (RStudio Team, 2022). With the *dartR* package 2.0.4 (Gruber et al., 2018), H_o , H_e , and F_{IS} were calculated using the “gl.He” function, the “gl.Ho” function, and the “gl.basic.stats” function, respectively. Next, the H_e values were used to calculate N_e . PIC was adopted from the information automatically calculated in the “genlight” file

(`genlight@other$loc.metrics$AvgPIC`). Histograms were drawn with the “`hist`” function in the *graphics* package 4.2.2 (R Core Team, 2022) to visualize the data, and the descriptive statistics were performed using the “`summary`” function in the *base* package 4.2.2 (R Core Team, 2022).



The “`gl2gi`” function in *dartR* package 2.0.4 (Gruber et al., 2018) was used to convert a “`genlight`” object to “`genind`” object. The “`about`” function in the *poppr* package 2.9.3 (Kamvar et al., 2014; 2015) was used to calculate Nei's genetic distance (Nei, 1972; 1978) and construct a NJ (Saitou and Nei, 1987) tree with a bootstrap (Felsenstein, 1985) test of 1,000 replicates. In addition, the “`as.treedata`” function in the *treeio* package 1.16.2 (Wang et al., 2019) was used to convert a tree object to “`treedata`” object, and the *ggtree* package 3.0.4 (Yu et al., 2017; 2018; Yu, 2020) was used to draw another tree layout with the daylight method.

To investigate the population structure and the degree of admixture, fastSTRUCTURE 1.0 software (Raj et al., 2014) designed for large SNP datasets was used. Clusters (K) ranging from two to six were tested. It was run with the default convergence criterion of 10^{-6} , a logistic prior, and 20 of test sets for cross-validation. The built-in “`chooseK.py`” function was used to determine the most likely cluster number (K), and K ranging from two to eight were tested. Finally, the results were visualized with STRUCTURE PLOT V2.0 (Ramasamy et al., 2014).

2.2 Coat color gene analysis of Taiwan swamp buffalo

2.2.1 Genome-wide association study (GWAS)

The GWAS was performed on 78 gray and 16 white Taiwan swamp buffaloes in HAPS using the 14,456 SNPs from the 90K Axiom® Buffalo Genotyping Array after quality control mentioned in (2.1.4.1) to investigate SNPs associated with buffalo coat color. With the parameter “--fisher” in PLINK 1.9 (Purcell et al., 2007), a standard case/control association analysis using Fisher's exact test to generate significance was performed. The parameter “--r2” in PLINK 1.9 (Purcell et al., 2007) was used to measure the pairwise linkage disequilibrium (LD) for multiple SNPs (genome-wide). The Manhattan Plot was drawn by *qqman* R package 0.1.8 (Turner, 2014; 2018).

2.2.2 *ASIP* genotyping

Liang et al. (2021) pointed out that the *LINE-1* insertion in the *ASIP* gene of white swamp buffalo may be the cause of the white coat color. According to Liang et al. (2021), two pairs of primers (Table 3) were designed based on the assembled white buffalo-specific *ASIP* sequence to detect *LINE-1* insertion. Five gray Taiwan swamp buffaloes and 15 white Taiwan swamp buffaloes from Hualien Animal Propagation Station were genotyped. PCR, electrophoresis and Sanger sequencing were performed.

The PCR was performed on Veriti® 96-well Thermal Cycler (Applied Biosystems, Waltham, Massachusetts, USA). It was set up in a final volume of 25 µL containing 12.5 µL of 2x Phanta Max Master Mix (Vazyme Biotech, Nanjing, China), 9.5 µL of ddH₂O, 5 pmol of each primer (forward and reverse primers in Table 3), and 50-100 ng of gDNA. PCR conditions were: 94°C for 5 minutes followed by 35 cycles of 94°C for

30 seconds, 60°C for 1 minute, and 72°C for 1 minute, and the final extension for 7 minutes at 72°C. Electrophoresis in 1.5% agarose gel was used to visualize the PCR products. The gel was stained in ethidium bromide for 15 minutes, soaked in ddH₂O for 15 minutes, and then the bands on the gel were visualized upon illumination with UV light.

The PCR products were also analyzed by Sanger sequencing (Sanger and Coulson, 1975; Crossley et al., 2020). The sequencing results were analyzed by Chromas 2.6.6 software (Technelysium Pty Ltd, South Brisbane, QLD, Australia).

Table 3. Primers designed for genotyping of the *LINE-1* insertion in the *ASIP* gene and for the *MC1R* gene sequencing of the Taiwan swamp buffalo

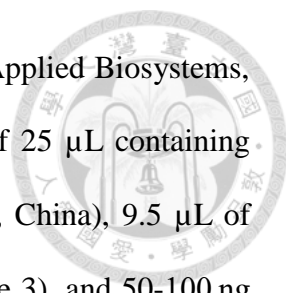
Primer pair	Primer sequence (5' → 3')*	Product size (bp)
<i>LINE-1</i> (Wild)	F: TCGGAAACGACTAAAGTGAC R: CTCCAAAGATGATGTACTAATGAACAAT	296
<i>LINE-1</i> (Mutation)	F: TTGTGGAATTTACTCGACGTT R: AAAGATTACCCACAGAAGGA	387
<i>MC1R</i> ¹	F: CTGAGAGCAAGCACCCCTTTC R: AGGCACAGCAGTACGACCTT	592
<i>MC1R</i> ²	F: ACCAGCCTGCTCTTCATCAC R: CCTCTTTGTCAAGGGACTGC	474

*F: forward primer; R: reverse primer.

¹*MC1R1*: the first fragment of *melanocortin 1 receptor* exon 1. ²*MC1R2*: the second fragment of *melanocortin 1 receptor* exon 1.

2.2.3 *MC1R* sequencing

According to da Cruz et al. (2020), two pairs of primers (Table 3) were designed to amplify the two overlapping fragments of the *MC1R* gene exon 1 in buffaloes by PCR. Twenty-seven gray Taiwan swamp buffaloes and 15 white Taiwan swamp buffaloes from HPAS were sequenced.



The PCR was performed on Veriti® 96-well Thermal Cycler (Applied Biosystems, Waltham, Massachusetts, USA). It was set up in a final volume of 25 μ L containing 12.5 μ L of 2x Phanta Max Master Mix (Vazyme Biotech, Nanjing, China), 9.5 μ L of ddH₂O, 5 pmol of each primer (forward and reverse primers in Table 3), and 50-100 ng of gDNA or cDNA. PCR conditions were: 94°C for 5 minutes followed by 35 cycles of 94°C for 30 seconds, 60°C for 1 minute, and 72°C for 1 minute, and the final extension for 7 minutes at 72°C. Electrophoresis in 1.5% agarose gel was used to visualize the PCR products. The gel was stained in ethidium bromide for 15 minutes, soaked in ddH₂O for 15 minutes, and then the bands on the gel were visualized upon illumination with UV light.

The PCR products were then analyzed by Sanger sequencing (Sanger and Coulson, 1975; Crossley et al., 2020). The first fragment was sequenced for the forward primer, and the second fragment was sequenced for the reverse primer. The sequencing results were analyzed by MultAlin software (Corpet, 1988), Chromas 2.6.6 software (Technelysium Pty Ltd, South Brisbane, QLD, Australia), and EMBOSS Needle pairwise sequence alignment tool (Madeira et al., 2022). The Chi-square test (χ^2) comparing genotype distribution and the Fisher's exact test comparing allele frequency between gray and white Taiwan swamp buffaloes were performed by R 4.1.3 (R Core Team, 2022), RStudio 2022.2.0.443 (RStudio Team, 2022), and Microsoft Office Excel 2019 (Microsoft Corporation, 2019).

2.2.4 TaqMan™ SNP Genotyping Assay

To verify the association between the *MC1R* c.901C>T and buffalo coat color and to genotype more samples efficiently, a custom TaqMan™ SNP Genotyping Assay was

designed to genotype buffalo *MC1R* c.901C>T using real-time PCR (quantitative PCR, qPCR). One hundred and fifteen gray Taiwan swamp buffaloes and 18 white Taiwan swamp buffaloes from Hualien Animal Propagation Station were genotyped.

The qPCR was performed on StepOnePlus™ Real-Time PCR System (Applied Biosystems, Foster City, California, USA). It was set up in a total volume of 15 µL containing 7.5 µL of KAPA PROBE FAST qPCR Master Mix (2x) ABI Prism® (Kapa Biosystems Ltd., London, UK), 6.125 µL of ddH₂O, 0.375 µL of primer probe mix (40x custom TaqMan™ SNP Genotyping Assay), and 50-100 ng of gDNA. PCR conditions were: 60°C for 30 seconds, 95°C for 10 minutes followed by 40 cycles of 95°C for 15 seconds, 60°C for 1 minute.

The results were analyzed by StepOne Software 2.3 (Applied Biosystems, Foster City, CA, USA). The Chi-square test (χ^2) comparing genotype distribution and the Fisher's exact test comparing allele frequency between gray and white Taiwan swamp buffaloes were performed by R 4.1.3 (R Core Team, 2022), RStudio 2022.2.0.443 (RStudio Team, 2022), and Microsoft Office Excel 2019 (Microsoft Corporation, 2019).

2.2.5 Amino acid substitution and protein function prediction

EMBOSS Transeq (Rice et al., 2000; Goujon et al., 2010) was used to predict the amino acid substitution *MC1R* c.901C>T might cause. PredictSNP (Bendl et al., 2014) was used to predict the potential effect of the amino acid substitution on MC1R protein structure or function.

2.2.6 Relative gene expression analysis

The skin tissue used for relative gene expression analysis was as follows. The ear,

abdomen, and back skin samples (Figure 5) were collected from one adult (10 years old) white Taiwan swamp buffalo (Figure 6) from HAPS when it was slaughtered. On the other hand, the ear skin samples (Figure 7) were collected from two gray (brown) Taiwan swamp buffalo calves (three weeks old) and one white Taiwan swamp buffalo calf (three weeks old) (Figure 8) in HAPS when they were earmarked.



Figure 5. The skin and the hair of the adult (10 years old) white Taiwan swamp buffalo from HAPS. (A) The ventral side ear, (B) the dorsal side ear, (C) the back, and (D) the abdomen skin tissue of the adult white Taiwan swamp buffalo from HAPS analyzed in this study.



Figure 6. The adult (10 years old) white Taiwan swamp buffalo from HAPS analyzed in this study. The photo was taken by courtesy of Pi-Hua Chuang, the director of HAPS.

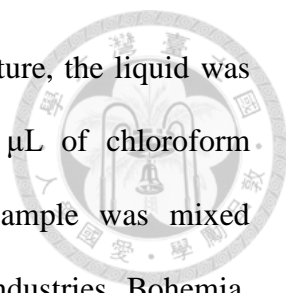


Figure 7. The ear skin tissue of the gray (brown) and white Taiwan swamp buffalo calves (three weeks old) from HAPS. (A) The ventral side ear of a gray (brown) calf, (B) the dorsal side ear of a gray (brown) calf, (C) the ventral side ear of a white calf, and (D) the dorsal side ear of a white calf from HAPS analyzed in this study.



Figure 8. The two gray (brown) Taiwan swamp buffalo calves (the left and the right ones) and one white Taiwan swamp buffalo calf (the middle one) from HAPS analyzed in this study. The calves were all three weeks old.

For the skin tissue collected mentioned above, skin hairs were shaved and fatty tissue was trimmed. The dorsal side and the ventral side of the ear skin were separated. All the skin samples were cut into small pieces and immediately placed in liquid nitrogen. Every skin sample was pulverized in liquid nitrogen using mortar and pestle, and it was transferred into a 1.5 mL microcentrifuge tube with 1 mL GENEzol™ reagent (Geneaid Biotech Ltd., New Taipei City, Taiwan) to isolate the total



RNA. After incubating the sample for 10 minutes at room temperature, the liquid was transferred to a new 1.5 mL microcentrifuge tube. Then, 200 μL of chloroform (Sigma-Aldrich Co., St. Louis, MO, USA) was added. The sample was mixed vigorously for 10 seconds by Vortex-Genie® 2 mixer (Scientific Industries, Bohemia, NY, USA) and then centrifuged at $14,000 \times g$ for 15 minutes at 4°C with a High-Speed Microcentrifuge (ScanSpeed 1730MR, Labogene, Denmark). The supernatant was transferred into a new 1.5 mL microcentrifuge tube. Next, one volume of isopropanol (Sigma-Aldrich Co., St. Louis, MO, USA) to the supernatant was added, and the tube was inverted several times to mix well. After incubating the sample for 10 minutes at room temperature, the sample was centrifuged at $14,000 \times g$ for 15 minutes at 4°C . The supernatant was removed, the RNA pellet was washed with 1 mL of 75% ethanol, and the tube was inverted several times. The washing step was repeated once again: the sample was centrifuged at $14,000 \times g$ for 5 minutes at 4°C , the supernatant was discarded, the RNA pellet was washed with 1 mL of 75% ethanol, and the tube was inverted several times. After centrifuging the sample at $14,000 \times g$ for 5 minutes at 4°C , the supernatant was removed carefully using a pipette, and the RNA pellet was dried with the tube inverted at room temperature for 5-10 minutes.

The air-dried RNA pellet was resuspended in 20 μL of DEPC H_2O . The sample was incubated at 57°C for 10 minutes to dissolve the RNA pellet. The RNA solution (1.0 μL) was used to evaluate RNA purity and concentration by NanoDrop® ND-1000 (Thermo Fisher Scientific, Waltham, MD, USA). RNA integrity was assessed by 1.0% agarose gel electrophoresis. The gel was stained in ethidium bromide for 15 minutes, soaked in dd H_2O for 15 minutes, and then the bands on the gel were visualized upon

illumination with UV light. The RNA samples were stored at -80°C for subsequent applications.

Reverse transcription was done using the High Capacity cDNA Reverse Transcription Kit with RNase Inhibitor (product number: 4374966) (Applied Biosystems, CA, USA) according to the manufacturer's instructions. The 2X RT master mix was prepared in a total volume of $10\ \mu\text{L}$ containing $2\ \mu\text{L}$ of 10X RT Buffer, $0.8\ \mu\text{L}$ of 25X dNTP Mix (100 mM), $2\ \mu\text{L}$ of 10X RT Random Primers, $1\ \mu\text{L}$ of MultiScribe™ Reverse Transcriptase, $1\ \mu\text{L}$ of RNase Inhibitor, and $3.2\ \mu\text{L}$ of DEPC H_2O . The cDNA reverse transcription reaction was set up in a final volume of $20\ \mu\text{L}$ containing $10\ \mu\text{L}$ of 2X RT master mix and $10\ \mu\text{L}$ of RNA sample. The PCR was performed on Veriti® 96-well Thermal Cycler (Applied Biosystems, Waltham, Massachusetts, USA). PCR conditions were: 25°C for 10 minutes, 37°C for 120 minutes, and 85°C for 5 minutes. The cDNA samples were stored at -20°C for subsequent applications.

Gene expression was analyzed by qPCR. The primers of the target genes (*MC1R*, *ASIP*, *MITF*, *TYR*, *TYRP1*, and *DCT*) (Table 4) were designed using NCBI Primer-BLAST online software (Ye et al., 2012). The *18S rRNA* was used as the endogenous reference gene, and the primer pairs (Table 4) were designed based on Liang et al. (2021). Primer efficiency tests were performed to ensure the qPCR primers were comparable.

Table 4. Primers designed for gene expression analysis of the *MC1R*, *ASIP*, *MITF*, *TYR*, *TYRPI*, *DCT*, and *18s rRNA* gene by qPCR in this study

Primer pair	Primer sequence (5' → 3')*	Product size (bp)
<i>MC1R</i> ^{a,1}	F: CCCTGATTTGCAGTGAAAGAGTCC R: TCACCGTCACAGGCATGAGG	198
<i>ASIP</i> ^{a,2}	F: CAAGCCCTCGGTGCCTAGAT R: TTACAAAGCATGGGCAGTGGC	151
<i>MITF</i> ^{a,3}	F: GCCTGTGTGTTTCATGCTGG R: AGGGCACGGCAACTTCATTA	180
<i>TYR</i> ^{a,4}	F: AGCAGGAGCACAGGCAAACA R: GCAGTTCCTCCATCCCAGGAC	188
<i>TYRPI</i> ^{a,5}	F: CTCCAGACAACCTGGGCTAT R: TCATAGTGGAAAGCTGTGGGT	152
<i>DCT</i> ^{a,6}	F: GGGACTGTTGGATGACTCTTGT R: GCCATCCATCTGTGGCTACT	162
<i>18s rRNA</i> ^b	F: GATGGGCGGGCGGAAAATTG R: TCCTCAACACCACATGAGCA	107

*F: forward primer; R: reverse primer.

^aYe et al. (2012) ^bLiang et al. (2021)

¹*MC1R*: melanocortin 1 receptor. ²*ASIP*: agouti signaling protein. ³*MITF*: melanocyte inducing transcription factor. ⁴*TYR*: tyrosinase. ⁵*TYRPI*: tyrosinase related protein 1. ⁶*DCT*: dopachrome tautomerase.

The qPCR was performed on StepOnePlus™ Real-Time PCR System (Applied Biosystems, Foster City, California, USA) using the PowerUp™ SYBR™ Green Master Mix Kit (Applied Biosystems, Foster City, California, USA). It was set up in a total volume of 20 µL containing 10 µL of 2X PowerUp™ SYBR™ Green Master Mix, 4.2 µL of ddH₂O, 0.4 µL of each primer (10 µM), and 5 µL of cDNA. PCR conditions were: 50°C for 2 minutes, 95°C for 10 minutes followed by 40 cycles of 95°C for 15 seconds and 60°C for 1 minute. Each qPCR analysis was performed in triplicate.

The results were analyzed by StepOne Software 2.3 (Applied Biosystems, Foster City, CA, USA). The relative gene expression levels were calculated using the 2^{-ΔΔCt} method (Livak and Schmittgen, 2001) by Microsoft Office Excel 2019 (Microsoft Corporation, 2019).

2.2.7 Histological examination and staining of the buffalo skin

The skin samples analyzed for histological examination and staining were the same as the relative gene expression analysis (2.2.6). These specimens were fixed in formalin and embedded in paraffin. The samples were then sectioned and subjected to Fontana-Masson (FM) staining using the Fontana-Masson stain Kit (ScyTek Lab., Logan, UT, USA) according to the manufacturer's instructions. The FM stain was used to detect melanin granules. The melanin was stained black, the nuclei was stained pink-red, and the cytoplasm was stained pale pink. The steps were as follows. Sections were deparaffinized and hydrated in ddH₂O. Slide was incubated in Fontana Silver Nitrate Solution at 56°C for 1 hour, and then rinsed by ddH₂O several times. Slide was toned in Gold Chloride Solution (0.2%) at room temperature for 5-10 minutes, and then rinsed by ddH₂O several times. Slide was incubated in Sodium Thiosulfate Solution (5%) at room temperature for 2 minutes, and then rinsed by ddH₂O several times. Slide was counterstained with Nuclear Fast Red Solution for 5 minutes, and then rinsed by ddH₂O for 1 minute. Lastly, slide was dehydrated, cleared and covered by a coverslip.

Chapter 3 Results



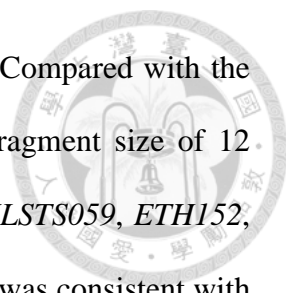
3.1 Population genetic structure analysis of Taiwan swamp buffalo

3.1.1 Microsatellite markers analysis results

3.1.1.1 Na and Ne results based on microsatellite markers

In this experiment, there were originally 132 Taiwan swamp buffaloes from HAPS analyzed by 15 microsatellite markers to estimate their population genetic structure. However, in order to compare with the results of 90K Axiom® Buffalo Genotyping Array, which is a 96-array plate, data of 94 Taiwan swamp buffaloes (78 gray and 16 white Taiwan swamp buffaloes) from HAPS which were analyzed by both the 15 microsatellite markers and 90K Axiom® Buffalo Genotyping Array was used for further analysis. The sample size of gray and white Taiwan swamp buffalo in different experiments in this study was summarized in Appendix table 1. The information including its father, mother, sex, and coat color of the 94 Taiwan swamp buffaloes analyzed in this study was in Appendix table 2.

The results showed that the marker, *ETH10*, had no polymorphism, so only the other 14 polymorphic microsatellite markers were used for further analysis in this study. The 14 microsatellite markers detected 60 alleles, and the detailed detected fragment size of all 15 microsatellite markers among 94 Taiwan swamp buffaloes was in Appendix table 3. The range of observed fragment size by the 14 microsatellite markers was listed in Table 5. Among the 14 microsatellite markers, the smallest range of observed fragment size was obtained by *CSSM061* (105-119 bp), and the largest range



of observed fragment size was obtained by *BM1818* (253-270 bp). Compared with the range of expected fragment size listed in Table 2, the observed fragment size of 12 microsatellite markers (*ILSTS058*, *INRA128*, *CSSM022*, *INRA005*, *ILSTS059*, *ETH152*, *BM1818*, *ILSTS033*, *ILSTS029*, *BM1824*, *CSSM061*, and *TGLA159*) was consistent with past literature (Tantia et al., 2006; Greyling et al., 2008; Zhang et al., 2008b; FAO, 2011; Hussain et al., 2017), and the other two microsatellite markers, *CSSM046* (Zhang et al., 2008b; FAO, 2011) and *CSSM008* (Tantia et al., 2006; Zhang et al., 2008b; FAO, 2011), detected fragments exceeding the range of the expected fragment size. The fragment detected by *CSSM046* exceeding expected fragment size was 148 bp, accounting for 48.94% of all observed fragments. The fragment detected by *CSSM008* exceeding expected fragment size was 177 bp, accounting for 33.87% of all observed fragments.

The range of the N_a among the 14 microsatellite markers was from 2 to 6. The lowest N_a was two observed by *ILSTS033* and *ILSTS029*. The highest N_a was six detected by *ILSTS058*, *INRA005* and *BM1824*. The average N_a among the 14 microsatellite markers was 4.3. The range of the N_e among the 14 microsatellite markers was from 1.214 to 4.856. The lowest N_e was 1.214 detected by *ILSTS029*. The highest N_e was 4.856 detected by *INRA005*. The average N_e among the 14 microsatellite markers was 2.620.

To avoid the effect of the null alleles on the results of the population genetic analysis, which is further explained in 3.1.1.3, the mean of the genetic parameters without two markers (*CSSM022* and *CSSM046*) were also calculated as Mean^b in Table 5. After removing the two markers, the average N_a and N_e values increased from 4.3 and 2.620 to 4.4 and 2.678, respectively.

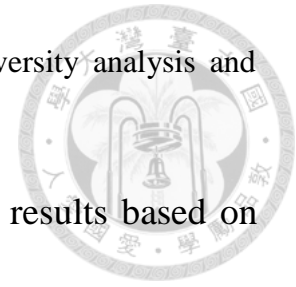
3.1.1.2 Ho, He, and PIC results based on microsatellite markers

Among the 14 microsatellite markers, the range of the Ho was from 0.160 to 0.915, and the range of the He was from 0.177 to 0.794. *INRA005* had the highest Ho (0.915) and He (0.794), while *CSSM046* had the lowest Ho (0.160), and *ILSTS029* had the lowest He (0.177). The average Ho and He among the 14 microsatellite markers were 0.525 and 0.577, respectively. The Ho of *CSSM022* (0.183), *ILSTS029* (0.196), and *CSSM046* (0.160) were less than 0.2. The Ho of *ILSTS033* was 0.456, and the other 10 microsatellite markers had Ho greater than 0.5. The He of *ILSTS029* was less than 0.2. The He of *CSSM022* and *ILSTS033* were 0.497 and 0.473, respectively, and the other 11 microsatellite markers had He greater than 0.5 (Table 5).

Among the 14 microsatellite markers, the range of the PIC was from 0.161 to 0.764. *INRA005* had the highest PIC (0.764), while *ILSTS029* had the lowest PIC (0.161). The average PIC among the 14 microsatellite markers was 0.514. The PIC of *ILSTS029* (0.161) was less than 0.25. The PIC of *INRA128* (0.434), *CSSM022* (0.423), *ILSTS033* (0.362), and *CSSM008* (0.459) were between 0.25 and 0.5. The other nine microsatellite markers had PIC greater than 0.5 (Table 5).

The average Ho (0.525), He (0.577), and PIC (0.514) obtained from the 14 microsatellite markers were all greater than 0.5, indicating that with the 14 microsatellite markers in this study, high polymorphism among the 94 Taiwan swamp buffaloes in HAPS could be detected. After removing the two markers (*CSSM022* and *CSSM046*) which might have null alleles, the average Ho, He and PIC values detected by the remaining 12 microsatellite markers increased from 0.525, 0.577, and 0.514 to 0.584, 0.581, and 0.521, respectively (Table 5). The overall genetic polymorphism of the 94 Taiwan swamp buffaloes from HAPS became higher, which indicated that the

existence of null alleles should affect the accuracy of genetic diversity analysis and decrease the values of genetic polymorphism.



3.1.1.3 F_{IS} , exact test of HWE, and null allele frequency results based on microsatellite markers

Among the 14 microsatellite markers, the range of the F_{IS} was from -0.147 to 0.740. *CSSM046* had the highest F_{IS} (0.740), while *INRA005* had the lowest F_{IS} (-0.147). The average F_{IS} among the 14 microsatellite markers was 0.092. The F_{IS} of 7 microsatellite markers were negative, while the other seven microsatellite markers had positive F_{IS} (Table 5). A positive value of F_{IS} indicates a higher proportion of homozygotes, which means a higher possibility of inbreeding (Zhang et al., 2007). Although the average F_{IS} among the 14 microsatellite markers was positive (0.092), the value was close to zero. Thus, the degree of inbreeding among the 94 Taiwan swamp buffaloes from HAPS should not be serious. Moreover, after removing the two markers (*CSSM022* and *CSSM046*) which might have null alleles, the average F_{IS} value decreased from 0.092 to -0.008. The degree of inbreeding among the 94 Taiwan swamp buffaloes from HAPS became lower, which again indicated that the existence of null alleles should decrease the genetic polymorphism in the study.

Among the 14 microsatellite markers, three microsatellite markers (*CSSM022*, *BM1824*, and *CSSM046*) were significantly deviated from Hardy-Weinberg equilibrium ($P < 0.01$) (Table 5). However, the disequilibrium due to heterozygote deficiency might be affected by the existence of the null alleles (Zhang et al., 2007; Carlsson, 2008; Berthouly et al., 2010; Wen et al., 2013). Among the three microsatellite markers that were deviated from HWE, *CSSM022* and *CSSM046* had high null allele frequency (0.462 and 0.584, respectively) and heterozygote deficiency ($H_o = 0.183$ and 0.160,

respectively). As for *BM1824*, it had low null allele frequency (0.098) and high H_o (0.617), so it was not removed for further analysis. The reason why *BM1824* was deviated from HWE might be contributed to the artificial selection in HAPS.

The average null allele frequency of the 14 microsatellite markers was 0.089. The null allele frequency of *CSSM022* (0.462) and *CSSM046* (0.584) were high. The null allele frequency of *BM1824* (0.098) and *CSSM061* (0.103) were less than 0.2. The other 10 microsatellite markers had no null allele frequency (Table 5). The average null allele frequency (0.089) of the 14 microsatellite markers was lower than 0.2, which was acceptable in the population genetic analysis (Wen et al., 2013). Nevertheless, the null allele frequency of *CSSM022* (0.462) and *CSSM046* (0.584) were higher than 0.2. These two microsatellite markers were at the same time significantly deviated from Hardy-Weinberg equilibrium ($P < 0.01$) and had heterozygote deficiency, which suggested a higher possibility of the existence of null alleles (Zhang et al., 2007; Carlsson, 2008; Berthouly et al., 2010; Wen et al., 2013). To avoid the effect of the null alleles on the results of the population genetic analysis, the mean of the genetic parameters without these two markers were calculated as Mean^b in Table 5.

Table 5. Analysis of genetic polymorphism of 94 Taiwan swamp buffaloes based on 14 microsatellite markers in this study

Locus	Observed fragment size (bp)	Na	Ne	Ho	He	PIC	F_{IS}	Null allele frequency	Exact test of HWE
<i>ILSTS058</i>	128-147	6	3.055	0.692	0.673	0.622	-0.023	0.000	NS
<i>INRA128</i>	162-171	5	2.169	0.553	0.539	0.434	-0.021	0.000	NS
<i>CSSM022</i>	203-209	4	1.986	0.183	0.497	0.423	0.635	0.462	**
<i>INRA005</i>	116-132	6	4.856	0.915	0.794	0.764	-0.147	0.000	NS
<i>ILSTS059</i>	158-164	3	2.673	0.628	0.626	0.547	0.003	0.000	NS
<i>ETH152</i>	190-215	5	2.372	0.649	0.578	0.534	-0.117	0.000	NS
<i>BM1818</i>	253-270	4	2.335	0.620	0.572	0.511	-0.078	0.000	NS
<i>ILSTS033</i>	148-150	2	1.897	0.456	0.473	0.362	0.042	0.000	NS
<i>ILSTS029</i>	155-159	2	1.214	0.196	0.177	0.161	-0.103	0.000	NS
<i>BM1824</i>	179-192	6	4.027	0.617	0.752	0.717	0.184	0.098	**
<i>CSSM061</i>	105-119	4	2.888	0.532	0.654	0.582	0.192	0.103	NS
<i>CSSM046</i>	148-154	3	2.548	0.160	0.608	0.528	0.740	0.584	**
<i>CSSM008</i>	177-187	5	2.172	0.570	0.540	0.459	-0.051	0.000	NS
<i>TGLA159</i>	222-235	5	2.481	0.585	0.597	0.558	0.025	0.000	NS
Mean ^a	-	4.3	2.620	0.525	0.577	0.514	0.092	0.089	-
Mean ^b	-	4.4	2.678	0.584	0.581	0.521	-0.008	0.017	-

Na: Number of observed alleles; Ne: Number of effective alleles; Ho: Observed heterozygosity; He: Expected heterozygosity; PIC: Polymorphic information content; F_{IS} : Wright's inbreeding coefficient; HWE: Hardy-Weinberg equilibrium, NS: not significant

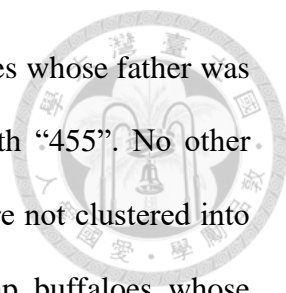
** Significant ($P < 0.01$) departure from the Hardy-Weinberg equilibrium.

Mean^a: Mean values for the 14 microsatellite markers; Mean^b: Mean values for the 12 microsatellite markers (removing *CSSM022* and *CSSM046*).

3.1.1.4 Phylogenetic tree results based on microsatellite markers

The neighbor-joining tree with a bootstrap test of 1,000 replicates of the 94 Taiwan swamp buffaloes based on 14 microsatellite markers was in Figure 9 and Figure 10. The two trees were basically the same but with different layouts. The radial form of the neighbor-joining tree was in Figure 9, and it showed a more clearly picture of the clustering of the 94 Taiwan swamp buffaloes but without bootstrap values on the nodes. Figure 10 showed the rectangular layout with numbers on the nodes indicating the percentage bootstrap values generated from 1,000 times of resampling. By labeling the fathers of the individuals with different color according to the pedigree data, the accuracy and the similarities of the phylogenetic trees drawn with different methods could be observed more clearly.

The phylogenetic tree based on 14 microsatellite markers showed that 94 Taiwan swamp buffaloes could be divided into three subpopulations by the node marked with a red circle, and the three clusters were framed by the green, blue, and red dotted-line frames (Figure 9 and Figure 10). The clustering could be observed more obviously in Figure 9. The “W” marked with red circle in the ID of the 16 white Taiwan swamp buffaloes highlighted the white buffaloes. However, the phylogenetic tree based on 14 microsatellite markers showed that not all of the 16 white Taiwan swamp buffaloes were grouped into the same subpopulation. Four white Taiwan swamp buffaloes (W644, W701, W641, and W464) were clustered into the green-framed subpopulation, while the other 12 white Taiwan swamp buffaloes were clustered into the red-framed subpopulation. According to the pedigree, the father of W644 and W641 was both “526”, but they were not clustered into the same subgroup (red-framed) with other white swamp buffaloes whose father was also “526”. Instead, W644 and W641 were clustered



into the green-framed subpopulation with other gray swamp buffaloes whose father was “300”. On the other hand, the father of W701 and W464 was both “455”. No other white swamp buffaloes’ father was “455”, but W701 and W464 were not clustered into the subgroups (red-framed and blue-framed) as other gray swamp buffaloes whose father was also “455”. Thus, the accuracy of the clustering results of these four white Taiwan swamp buffaloes (W644, W701, W641, and W464) might be questioned.

In addition, the robustness of the phylogenetic tree based on 14 microsatellite markers might be low according to the low bootstrap support (mostly below 50%) on the nodes of the tree (Figure 10). There were in total 91 bootstrap values in the tree, ranging from 0 to 92.6, and the average bootstrap value was 15.09. Low bootstrap values indicated that the grouping was unstable and no clustering was observed at a significantly high frequency. The reason might be that the individuals estimated are very closely related and there were short internal branches in the tree (Kamara et al., 2007). In addition, it was also inferred that the low bootstrap values meant that the clustering was sensitive to the combinations of genotypes that were evaluated, and when more data is included, the grouping results might alter (de Oliveira et al., 2010).

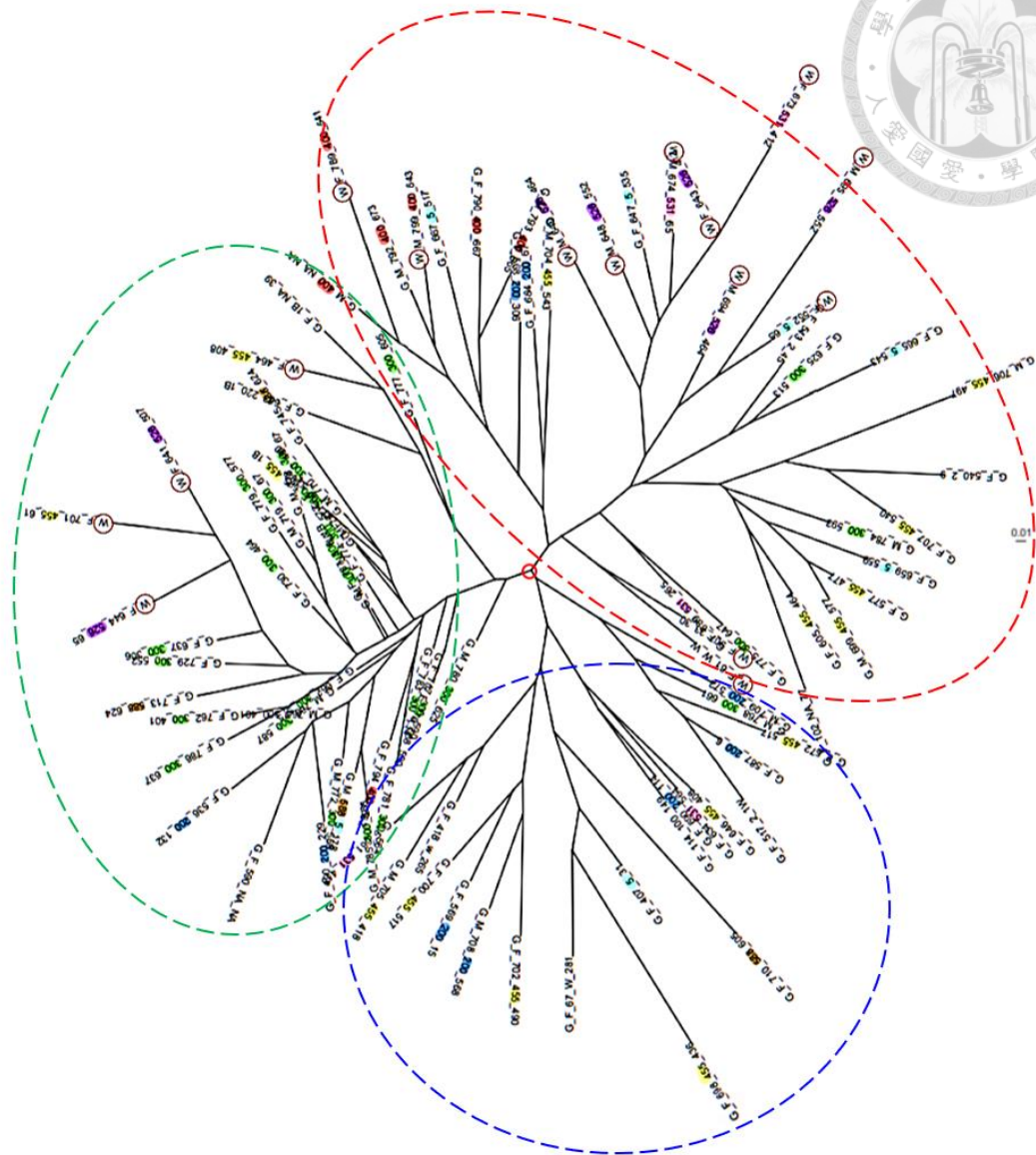
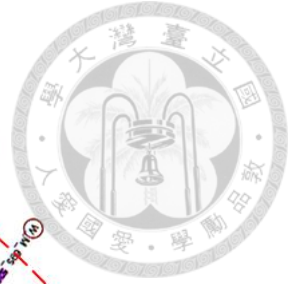


Figure 9. The neighbor-joining tree (daylight method) based on the 14 microsatellite markers for the population of the 94 Taiwan buffaloes from HAPS in this study. The labels of the 94 Taiwan buffalo individuals represent the information as follows. The first letter represents its coat color (gray: G, white: W), and the second letter represents its gender (male: M, female: F). The first number represents its ID, the second number represents its father's ID, and the last number represents its mother's ID. "NA" means that there was a lack of the record. The color on the labels corresponds to the ID of sire (red: 400, pink: 531, yellow: 455, green: 300, dark blue:200, light blue:5, purple: 526, brown:

588). “W” marked with red circle represents the white buffalo. Three subpopulations were identified by the node marked with a red circle, and the three clusters were framed by the green, blue, and red dotted-line frames. The bar at the middle right of the figure provides a scale for the length of branch that represents an amount of genetic distance of 0.01.

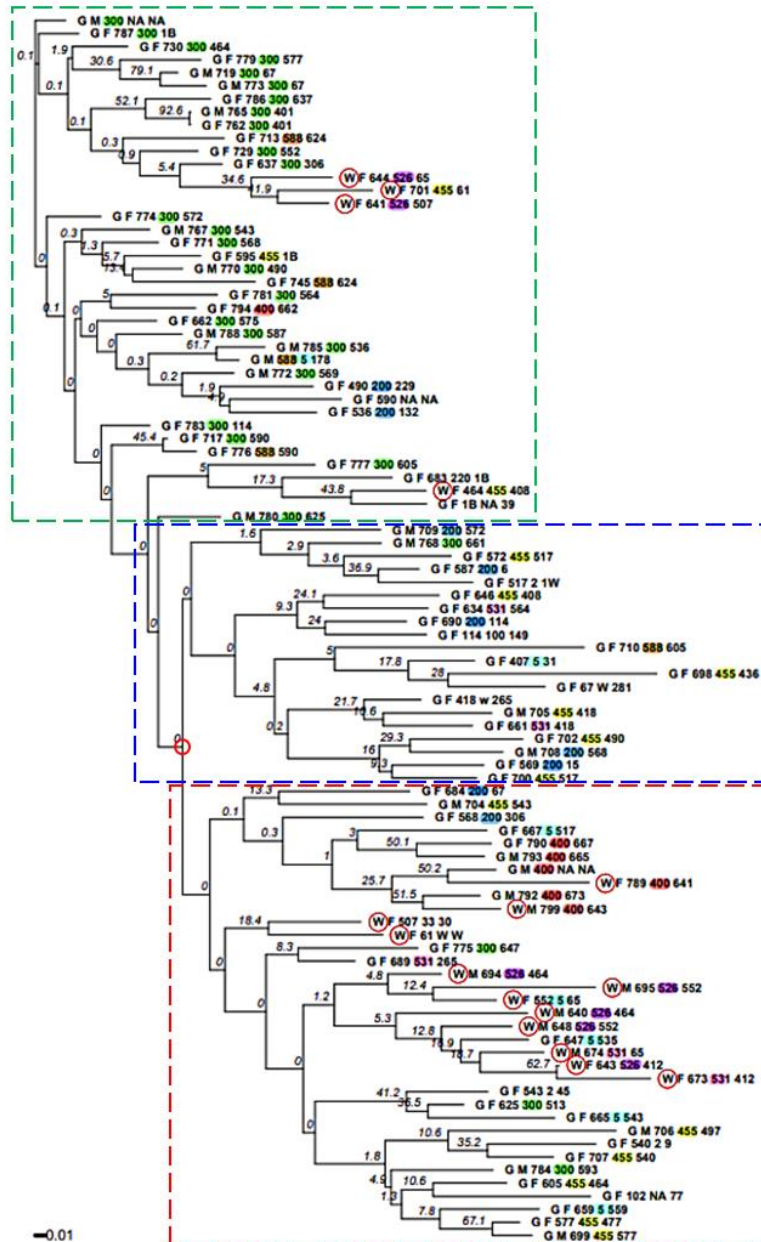
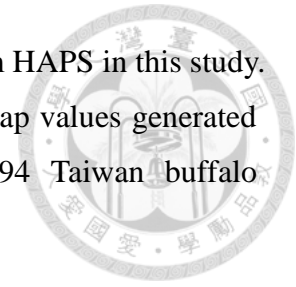


Figure 10. The neighbor-joining tree (rectangular layout) based on the 14 microsatellite

markers for the population of the 94 Taiwan buffaloes from HAPS in this study. The numbers on the nodes indicate the percentage bootstrap values generated from 1,000 times of resampling. The labels of the 94 Taiwan buffalo individuals and the footnotes were as in Figure 9.

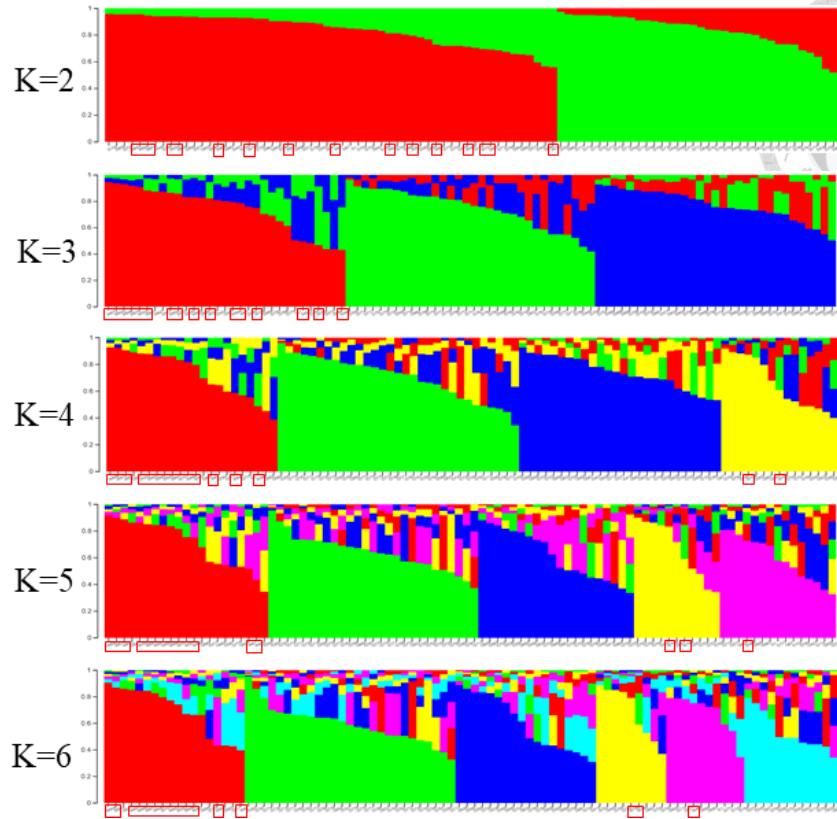


3.1.1.5 STRUCTURE results based on microsatellite markers

The plots of STRUCTURE cluster analysis ($K = 2$ to 6) based on 14 microsatellite markers were presented in Figure 11A. The results showed that when K was two or three, the 16 white swamp buffaloes were all classified into the same cluster. When K was four, two white swamp buffaloes (W789 and W799) were divided into a different cluster from other 14 white swamp buffaloes. When K was five or six, one white swamp buffalo (W464) was further assigned into a third cluster.

The results of Evanno method showed that the most optimal K value was three (Figure 11B), indicating that the 94 Taiwan swamp buffaloes could be divided into three subpopulations based on the 14 microsatellite markers. Furthermore, white swamp buffaloes were all clustered into one subpopulation, whereas other gray swamp buffaloes could be differentiated into two subpopulations.

(A)



(B)

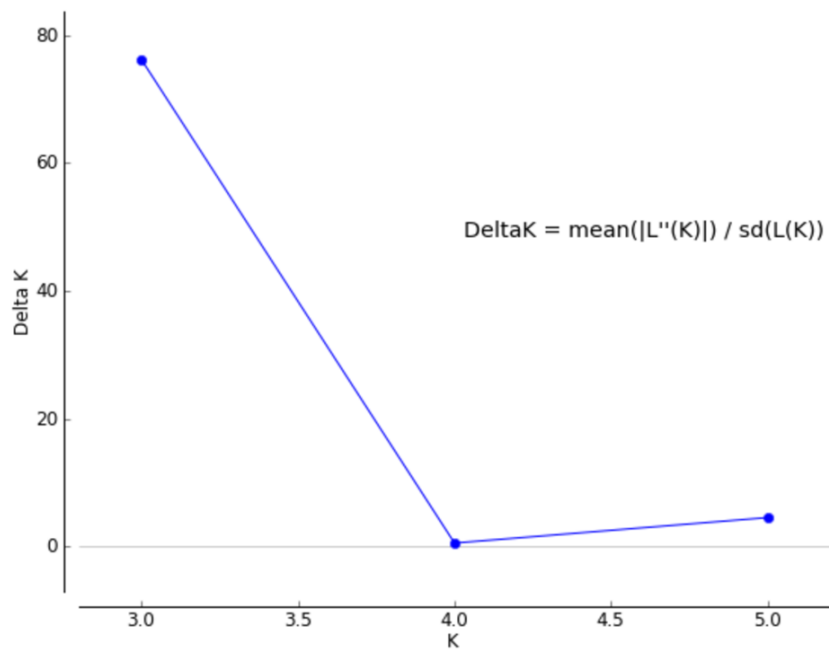


Figure 11. STRUCTURE analysis based on the 14 microsatellite markers for the population of the 94 Taiwan buffaloes from HAPS in this study. (A) The

STRUCTURE cluster analysis plot ($K = 2$ to 6). The K value ($K = 2$ to 6) is the number of clusters assumed in the analysis, and different colors correspond to different clusters. The horizontal axis shows individuals, and each bar represents one individual. The vertical axis shows the proportion of different clusters an individual stand for. The red frame indicates 16 white swamp buffaloes. (B) The ΔK values at different K values calculated by the method of Evanno. When K was three, 94 Taiwan swamp buffaloes were clearly grouped into three clusters.

3.1.2 HD SNP genotyping array analysis results

3.1.2.1 N_a and N_e results based on HD SNP genotyping array

In this experiment, 14,456 SNPs from the 90K Axiom® Buffalo Genotyping Array after quality control in 2.1.4 were used to analyze population genetic structure of the 94 Taiwan swamp buffaloes (78 gray and 16 white Taiwan swamp buffaloes) from HAPS, which were also analyzed by 15 microsatellite markers, in this study. The results showed that the SNPs all had two observed alleles ($N_a = 2$), and the average N_e was 1.616. N_e among the 14,456 SNPs ranged from 1.112 to 2.000 (Table 6). The distribution of the 14,456 SNPs for N_e was visualized in Figure 12A.

3.1.2.2 H_o , H_e , and PIC results based on HD SNP genotyping array

Among the 14,456 SNPs, the average H_o was 0.372, ranging from 0.021 to 0.691 (Table 6). H_o of 4,478 (64+1,904+2,510) (30.98%) SNPs were less than 0.3. H_o of 7,527 (2,912+4,615) (52.07%) SNPs were between 0.3 and 0.5. H_o of 2,451 (2,301+150) (16.95%) SNPs were greater than 0.5 (Figure 12B).

Among the 14,456 SNPs, the average H_e was 0.360, ranging from 0.101 to 0.500 (Table 6). H_e of 4,583 (2,164+2,419) (31.70%) SNPs were less than 0.3. H_e of 9,873

(2,966+6,907) (68.30%) SNPs were between 0.3 and 0.5 (Figure 12C).

Among the 14,456 SNPs, the average PIC was 0.282, ranging from 0.095 to 0.463 (Table 6). PIC of 4,619 (147+2,591+1,881) (31.95%) SNPs were less than 0.25. PIC of 9,837 (2,528+7,029+280) (68.05%) SNPs were between 0.25 and 0.5 (Figure 12D).

3.1.2.3 F_{IS} and exact test of HWE based on HD SNP genotyping array

Among the 14,456 SNPs, the average F_{IS} was -0.029, ranging from -0.436 to 0.791 (Table 6). F_{IS} of 9,325 (2+35+496+3,180+5,612) (64.51%) SNPs were less than or equal to zero. F_{IS} of 5,131 (3,476+1,302+265+60+19+7+2) (35.49%) SNPs were positive (Figure 12E).

Among the 14,456 SNPs, 638 (4.4%) SNPs were significantly deviated from Hardy-Weinberg equilibrium ($P < 0.05$) (Figure 12F). The average P -value of 14,456 SNPs was 0.587 (Table 6).

Table 6. Analysis of the genetic polymorphism of the 94 Taiwan swamp buffaloes from HAPS based on the 14,456 SNPs from the 90K Axiom® Buffalo Genotyping Array

	Na	Ne	Ho	He	PIC	F_{IS}	HWE test P -value
Min	2	1.112	0.021	0.101	0.095	-0.436	0.0000012
Max	2	2.000	0.691	0.500	0.462	0.791	1.000
Mean	2	1.616	0.372	0.360	0.282	-0.029	0.587

Na: Number of observed alleles; Ne: Number of effective alleles; Ho: Observed heterozygosity; He: Expected heterozygosity; PIC: Polymorphic information content; F_{IS} : Wright's inbreeding coefficient; HWE: Hardy-Weinberg equilibrium.

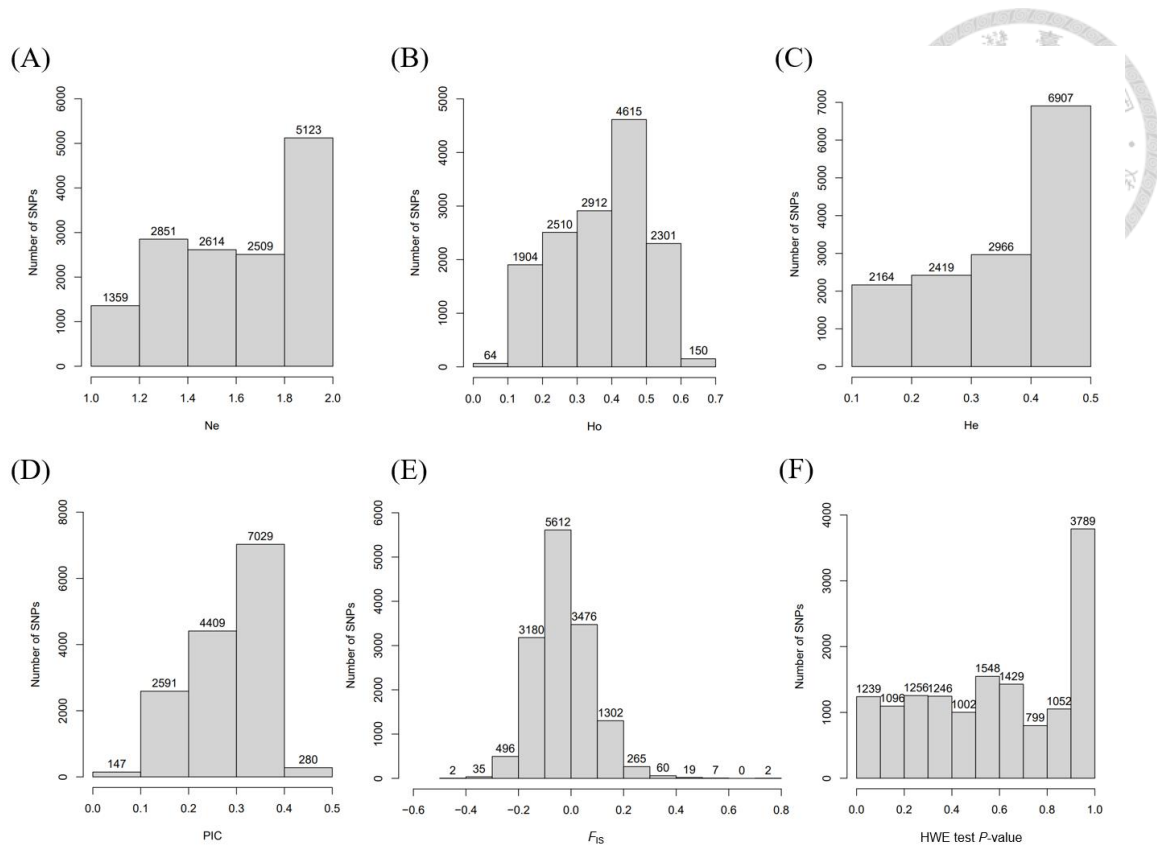


Figure 12. Distribution of the 14,456 SNPs for the genetic parameters among the 94 Taiwan swamp buffaloes from HAPS. (A) Ne, (B) Ho, (C) He, (D) PIC, (E) F_{IS} , and (F) P -value of HWE test. Ne: Number of effective alleles; Ho: Observed heterozygosity; He: Expected heterozygosity; PIC: Polymorphic information content; F_{IS} : Wright's inbreeding coefficient; HWE: Hardy-Weinberg equilibrium. $P < 0.05$ departure from the HWE.

3.1.2.4 Phylogenetic tree results based on HD SNP genotyping array

The neighbor-joining tree with a bootstrap test of 1,000 replicates of the 94 Taiwan swamp buffaloes based on 14,456 SNPs from the 90K Axiom® Buffalo Genotyping Array after quality control in 2.1.4 was in Figure 13 and Figure 14. The two trees were basically the same but with different layouts. The radial form of the neighbor-joining tree was in Figure 13, and it showed a more clearly picture of the clustering of the 94 Taiwan swamp buffaloes but without bootstrap values on the nodes. Figure 14 showed

the rectangular layout with numbers on the nodes indicating the percentage bootstrap values generated from 1,000 times of resampling. By labeling the fathers of the individuals with different color according to the pedigree data, the accuracy and the similarities of the phylogenetic trees drawn with different methods could be observed more clearly.

The phylogenetic tree based on 14,456 SNPs from the 90K Axiom® Buffalo Genotyping Array showed that 94 Taiwan swamp buffaloes could be divided into three subpopulations by the two nodes marked with red circles, and the three clusters were framed by the green, blue, and red dotted-line frames (Figure 13 and Figure 14). The clustering could be observed more obviously in Figure 13. The “W” marked with red circle in the ID of the 16 white Taiwan swamp buffaloes highlighted the white buffaloes. All of the 16 white swamp buffaloes were clustered into the red-framed subpopulation in the phylogenetic tree based on the 14,456 SNPs from the 90K Axiom® Buffalo Genotyping Array, which was more reasonable and in accordance with the pedigree compared with the tree based on 14 microsatellite markers.

Moreover, the robustness of the phylogenetic tree based on the 14,456 SNPs from the 90K Axiom® Buffalo Genotyping Array was higher according to the high bootstrap support on the nodes of the tree (Figure 14). There were in total 91 bootstrap values in the tree, ranging from 4 to 100, and the average bootstrap value was 72.11. Many of the bootstrap values were between 99 to 100%, and only a few were lower than 50%.

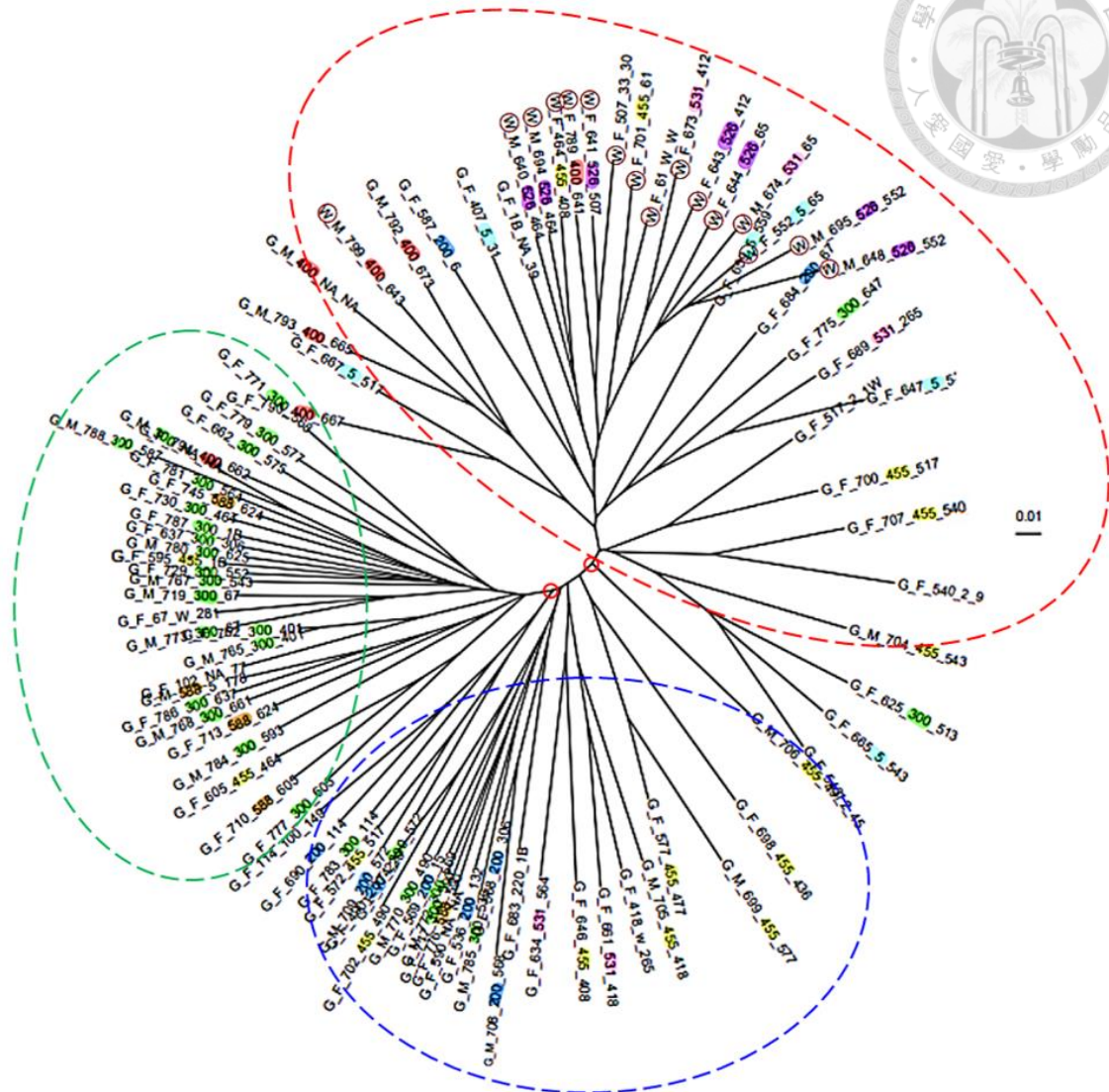


Figure 13. The neighbor-joining tree (daylight method) based on the 14,456 SNPs for the population of the 94 Taiwan buffaloes from HAPS in this study. The labels of the 94 Taiwan buffalo individuals and the footnotes were as in Figure 9.

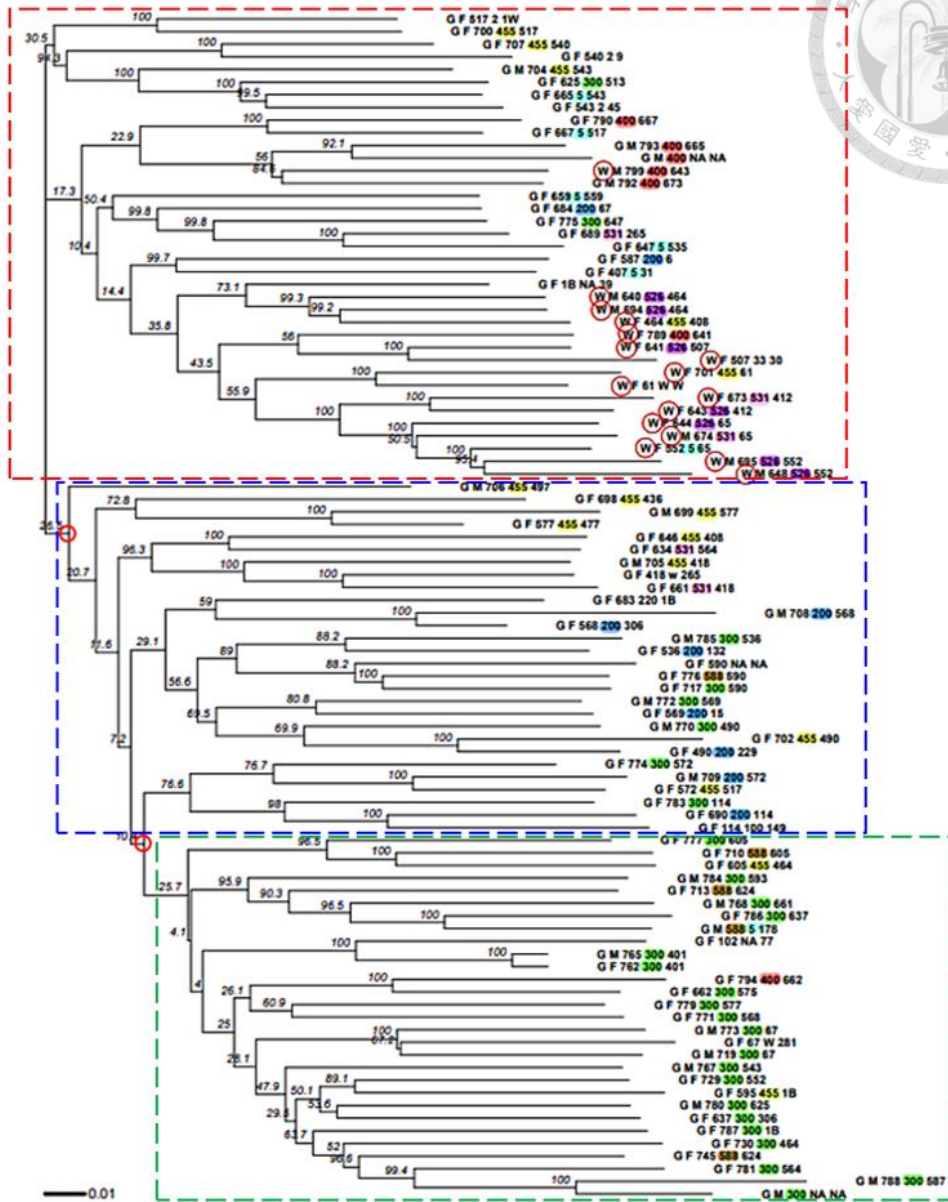


Figure 14. The neighbor-joining tree (rectangular layout) based on the 14,456 SNPs for the population of the 94 Taiwan buffaloes from HAPS in this study. The numbers on the nodes indicate the percentage bootstrap values generated from 1,000 times of resampling. The labels of the 94 Taiwan buffalo individuals and the footnotes were as in Figure 9.

3.1.2.5 fastSTRUCTURE results based on HD SNP genotyping array

The plots of fastSTRUCTURE cluster analysis ($K = 2$ to 6) based on 14,456 SNPs were presented in Figure 15. The results showed that when K was two or three, the 16 white swamp buffaloes were all classified into the same cluster. When K was four, one white swamp buffalo (W464) was divided into a different cluster from other 15 white swamp buffaloes. When K was five, two white swamp buffaloes (W789 and W799) were further assigned into a third cluster. When K was six, two white swamp buffaloes (W507 and W61) were assigned into the third cluster the same as W789 and W799.

The built-in chooseK.py function in fastSTRUCTURE outputs a range of reasonable values for model complexity (number of populations) appropriate for the dataset, but not a specific number for best K . It shows two K values: one represents model complexity that maximizes marginal likelihood, and another represents model components used to explain structure in data. When the test dataset for choices of K ranged from 2 to 6 in this study, the results of chooseK.py showed that $K = 6$ maximized marginal likelihood, and $K = 2$ was used to explain structure in data. However, when K ranged from 2 to 7, the results showed that $K = 7$ maximized marginal likelihood, and $K = 6$ was used to explain structure in data. Similarly, when K ranged from 2 to 8, the results showed that $K = 8$ maximized marginal likelihood, and $K = 6$ was used to explain structure in data. As a result, it might be indicated that the most likely number of populations (K) based on the 14,456 SNPs was six.

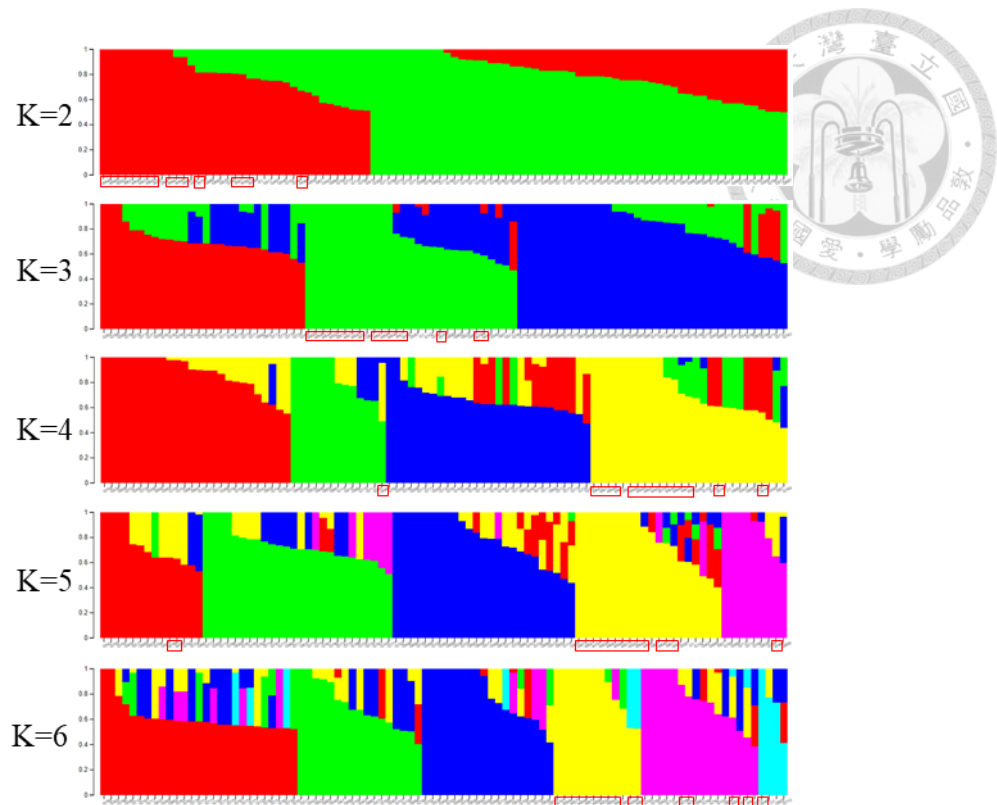


Figure 15. The fastSTRUCTURE cluster analysis plot ($K = 2$ to 6) of the 94 Taiwan buffaloes based on the 14,456 SNPs. The K value is the number of clusters assumed in the analysis, and different colors correspond to different clusters. The horizontal axis shows individuals, and each bar represents one individual. The vertical axis shows the proportion of different clusters an individual stand for. The red frame indicates 16 white swamp buffaloes.

3.2 Coat color gene analysis of Taiwan swamp buffalo

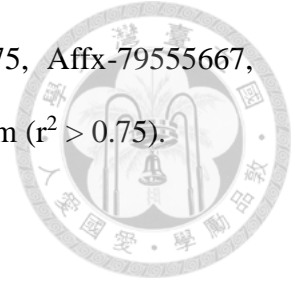
3.2.1 Genome-wide association study (GWAS) results

The GWAS was performed on 94 Taiwan swamp buffaloes (78 gray and 16 white Taiwan swamp buffaloes) in HAPS using the 14,456 SNPs from the 90K Axiom® Buffalo Genotyping Array after quality control in 2.1.4.1 to investigate SNPs associated with the white coat color of the Taiwan swamp buffalo. The Manhattan plot (Figure 16) visualized the results of the GWAS. The 17 most significant SNPs ($P < 1 \times 10^{-11}$) associated with the white coat color of the Taiwan swamp buffalo were identified and 26 related genes were listed in Table 7. The heatmap showed the difference of genotypes of the 17 most significant SNPs among the 94 Taiwan swamp buffaloes was in Appendix figure 1.

However, none of the 17 SNPs or 26 genes has been reported to be associated with pigmentation before. Therefore, it was checked that if any well-known pigmentation-related genes (Table 8) were near the 17 significant SNPs in the GWAS results. It turned out that only the *MC1R* gene was located near the significant SNPs in the GWAS results. The two most significant SNPs, Affx-79526737 and Affx-79522943, in the GWAS ($P < 1 \times 10^{-17}$) were found to be located near the *MC1R* gene (Figure 17). The *MC1R* gene, also known as *TUBB3*, was located at chromosome 18 (NC_059174.1) 14,365,823-14,378,088. Affx-79526737 was 985,604 nt upstream the *MC1R* gene, and Affx-79522943 was 1,730,340 nt downstream the *MC1R* gene.

In addition, a GWAS hit was on chromosome 18. The Manhattan plot subset of chromosome 18 was in Figure 17. The two most significant SNPs marked with red frames (Affx-79526737 and Affx-79522943) were in linkage equilibrium ($r^2 = 0.98$).

The other four SNPs marked with green frames (Affx-79541775, Affx-79555667, Affx-79562669, and Affx-79529804) were also in linkage equilibrium ($r^2 > 0.75$).



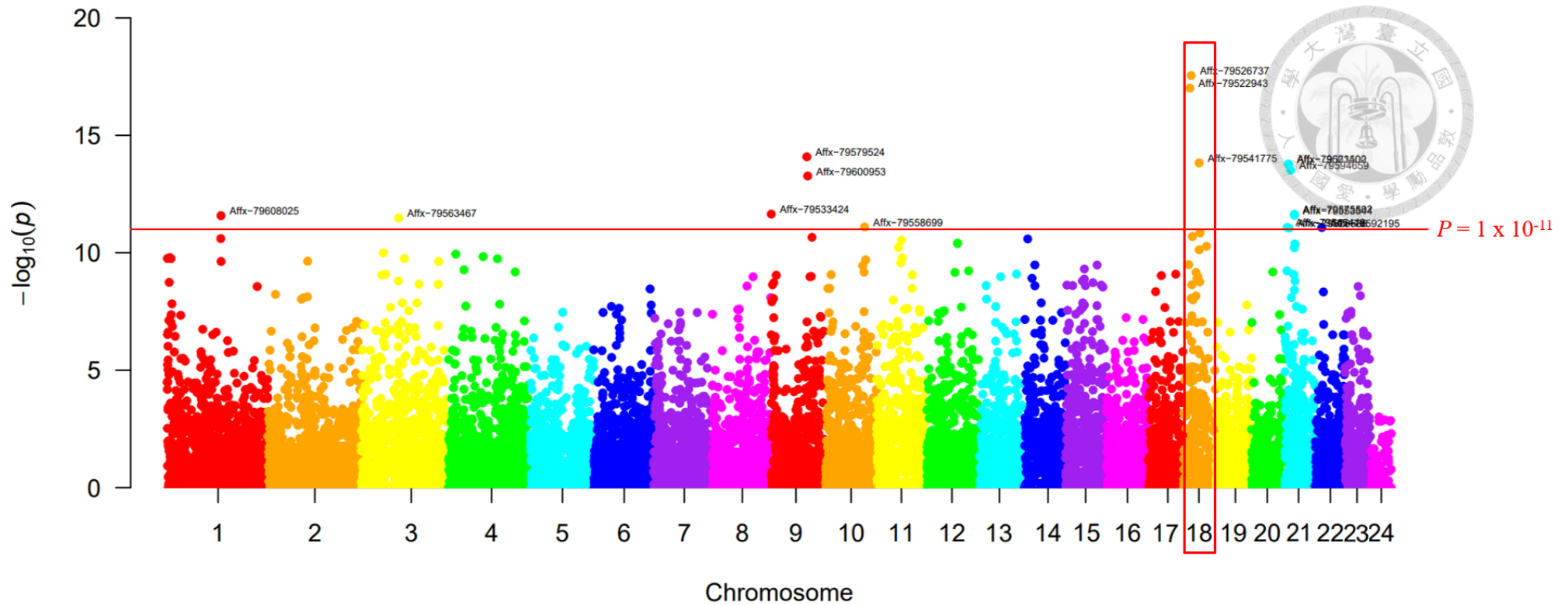


Figure 16. The Manhattan plot showing SNPs associated with the white coat color among 94 Taiwan swamp buffaloes (16 white and 78 gray) based on the 14,456 SNPs from the 90K Axiom® Buffalo Genotyping Array. The x-axis represents the SNP position on the chromosome in order (genome assembly: UOA_WB_1). The value on the y-axis represents the $-\log_{10}$ of the P -value of the GWAS. The dots represent the 14,456 SNPs. The 17 most significant SNPs associated with the white coat color of the Taiwan swamp buffalo were above the red line ($P < 1 \times 10^{-11}$) and were annotated with the Affymetrix (Affy) SNP ID. A GWAS hit was on the chromosome 18 and was marked with a red frame.

Table 7. The information of the top 17 SNPs and 26 related genes which are most significantly associated with coat color among Taiwan swamp buffaloes

Affy SNP ID	P-value	Chr.	Position*	Allele	Associated Gene†
Affx-79526737	2.84E-18	18	16108428	T/C	<i>PHKB</i> ¹ , <i>ABCC12</i> ²
Affx-79522943	9.78E-18	18	13380219	A/C	<i>ZFPM1</i> ³
Affx-79579524	8.20E-15	9	71679648	T/C	<i>COL23A1</i> ⁴
Affx-79541775	1.49E-14	18	31777934	A/G	<i>CDH8</i> ⁵ , <i>CDH11</i> ⁶
Affx-79601400	1.68E-14	21	7172215	A/G	<i>CNOT10</i> ⁷
Affx-79573502	1.68E-14	21	7495311	A/G	<i>GLB1</i> ⁸ , <i>CRTAP</i> ⁹
Affx-79594659	3.03E-14	21	11934641	T/C	<i>SCN5A</i> ¹⁰ , <i>EXO G</i> ¹¹
Affx-79600953	5.38E-14	9	73420245	A/G	<i>COMMD10</i> ¹²
Affx-79533424	2.26E-12	9	419413	A/G	<i>WDR36</i> ¹³ , <i>CAMK4</i> ¹⁴
Affx-79575502	2.27E-12	21	19364448	A/G	<i>GRM7</i> ¹⁵
Affx-79553544	2.56E-12	21	19269295	C/G	<i>GRM7</i> ¹⁵
Affx-79608025	2.62E-12	1	108315428	A/G	<i>LSAMP</i> ¹⁶ , <i>IGSF11</i> ¹⁷
Affx-79563467	3.28E-12	3	74936894	T/C	<i>ACO1</i> ¹⁸ , <i>LINGO2</i> ¹⁹
Affx-79558699	7.98E-12	10	78497363	A/G	<i>HDDC2</i> ²⁰ , <i>HEY2</i> ²¹
Affx-79545448	8.26E-12	21	4807661	A/G	<i>TGFBR2</i> ²² , <i>RBMS3</i> ²³
Affx-79592195	8.44E-12	22	13871627	A/G	<i>CTIF</i> ²⁴
Affx-79528536	8.96E-12	21	8896194	A/G	<i>ARPP21</i> ²⁵ , <i>PDCD6IP</i> ²⁶

*Genome version is NDDDB_SH_1, except for Affx-79558699, which can't be found in NDDDB_SH_1. Genome version of Affx-79558699 position is UOA_WB_1.

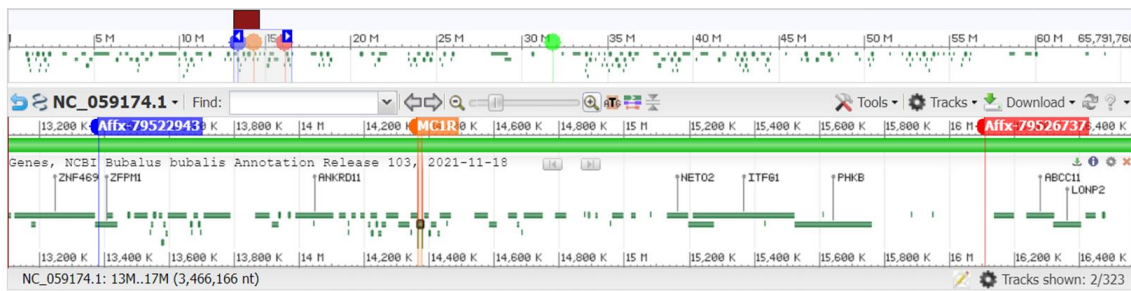
†Netaffx annotation version: 35.r2.a2

¹*PHKB*: Phosphorylase kinase regulatory subunit beta. ²*ABCC12*: ATP binding cassette subfamily C member 12. ³*ZFPM1*: Zinc finger protein, FOG family member 1. ⁴*COL23A1*: Collagen type XXIII alpha 1 chain. ⁵*CDH8*: Cadherin 8. ⁶*CDH11*: Cadherin 11. ⁷*CNOT10*: CCR4-NOT transcription complex subunit 10. ⁸*GLB1*: Galactosidase beta 1. ⁹*CRTAP*: Cartilage associated protein. ¹⁰*SCN5A*: Sodium voltage-gated channel alpha subunit 5. ¹¹*EXO G*: Exo/endonuclease G. ¹²*COMMD10*: COMM domain containing 10. ¹³*WDR36*: WD repeat domain 36. ¹⁴*CAMK4*: Calcium/calmodulin dependent protein kinase IV. ¹⁵*GRM7*: Glutamate metabotropic receptor 7. ¹⁶*LSAMP*: Limbic system associated membrane protein. ¹⁷*IGSF11*: Immunoglobulin superfamily member 11. ¹⁸*ACO1*: Aconitase 1. ¹⁹*LINGO2*: Leucine rich repeat and Ig domain containing 2. ²⁰*HDDC2*: HD domain containing 2. ²¹*HEY2*: Hes related family bHLH transcription factor with YRPW motif 2. ²²*TGFBR2*: Transforming growth factor beta receptor 2. ²³*RBMS3*: RNA binding motif single stranded interacting protein 3. ²⁴*CTIF*: Cap binding complex dependent translation initiation factor. ²⁵*ARPP21*: cAMP regulated phosphoprotein 21. ²⁶*PDCD6IP*: Programmed cell death 6 interacting protein.

Table 8. The location of the well-known pigmentation-related genes in the buffalo

Gene symbol	Gene description	Chr.	Position*	Reference
<i>OCA2</i>	<i>OCA2</i> <i>melanosomal transmembrane protein</i>	2	52640656..52958072	Grønskov et al. (2007); Lao et al. (2007); Du et al. (2017)
<i>PAX3</i>	<i>paired box 3</i>	2	162672501..162772751	Pingault et al. (2010); Pausch et al. (2012)
<i>TYRP1</i>	<i>tyrosinase related protein 1</i>	3	94297146..94313631	Rieder et al. (2001); Guibert et al. (2004); Lao et al. (2007)
<i>SOX10</i>	<i>SRY-box transcription factor 10</i>	4	10196777..10207847	Stanchina et al. (2006); Murisier et al. (2007); Pingault et al. (2010)
<i>PMEL</i>	<i>premelanosome protein</i>	4	63011426..63020226	Schmutz and Dreger (2013); Knaust et al. (2020)
<i>KITLG</i>	<i>KIT ligand</i>	4	101849770..101907034	Lao et al. (2007); Pausch et al. (2012); Weich et al. (2020)
<i>TYR</i>	<i>tyrosinase</i>	5	86853089..86963873	Oetting (2000); Guibert et al. (2004); Damé et al. (2012)
<i>KIT</i>	<i>KIT</i> <i>proto-oncogene, receptor tyrosine kinase</i>	7	47139439..47225867	Haase et al. (2007); Holland et al. (2016)
<i>DCT</i> (<i>TYRP2</i>)	<i>dopachrome tautomerase</i> (<i>tyrosinase related protein 2</i>)	13	20846553..20887813	Guibert et al. (2004); Lao et al. (2007)
<i>EDNRB</i>	<i>endothelin receptor type B</i>	13	36722487..36755472	Stanchina et al. (2006); Pingault et al. (2010)
<i>ASIP</i>	<i>agouti signaling protein</i>	14	19998890..20091365	Hida et al. (2009); Liang et al. (2021); Kumari et al. (2023)
<i>EDN3</i>	<i>endothelin 3</i>	14	26512071..26536911	Stanchina et al. (2006); Pingault et al. (2010)
<i>MC1R</i> (<i>TUBB3</i>)	<i>melanocortin 1 receptor</i> (<i>tubulin beta 3 class III</i>)	18	14365823..14378088	Miao et al. (2010); da Cruz et al. (2020); Ali et al. (2022)
<i>MITF</i>	<i>melanocyte inducing transcription factor</i>	21	31544437..31775071	Yajima et al. (2011); Yusnizar et al. (2015); Nguyen and Fisher (2019)

*The information was referred to NCBI *Bubalus bubalis* Annotation Release 103



(O'Leary et al., 2016)

Figure 17. The location of the two most significant ($P < 1 \times 10^{-17}$) SNPs associated with the white coat color among 94 Taiwan swamp buffaloes (16 white and 78 gray) in the GWAS results and the *MC1R* gene on the buffalo chromosome 18. The two SNPs (Affx-79526737 marked with red frame and Affx-79522943 marked with blue frame) were located near the *MC1R* gene, which is a well-known pigmentation-related gene. The figure was screenshot from the NCBI website. The reference sequence is NC_059174.1, and its definition is “*Bubalus bubalis* isolate 160015118507 breed Murrah chromosome 18, NDDDB_SH_1, whole genome shotgun sequence”.

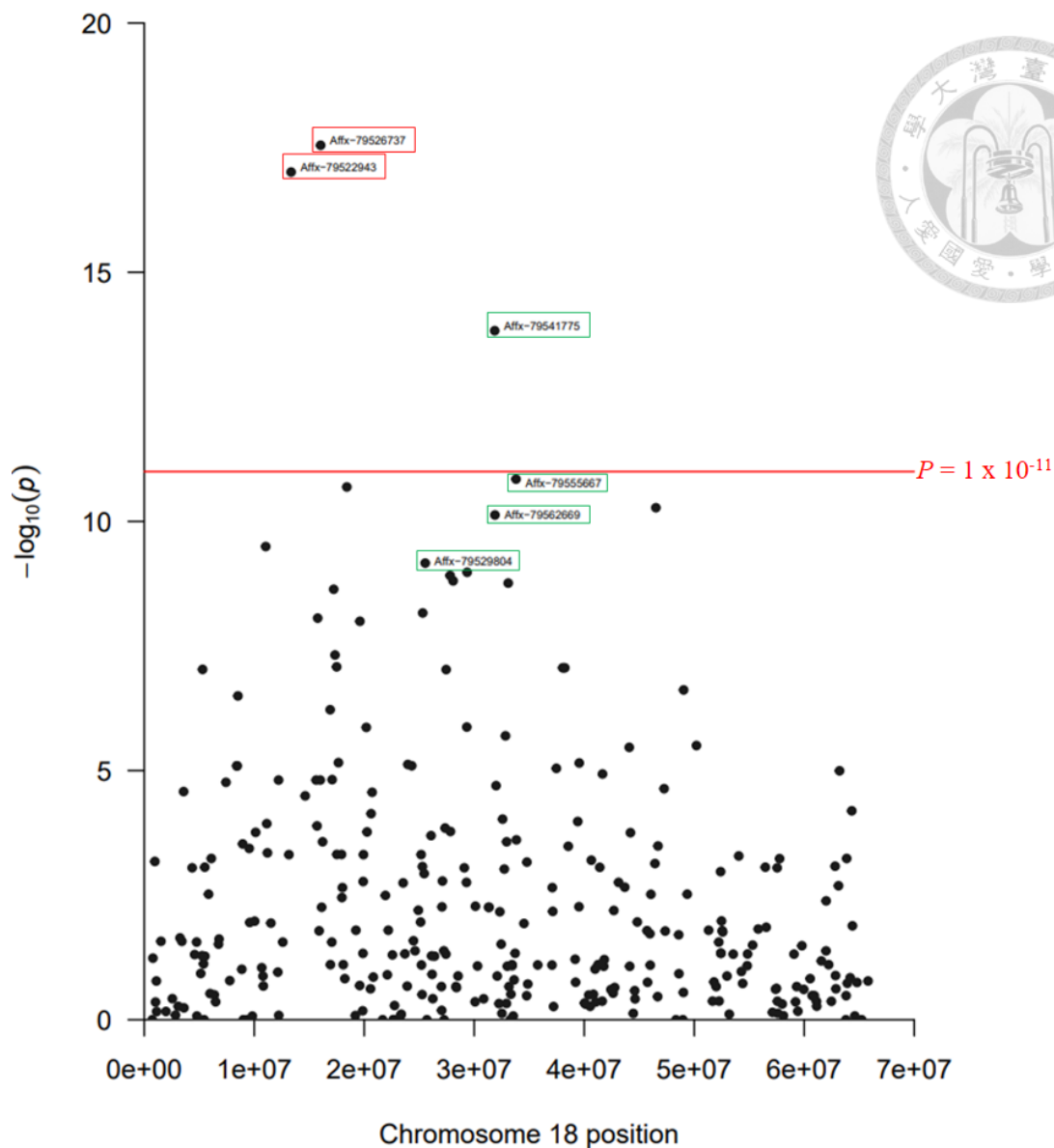


Figure 18. Manhattan plot subset of the chromosome 18 showing SNPs associated with the white coat color among 94 Taiwan swamp buffaloes (16 white and 78 gray) based on the 14,456 SNPs from the 90K Axiom® Buffalo Genotyping Array. The x-axis represents the SNP position on the chromosome in order. The value on the y-axis represents the $-\log_{10}$ of the P -value of the GWAS. The dots represent the 14,456 SNPs. SNPs marked with red frames (Affx-79526737 and Affx-79522943) were in linkage equilibrium ($r^2 = 0.98$). SNPs marked with green frames (Affx-79541775, Affx-7955667, Affx-79562669, and Affx-79529804) were in linkage equilibrium ($r^2 > 0.75$).

3.2.2 *ASIP* genotyping results

Liang et al. (2021) pointed out that the *LINE-1* insertion in the *ASIP* gene of white swamp buffalo may be the cause of the white coat color. However, the GWAS results in this study did not identify the *ASIP* gene to be associated with the white coat color of the Taiwan swamp buffalo. In order to verify whether the *LINE-1* insertion existed in the *ASIP* gene of the white Taiwan swamp buffalo, 15 white Taiwan swamp buffaloes from HAPS of which gDNA stock was available and five wild-type gray Taiwan swamp buffaloes randomly selected from the gDNA stock of the 94 Taiwan swamp buffaloes were genotyped for the *LINE-1* insertion in the *ASIP* gene using the allele-specific PCR (Table 3). The 1.5% agarose gel electrophoresis results (Figure 19) showed that 5 gray Taiwan swamp buffaloes (G1~G5) and 14 white Taiwan swamp buffaloes (W1~W15, except for W4) had wild-type alleles (296 bp). There was neither wild-type nor mutant-type band in one white Taiwan swamp buffalo (W4) maybe because of its low gDNA quality and quantity. No mutant allele indicating the existence of the *LINE-1* insertion in the *ASIP* gene was found in any gray or white Taiwan swamp buffaloes in this study. Thus, the cause for the white coat color of the Taiwan swamp buffalo should be different from what Liang et al. (2021) discovered in their white swamp buffaloes.

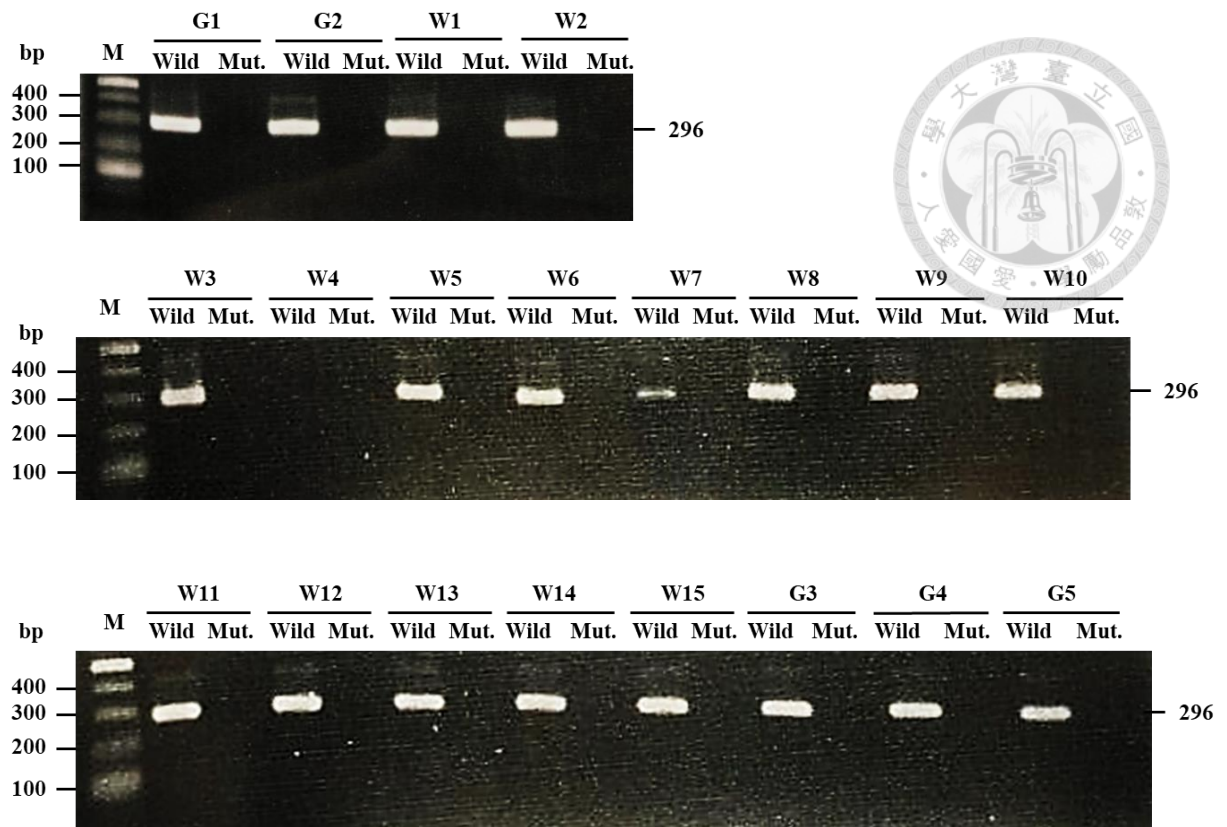


Figure 19. The 1.5% agarose gel electrophoresis results of genotyping the *LINE-1* insertion in the *ASIP* gene using the allele-specific PCR. PCR product of wild-type allele is 296 bp. PCR product of mutant allele indicating the existence of the *LINE-1* insertion in the *ASIP* gene is 387 bp. Five gray Taiwan swamp buffaloes (G1~G5) and 14 white Taiwan swamp buffaloes (W1~W15, except for W4) were all wild type, which detected a 296 bp band with the wild-type primer pairs. There were neither bands in one white Taiwan swamp buffalo (W4). No mutant allele indicating the existence of the *LINE-1* insertion in the *ASIP* gene was found with the mutant-type primer pairs in these 20 Taiwan swamp buffaloes. Lane “M” was the 100 bp DNA ladder.

The PCR products were also analyzed by Sanger sequencing. The results (Figure 20) showed that five gray Taiwan swamp buffaloes (G1~G5) and 13 white Taiwan swamp buffaloes (W1~W15, except for W4 and W7) had wild-type alleles without the *LINE-1* insertion in their *ASIP* genes. The Sanger sequencing results showed that the PCR products of two white Taiwan swamp buffaloes (W4 and W7) were lack of concentration. The results verified that no *LINE-1* insertion was found in the *ASIP* gene in any gray or white Taiwan swamp buffaloes in this study.

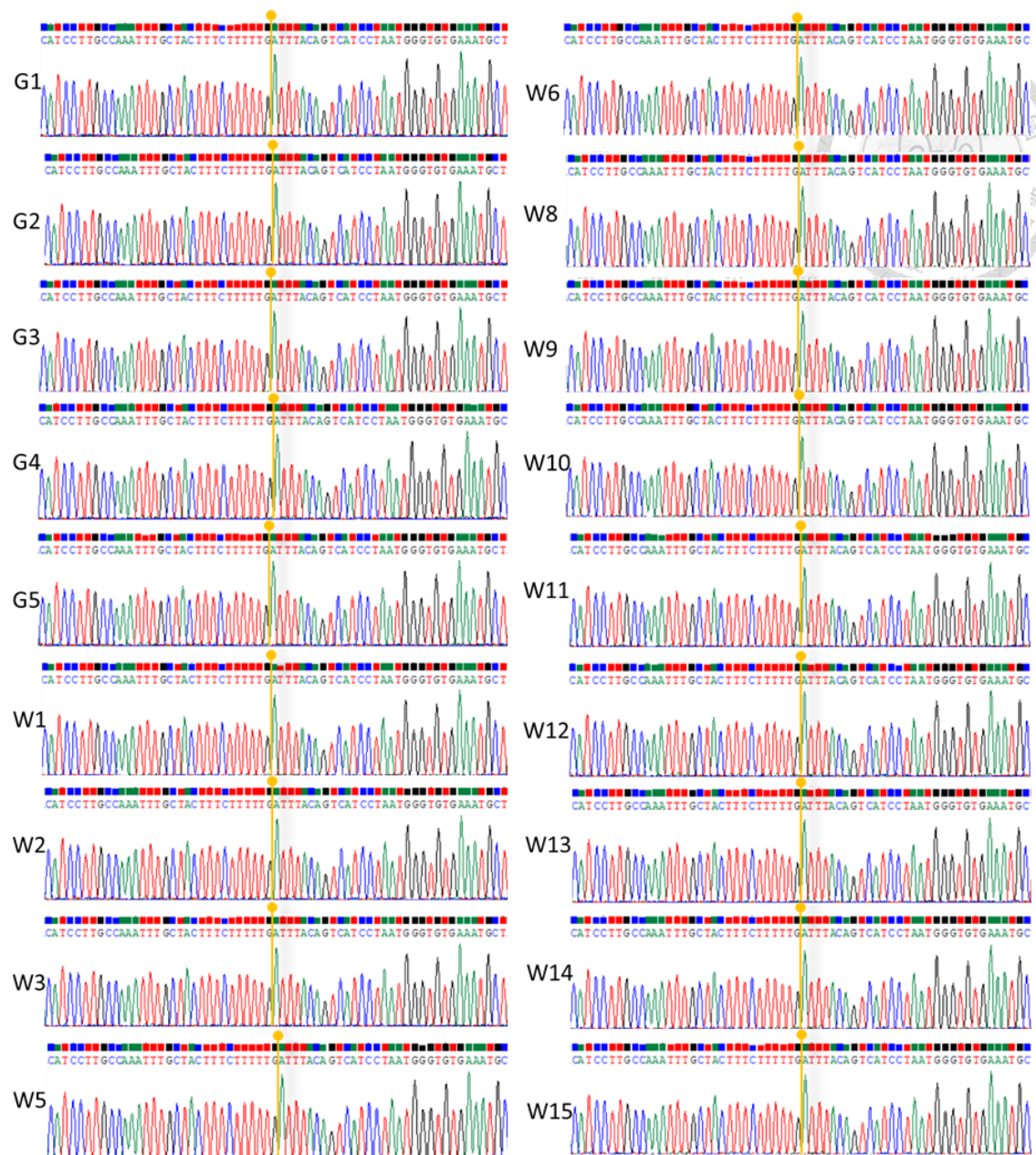


Figure 20. The Sanger sequencing results of genotyping the *LINE-1* insertion in the *ASIP* gene using the allele-specific PCR. The results showed that 5 gray Taiwan swamp buffaloes (G1~G5) and 13 white Taiwan swamp buffaloes (W1~W15, except for W4 and W7) had wild-type alleles. There was no *LINE-1* insertion in their *ASIP* genes. The *LINE-1* insertion will be at the yellow line position if it is a mutant-type allele. The *ASIP* gene sequence shown in the figure was from 42,922 nt to 42,983 nt (NCBI Reference Sequence: NC_059170.1).

3.2.3 *MC1R* sequencing results

The *MC1R* gene of 27 gray Taiwan swamp buffaloes randomly selected from the gDNA stock of the 94 Taiwan swamp buffaloes and 15 white Taiwan swamp buffaloes from HAPS of which gDNA stock was available were sequenced by Sanger sequencing. Figure 21 showed the alignment of *MC1R* nucleotide sequences of the river buffalo from NCBI database (NC_059174.1) (O'Leary et al., 2016), the swamp buffalo from NCBI database (GU121301.1) (Miao et al., 2010; O'Leary et al., 2016), and the gray and white Taiwan swamp buffaloes analyzed in this study. The obtained coding sequences of both gray and white Taiwan swamp buffalo *MC1R* gene were 951 bp long and encoded 317 amino acids. Compared with the river buffalo, four variations at position 310 (c.310A>G), position 384 (c.384T>G), position 618 (c.618C>G), and position 901 (c.901C>T) in the *MC1R* gene were found in both gray and white Taiwan swamp buffaloes. Three of the four variations (c.310A>G, c.384T>G, and c.618C>G) had been found in the swamp buffalo in the study of Miao et al. (2010). Only the variation at position 901 (c.901C>T) was found exclusively in the gray and white Taiwan swamp buffaloes in this study (Figure 21).



Figure 21. Alignment of *MC1R* nucleotide sequences of the river buffalo and swamp buffalo from NCBI database, and gray and white Taiwan swamp buffaloes in this study. Accession number: ¹NC_059174.1 and ²GU121301.1. Dashes (-)

denote identity with the river buffalo *MC1R* nucleotide sequence, which was used as a reference sequence. Compared with the river buffalo, four variations at position 310 (c.310A>G), position 384 (c.384T>G), position 618 (c.618C>G), and position 901 (c.901C>T) were found in both gray and white Taiwan swamp buffaloes. Compared with the swamp buffalo from NCBI database, the variations at position 901 (c.901C>T) were found in both gray and white Taiwan swamp buffaloes in this study.

In further analysis, we found that the variation at position 901 (c.901C>T) in the *MC1R* gene (Figure 22) was significantly associated ($P < 0.05$) with Taiwan swamp buffalo coat color (Table 9). The results showed that 11 gray and zero white Taiwan swamp buffaloes were homozygous for the wild-type C allele, 16 gray and one white Taiwan swamp buffaloes were heterozygous for the variant, and zero gray and 14 white Taiwan swamp buffaloes were homozygous for the variant T allele.

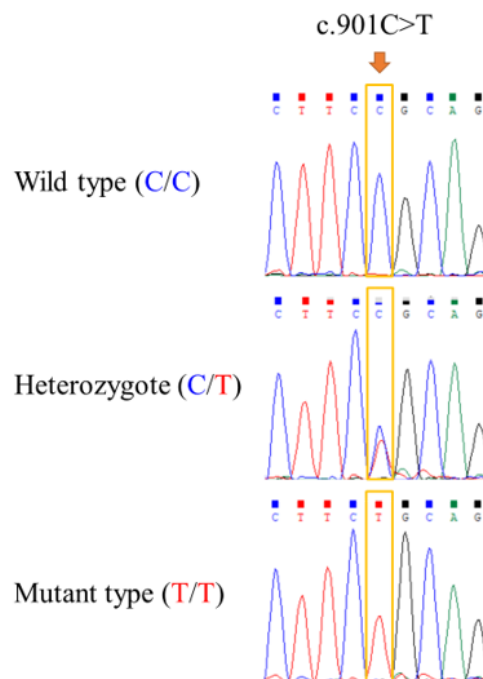


Figure 22. Sanger sequencing of gDNA in gray and white Taiwan swamp buffaloes revealed a mutation (c.901C>T) in the *MC1R* gene. The figure shows partial

chromatogram obtained from the assembly of *MC1R* sequences from wild-type (C/C), heterozygote (C/T), and mutant-type (T/T) Taiwan swamp buffaloes. The normal C at the 5th nucleotide position shown in the picture was observed in the wild-type *MC1R* sequence. A double peak (C/T) was observed in the heterozygote sequence, and a point mutation (C to T) was observed in the mutant-type sequence. The results showed that 11 gray Taiwan swamp buffaloes were wild-type (C/C), 16 gray and one white Taiwan swamp buffaloes were heterozygote (C/T), and 14 white Taiwan swamp buffaloes were mutant-type (T/T).

Table 9. Genotype distribution and allele frequency of the mutation (c.901C>T) in the *MC1R* gene in 27 gray and 15 white Taiwan swamp buffaloes by Sanger sequencing

Phenotype	n	Genotype frequency (%)			χ^2 (P) ¹	Allele frequency (%)		P ²
		C/C	C/T	T/T		C	T	
Gray	27	11 (40.7)	16 (59.3)	0 (0)	37.901	38 (70.4)	16 (29.6)	5.04 x 10 ⁻⁹
White	15	0 (0)	1 (6.6)	14 (93.3)	(5.89 x 10 ⁻⁹)	1 (3.3)	29 (96.7)	

¹Chi-square test (χ^2) comparing genotype distribution between gray and white Taiwan swamp buffaloes

²Fisher's exact test comparing allele frequency between gray and white Taiwan swamp buffaloes

n: sample size

The number in the parentheses represents the percentage.

3.2.4 *MC1R* c.901C>T genotyping using TaqMan™ SNP Genotyping

Assay results

To further verify the association between the *MC1R* c.901C>T and the coat color of the Taiwan swamp buffalo and to genotype more samples efficiently, TaqMan™ SNP Genotyping Assay was designed to genotype the buffalo *MC1R* c.901C>T variation using qPCR (Figure 23). New samples from HAPS were added in this experiment.

There were in total 133 Taiwan swamp buffaloes (115 gray and 18 white Taiwan swamp

buffaloes) genotyped using the qPCR method, and some samples overlapped with the Sanger sequencing experiment mentioned above. The results showed that 78 gray Taiwan swamp buffaloes were homozygous for the wild-type C allele, 37 gray and one white Taiwan swamp buffaloes were heterozygous for the variant, and 17 white Taiwan swamp buffaloes were homozygous for the variant T allele. The association between *MC1R* c.901C>T and the gray and white coat color of Taiwan swamp buffalo was highly significant ($P < 0.05$) (Table 10).

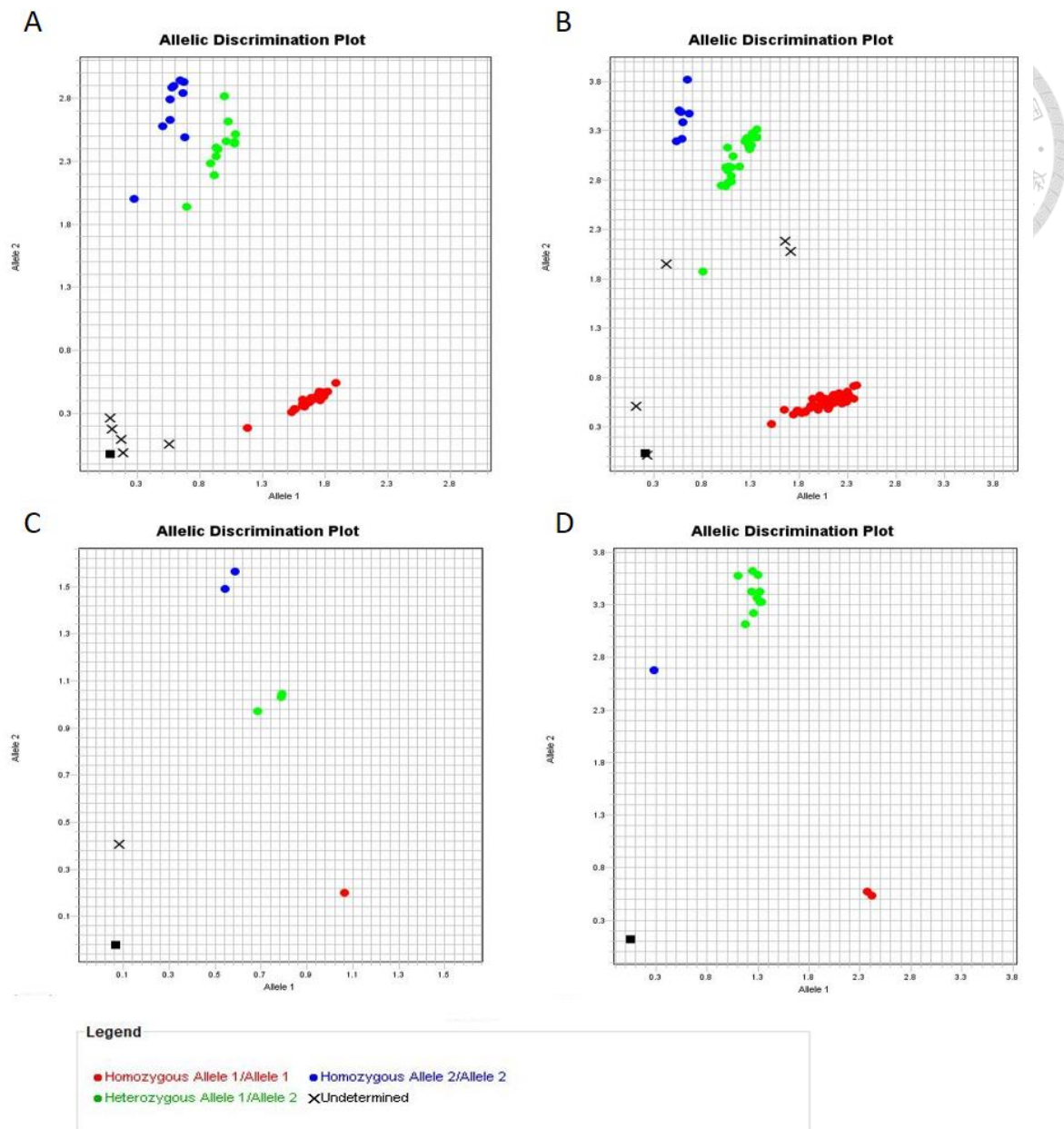


Figure 23 Allelic discrimination plots obtained for genotyping of *MC1R* c.901C>T in grey and white Taiwan swamp buffaloes using TaqMan™ SNP Genotyping Assay with qPCR. In these four allelic discrimination plots, red spots near the X-axis indicate samples that were C/C genotype (homozygous allele 1), blue spots near the Y-axis indicate samples that were T/T genotype (homozygous allele 2), and samples that were C/T genotype (heterozygous alleles) were plotted as green dots in the middle between the two axes. “X” indicates undetermined samples. The squares on the bottom left of the plot are no-template control. (A) Twenty-three samples were C/C genotype, eight samples were C/T genotype, and ten samples were T/T genotype.

were undetermined. (B) Fifty-four samples were C/C genotype, 17 samples were C/T genotype, and seven samples were T/T genotype. Five samples were undetermined. (C) One sample was C/C genotype, three samples were C/T genotype, and two samples were T/T genotype. One sample was undetermined. (D) Two samples were C/C genotype, nine samples were C/T genotype, and one sample was T/T genotype.

Table 10. Genotype distribution and allele frequency of the missense mutation (c.901C>T) in the *MC1R* gene in 115 gray and 18 white Taiwan swamp buffaloes by qPCR

Phenotype	n	Genotype frequency (%)			χ^2 (P) ¹	Allele frequency (%)		P ²
		C/C	C/T	T/T		C	T	
Gray	115	78 (67.8)	16 (32.2)	0 (0)	124.68	193 (83.6)	37 (16.4)	1.891 x 10 ⁻²²
White	18	0 (0)	1 (5.6)	17 (94.4)	(8.44 x 10 ⁻²⁸)	1 (2.6)	35 (97.4)	

¹Chi-square test (χ^2) comparing genotype distribution between gray and white Taiwan swamp buffaloes

²Fisher's exact test comparing allele frequency between gray and white Taiwan swamp buffaloes

n: sample size

The number in the parentheses represents the percentage.

3.2.5 Amino acid substitution and protein function prediction results

The variations in the *MC1R* gene found at position 310 (c.310A>G), position 384 (c.384T>G), and position 901 (c.901C>T) were nonsynonymous (missense variants), causing p.S104G, p.I128M, and p.R301C amino acid changes in the MC1R protein, respectively. On the other hand, the variation at position 618 (c.618C>G) was synonymous, causing no amino acid substitution (Figure 24).

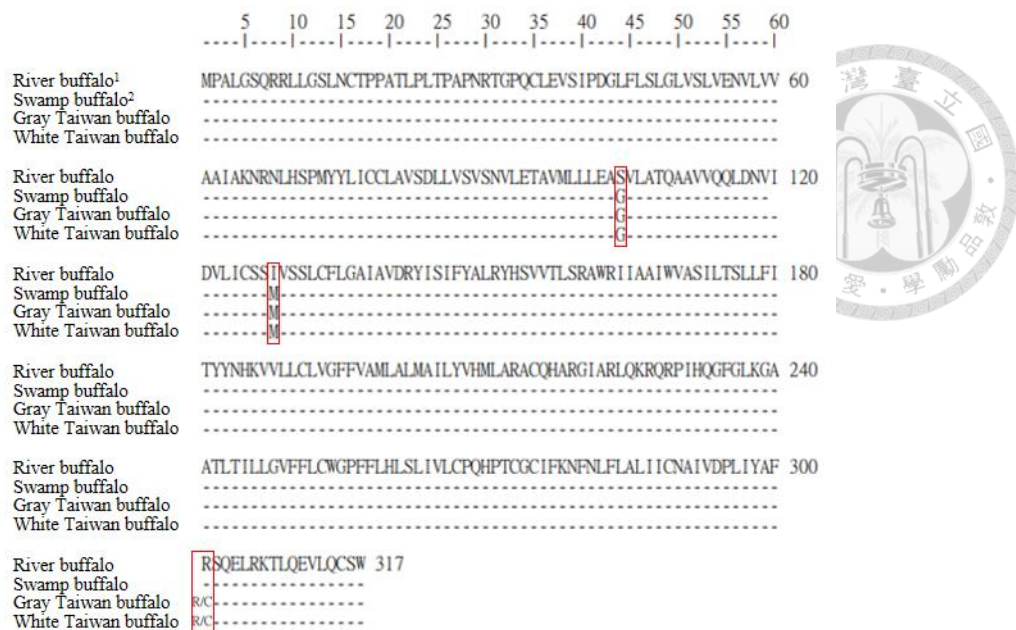


Figure 24. Alignment of the MC1R amino acid sequences of the river buffalo and swamp buffalo from NCBI database, and gray and white Taiwan swamp buffaloes in this study. Accession number: ¹NC_059174.1 and ²GU121301.1. Dashes (-) denote identity with the river buffalo MC1R amino acid sequence, which was used as a reference sequence. Compared with the river buffalo, amino acid substitutions from serine (S) to glycine (G) at position 104, isoleucine (I) to methionine (M) at position 128, and arginine (R) to cysteine (C) at position 301 were observed in both gray and white Taiwan swamp buffaloes. Compared with the swamp buffalo from NCBI database, the amino acid substitutions from arginine (R) to cysteine (C) at position 301 were found in both gray and white Taiwan swamp buffaloes in this study.

Because the association between *MC1R* c.901C>T and the gray and white coat color of Taiwan swamp buffalo was highly significant, PredictSNP (Bendl et al., 2014) was used to predict the potential effect of the p.R301C on MC1R protein structure or function. PredictSNP is a web interface that allows an easy access to the other seven prediction tools: MAPP (Stone and Sidow, 2005), PhD-SNP (Capriotti et al., 2006), PolyPhen-1 (Ramensky et al., 2002), PolyPhen-2 (Adzhubei et al., 2010), SIFT (Ng and

Henikoff, 2003), SNAP (Bromberg and Rost, 2007), and PANTHER (Thomas and Kejariwal, 2004). Predictions from the computational tools are supplemented by experimental annotations from Protein Mutant Database (Kawabata et al., 1999) and UniProt database (UniProt Consortium, 2012). The results showed that all of the eight tools in this study predicted the variant (p.R301C) to be deleterious, and the expected accuracy was between 45 to 89% (Table 11). In addition, the amino-acid biochemical properties changed from basic to polar when the amino acid changed from arginine to cysteine. As a result, the variation p.R301C might really cause some harmful and structural impact on the MC1R protein.

Table 11. Potential effect of amino acid substitution (p.R301C) on MC1R structure or function by eight prediction tools

Amino acid substitution prediction tool	Version	Results	Expected accuracy (%)
PredictSNP ¹	-	Deleterious	87
MAPP ²	28.6.05	Deleterious	86
PhD-SNP ³	2.06	Deleterious	82
PolyPhen-1 ⁴	1.18	Deleterious	59
PolyPhen-2 ⁵	2.2.2	Deleterious	45
SIFT ⁶	4.0.4	Deleterious	53
SNAP ⁷	1.1.30	Deleterious	89
PANTHER ⁸	1.02	Deleterious	74

¹Bendl et al. (2014). ²Stone and Sidow (2005). ³Capriotti et al. (2006). ⁴Ramensky et al. (2002). ⁵Adzhubei et al. (2010). ⁶Ng and Henikoff (2003). ⁷Bromberg and Rost (2007). ⁸Thomas and Kejariwal (2004).

3.2.6 Relative gene expression analysis results

3.2.6.1 Relative gene expression among different parts of skin tissue of an adult white Taiwan swamp buffalo

The mean Ct and delta Ct values in the relative gene expression analysis among

different parts of skin tissue of an adult white Taiwan swamp buffalo was in Appendix table 4. The results showed that gene expression between different parts of skin tissue of an adult white Taiwan swamp buffalo were different (Figure 25). For the *MC1R* gene expression, the ventral side ear (0.26) was 1.6 times higher than the dorsal side ear (0.16), and the back (0.11) was 1.8 times higher than the abdomen (0.06). For the *ASIP* gene expression, the ventral side ear (0.01) was 46 times lower than the dorsal side ear (0.46), and the back (0.08) was 1.3 times lower than the abdomen (0.06). For the *MITF* gene expression, the ventral side ear (0.06) was 14 times lower than the dorsal side ear (0.84), and the back (0.18) was 1.4 times lower than the abdomen (0.25). For the *TYR* gene expression, the ventral side ear (0.02) was 17.5 times lower than the dorsal side ear (0.35), and the back (0.08) was 1.1 times lower than the abdomen (0.09). For the *TYRP1* gene expression, the ventral side ear (0.05) was 20 times lower than the dorsal side ear (1.00), and the back (0.20) was 1.2 times lower than the abdomen (0.24). For the *DCT* gene expression, the ventral side ear (0.02) was 18.5 times lower than the dorsal side ear (0.37), and the back (0.09) was the same as the abdomen (0.09).

In the ventral side ear, the *MC1R* gene expression (0.26) was 26 times higher than the *ASIP* gene expression (0.01). In the dorsal side ear, the *MC1R* gene expression (0.16) was 2.9 times lower than the *ASIP* gene expression (0.46). In the back, the *MC1R* gene expression (0.11) was 1.4 times higher than the *ASIP* gene expression (0.08). In the abdomen, the *MC1R* gene expression (0.06) was 1.8 times lower than the *ASIP* gene expression (0.11).

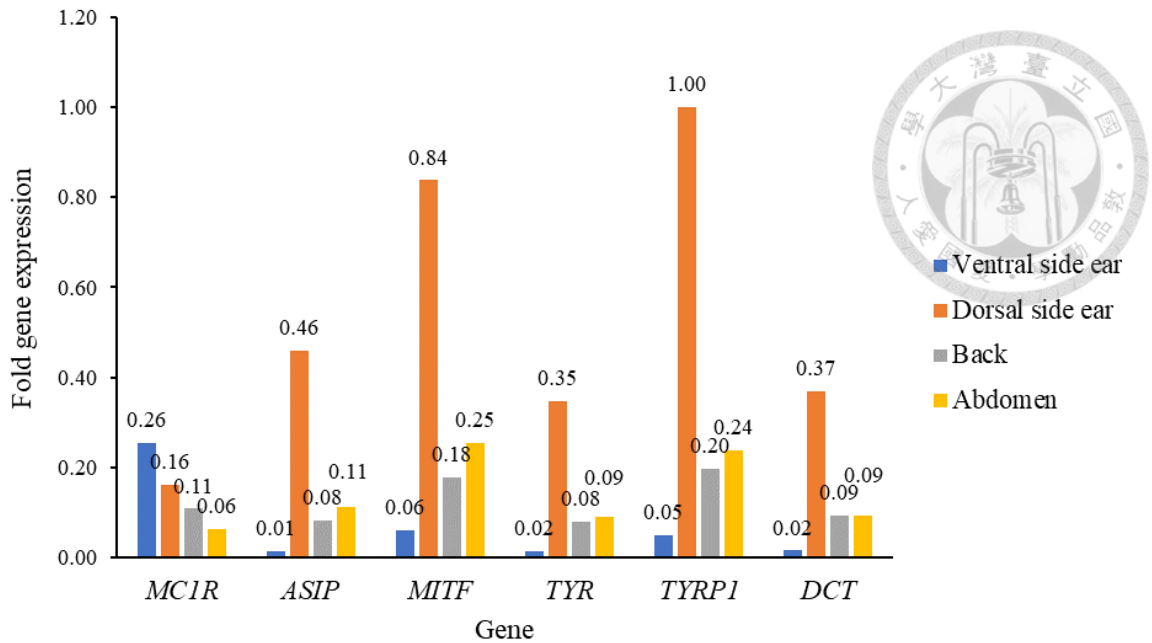


Figure 25. Gene expression (*MC1R*, *ASIP*, *MITF*, *TYR*, *TYRP1*, and *DCT* gene) comparison of different parts of skin tissue (ventral side ear, dorsal side ear, back, and abdomen) of an adult white Taiwan swamp buffalo using qPCR analysis. The X-axis represents the target genes: *MC1R* (*melanocortin 1 receptor*), *ASIP* (*agouti signaling protein*), *MITF* (*melanocyte inducing transcription factor*), *TYR* (*tyrosinase*), *TYRP1* (*tyrosinase related protein 1*), and *DCT* (*dopachrome tautomerase*). The Y-axis represents the fold gene expression of every gene relative to the gene expression level of *TYRP1* gene in the dorsal side ear. The *18S rRNA* was used as the endogenous reference gene. Each qPCR analysis was performed in triplicate. The relative gene expression levels were calculated using the $2^{-\Delta\Delta C_t}$ method. The adult white Taiwan swamp buffalo analyzed was *MC1R* c.901 (T/T) mutant type. n = 1.

3.2.6.2 Relative gene expression among ear skin tissue of gray (brown) and white Taiwan swamp buffalo calves

The mean Ct and delta Ct values in the relative gene expression analysis among ear skin tissue of gray (brown) and white Taiwan swamp buffalo calves was in Appendix table 5. The results showed that gene expression between two gray (brown) calves and

one white calf had no significant difference (Figure 26). The white calf had normal gene expression as the two gray (brown) calves. There was no clear association observed between gene expression and the gray (brown) and white coat color.

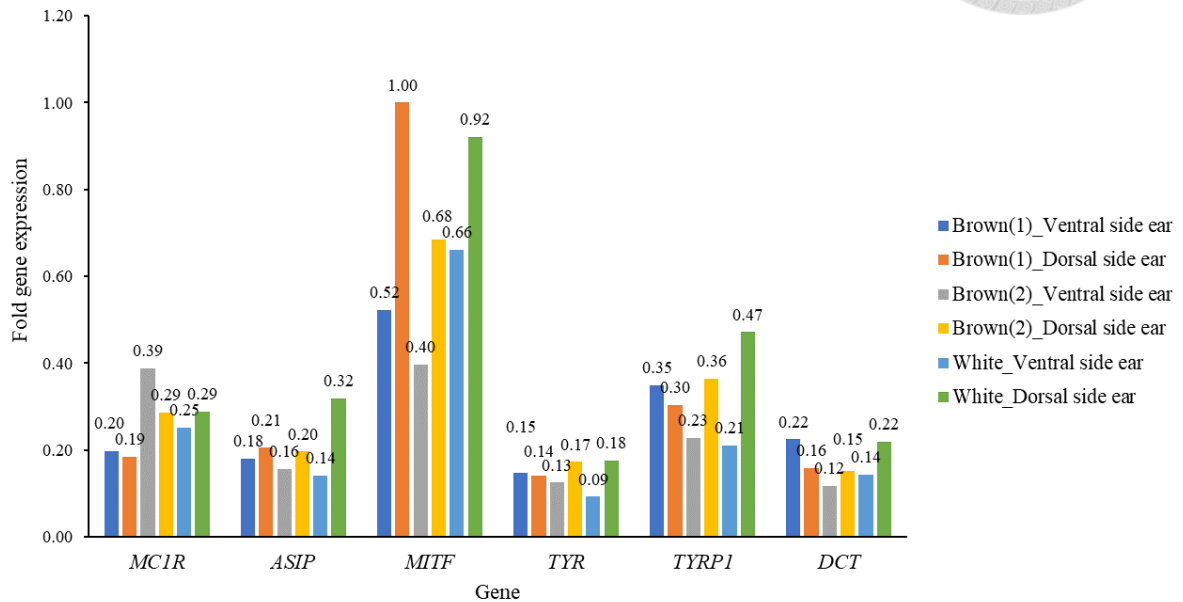
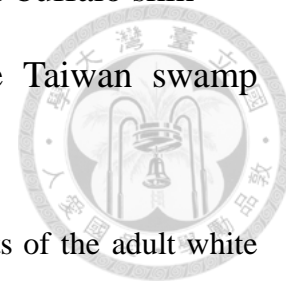


Figure 26. Gene expression (*MC1R*, *ASIP*, *MITF*, *TYR*, *TYRP1*, and *DCT* gene) comparison of the ventral side and dorsal side ear skin tissue of two gray (brown) Taiwan swamp buffalo calves and one white Taiwan swamp buffalo calf using qPCR analysis. The X-axis represents the target genes: *MC1R* (*melanocortin 1 receptor*), *ASIP* (*agouti signaling protein*), *MITF* (*melanocyte inducing transcription factor*), *TYR* (*tyrosinase*), *TYRP1* (*tyrosinase related protein 1*), and *DCT* (*dopachrome tautomerase*). The Y-axis represents the fold gene expression of every gene relative to the gene expression level of *MITF* gene in the dorsal side ear of “Brown(1)”. The *18S rRNA* was used as the endogenous reference gene. Each qPCR analysis was performed in triplicate. The relative gene expression levels were calculated using the 2 $-\Delta\Delta$ Ct method. “Brown(1)” was a gray (brown) swamp buffalo calf with *MC1R* c.901 (C/C) wild type, “Brown(2)” was a gray (brown) swamp buffalo calf with *MC1R* c.901 (C/T) heterozygous type, and “White” was a white swamp buffalo calf with *MC1R* c.901 (T/T) mutant type. n = 1.

3.2.7 Histological examination and staining results of the buffalo skin

3.2.7.1 Different parts of skin tissue of an adult white Taiwan swamp buffalo



The Fontana-Masson staining results showed that all four parts of the adult white Taiwan swamp buffalo skin tissue had melanin deposition, with less melanin deposition in the dorsal side ear and abdomen skin, and significantly more melanin deposition in the ventral side ear and back skin (Figure 27).

In the skin tissue of the ventral side ear, melanin deposition was all over the epidermis (Figure 27A). In the skin tissue of the dorsal side ear, some melanin deposition was in the basal layer of the epidermis (Figure 27B). There was much more melanin deposition all over the epidermis in the skin tissue of the back (Figure 27C), while there was little melanin deposition in the basal layer of the epidermis in the skin tissue of the abdomen (Figure 27D).

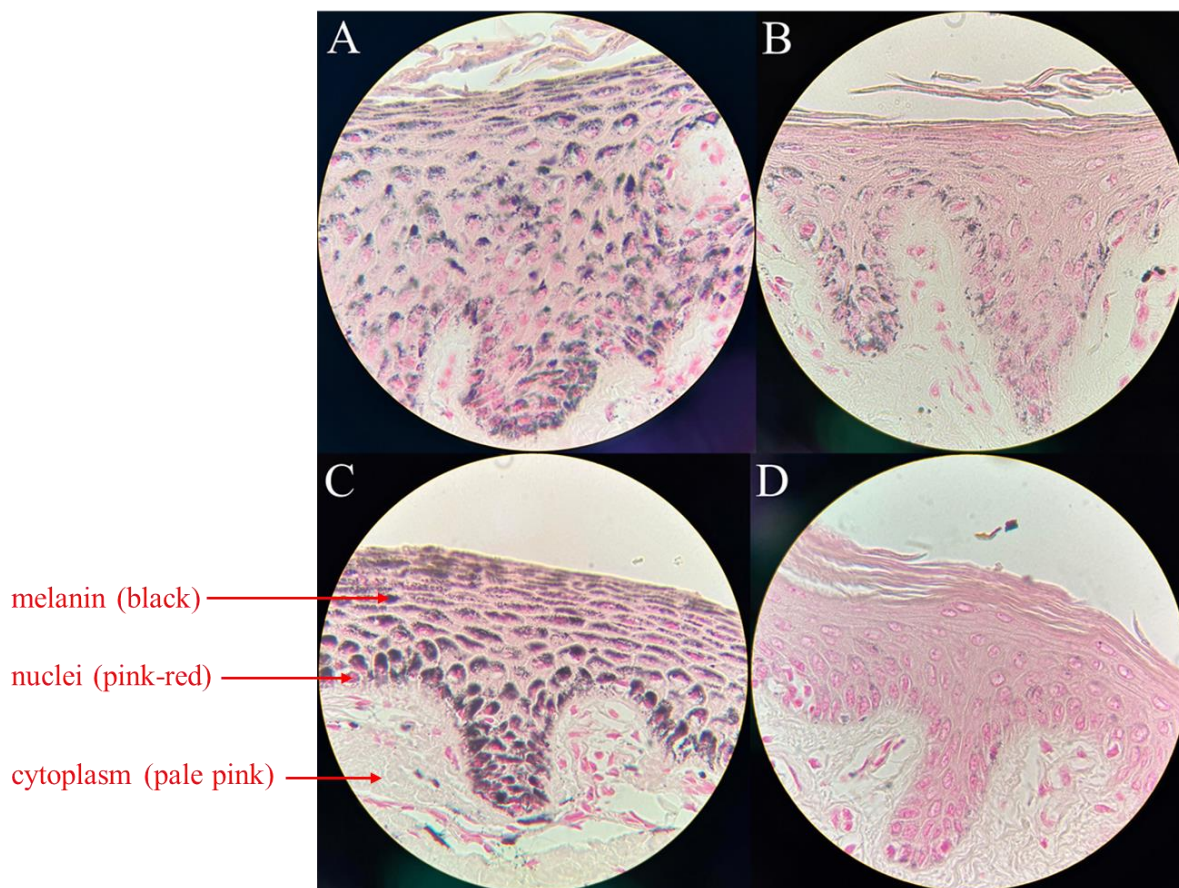


Figure 27. Fontana-Masson staining of four parts of a white Taiwan swamp buffalo skin tissue. (A) The ventral side ear, (B) the dorsal side ear, (C) the back, and (D) the abdomen of a white Taiwan swamp buffalo. The total magnification of microscope was 1000X (100X objective lens \times 10X eyepieces). The Fontana-Masson stain was used to detect melanin granules. The melanin was stained black, the nuclei was stained pink-red, and the cytoplasm was stained pale pink. n = 1.

3.2.7.2 Ear skin tissue of gray (brown) and white Taiwan swamp buffalo calves

The Fontana-Masson staining results showed difference of melanin content between ear skin tissue of gray (brown) and white Taiwan swamp buffalo calves (Figure 28). The ventral side ear of the gray (brown) calf had much more melanin deposition all over the epidermis than its dorsal side ear, which had nearly no melanin deposition

(Figure 28A and Figure 28B). For the white calf, both the ventral side ear and the dorsal side ear had melanin deposition, and the ventral side ear had slightly more melanin deposition (Figure 28C and Figure 28D). The ventral side ear of the gray (brown) calf had significantly more melanin deposition than that of the white calf.

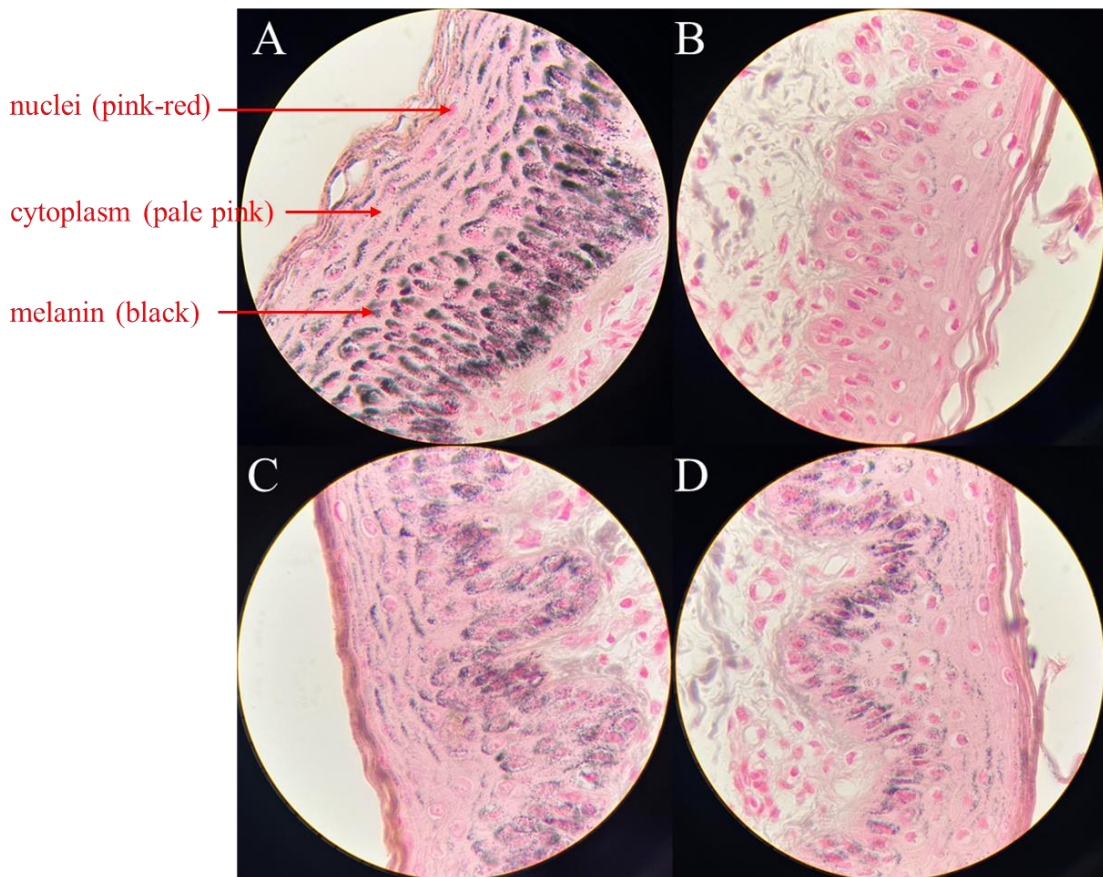
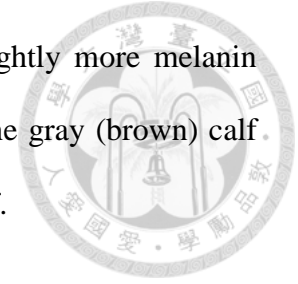


Figure 28. Fontana-Masson staining of ear skin tissue of gray (brown) and white Taiwan swamp buffalo calves. (A) The ventral side ear of a gray (brown) calf, (B) the dorsal side ear of a gray (brown) calf, (C) the ventral side ear of a white calf, and (D) the dorsal side ear of a white calf. The total magnification of microscope was 1000X (100X objective lens \times 10X eyepieces). The Fontana-Masson stain was used to detect melanin granules. The melanin was stained black, the nuclei was stained pink-red, and the cytoplasm was stained pale pink. $n = 1$.

Chapter 4 Discussion

4.1 Population genetic structure analysis of Taiwan swamp buffalo



4.1.1 Microsatellite markers analysis

In Taiwan, Lin et al. (2013) used 12 microsatellite markers to analyze the population genetic structure of 114 Taiwan swamp buffaloes in HAPS. The 12 microsatellite markers included *CSSM19*, *CSSM32*, *CSSM33*, *CSSM38*, *CSSM41*, *CSSM43*, *CSSM45*, *CSSM47*, *CSSM60*, *CSSME070*, *BMC1013*, and *BRN*. None of the 12 microsatellite markers were used in this study. The results showed that removing the non-polymorphic marker (*CSSM045*) and the marker (*CSSME070*) with low PIC (0.149), the average N_a was 4.7, N_e was 2.7, H_o was 0.590, H_e was 0.622, PIC was 0.561, and F_{IS} was 0.052 among the 10 microsatellite markers (Lin et al., 2013). Compared with the results of the 12 microsatellite markers in this study, we got slightly lower N_a (4.4), N_e (2.678), H_o (0.584), H_e (0.581), PIC (0.521), and F_{IS} (-0.008) in 94 Taiwan swamp buffaloes from HAPS. Compare with the results of Lin et al. (2013), the genetic polymorphism detected among Taiwan swamp buffaloes from HAPS in this study was a little lower, but the degree of inbreeding in this study was milder. On the other hand, based on the analysis of STRUCTURE 2.3 (Pritchard et al., 2000) and the UPGMA (unweighted pair group method with arithmetic mean) phylogenetic tree drawn with PHYLIP 3.6 (Felsenstein, 2002) using D_A genetic distances (Saitou and Nei, 1987), Taiwan swamp buffaloes in the study of Lin et al. (2013) could be clustered into three subpopulations. The results corresponded to the observation of this study that the 94 Taiwan swamp buffaloes in HAPS could be divided into three subpopulations. However, Lin et al. (2013) did not mention the difference between the gray and white

Taiwan swamp buffaloes in HAPS in their study, while the STRUCTURE cluster analysis results in this study showed that the white Taiwan swamp buffaloes tended to be clustered into one subgroup.

Barker et al. (1997) estimated swamp buffaloes from Thailand (25), Malaysia (75), Indonesia (50), Philippines (26), and Australia (23) by 21 microsatellite markers, including *CSSM008*, *CSSM022*, *CSSM46*, and *CSSM61*, which were also used in this study. The average Na (4.4) detected by the 12 microsatellite markers among Taiwan swamp buffaloes in this study was lower than that (Na: 7.10) reported in multiple swamp buffaloes in the study of Barker et al. (1997), which might be because of the diversity of their sample sources. However, when Ho and He were first calculated in different populations separately, the average Ho (0.483) and He (0.506) among multiple swamp buffalo populations (Barker et al., 1997) were lower than the Ho (0.584) and He (0.577) in the Taiwan swamp buffalo population in this study. Notably, it was pointed out that *CSSM022* and *CSSM46* showed significant deviations from HWE and observed deficiency of heterozygotes, which corresponded to the results in this study. It might imply that *CSSM022* and *CSSM046* were not appropriate microsatellite markers to be used in population genetic analysis among swamp buffaloes.

Zhang et al. (2007) analyzed 18 Chinese indigenous swamp buffalo populations by 30 microsatellite markers, including *CSSM008*, *CSSM022*, *CSSM46*, *CSSM61*, and *ILSTS033*, which were also used in this study. Among the 30 microsatellite markers, the average Na (8.13) in 18 Chinese swamp buffalo populations was higher than that (4.4) in Taiwan swamp buffaloes among 12 microsatellite markers in this study. However, the average Ho (0.581) was higher among Taiwan swamp buffaloes in this study than that (0.535) in 18 Chinese swamp buffalo populations. It was indicated that *CSSM022* showed significant deviations ($P < 0.05$) from HWE due to heterozygote deficiency,

which might be attributable to the presence of null alleles. The assumption matched the results of *CSSM022* in this study.

Berthouly et al. (2010) estimated 744 Vietnamese swamp buffaloes from 13 locations in Vietnam by 20 microsatellite markers, including *CSSM008*, *CSSM022*, and *CSSM46*, which were also used in this study. It was indicated that there could be null alleles in *CSSM46*, and the observation corresponded to the results in this study that *CSSM046* had high null allele frequency (0.584). Three markers with possibility of null alleles were removed from the analysis in the study of Berthouly et al. (2010). Among the remaining 17 microsatellite markers, the average N_a (5.7) in Vietnamese swamp buffalo were higher than that (4.4) in Taiwan swamp buffaloes among 12 microsatellite markers in this study. However, the average H_o (0.584) was higher and F_{IS} (-0.008) was lower among Taiwan swamp buffaloes in this study than those (0.560 and 0.214, respectively) of the Vietnamese population. In addition, Berthouly et al. (2010) inferred that *CSSM022* deviated from HWE and was in heterozygote deficiency, which could indicate the presence of null alleles. This observation was again similar to the results of this study that *CSSM022* was significantly deviated from HWE ($P < 0.01$) and had high null allele frequency (0.462).

Saputra et al. (2020) estimated 80 Thai swamp buffaloes from seven locations in Thailand by ten microsatellite markers, including *BM1818*, *BM1824*, *ETH152*, and *CSSM46*, which were also used in this study. The average N_a (4.4) detected by the 12 microsatellite markers among 94 Taiwan swamp buffaloes in this study was lower than that reported in seven swamp buffalo populations in Thailand (4.7). It was emphasized that *ETH152* gave the highest level of diversity with eight alleles in the study of Saputra et al. (2020), but there were only five alleles observed in this study among Taiwan swamp buffaloes.

Singh et al. (2022) analyzed 76 Bhangor swamp buffaloes from India by 15 microsatellite markers, including *BM1818*, *ILSTS029*, *ILSTS033*, and *ILSTS058*, which were also used in this study. Among the 15 microsatellite markers, the average N_a (7.60), N_e (3.76), H_e (0.67), and PIC (0.63) in Bhangor swamp buffaloes from India were higher than those (4.4, 2.678, 0.581, and 0.521, respectively) in Taiwan swamp buffaloes among 12 microsatellite markers in this study. However, the average H_o (0.584) was higher and F_{IS} (-0.008) was lower among Taiwan swamp buffaloes in this study than those (0.53 and 0.114, respectively) in the study of Singh et al. (2022).

In summary, the N_a (4.4) of Taiwan swamp buffaloes estimated by 12 microsatellite markers in this study was generally lower than that in other swamp buffalo populations worldwide. However, the H_o (0.584) and H_e (0.581) in this study were almost as high or even higher compared with swamp buffaloes in other research. Moreover, the degree of inbreeding among Taiwan swamp buffaloes in this study was relatively milder (Table 5). In addition, it could be suggested that *CSSM022* and *CSSM046* were not appropriate microsatellite markers to be used in population genetic analysis among swamp buffaloes because of the existence of null alleles.

4.1.2 HD SNP genotyping array analysis

Colli et al. (2018) analyzed 15 swamp buffalo populations from China, Philippines, Thailand, Indonesia, and Brazil with the 90K Axiom® Buffalo Genotyping Array. A total of 14,456 polymorphic SNPs among Taiwan swamp buffaloes were remained after QC in this study. As for in the study of Colli et al. (2018), the polymorphic SNPs were 12,453 to 14,738 (Indonesia), 15,864 to 16,876 (China), 16,010 (Brazil), 16,433 to 16,653 (Thailand), and 19,451 (Philippines). The average H_o among Taiwan swamp buffaloes was 0.372 (Table 6), which was more than that in the swamp buffalo

populations in Indonesia (0.220 to 0.281), China (0.262 to 0.277), Brazil (0.292), and Thailand (0.272 to 0.294), but less than that in Philippines (0.413) (Colli et al., 2018). Similarly, the average H_e among Taiwan swamp buffaloes was 0.360 (Table 6), which was more than that in the swamp buffalo populations in Indonesia (0.216 to 0.271), China (0.260 to 0.267), Brazil (0.262), and Thailand (0.273 to 0.276), but less than that in Philippines (0.380) (Colli et al., 2018). As for the inbreeding degree, the average F_{IS} among Taiwan swamp buffaloes was -0.029 (Table 6), which was less than those in the swamp buffalo populations in Indonesia (-0.005 to 0.066), China (-0.006 to 0.045), and Thailand (0.026 to 0.067), but more than those in Brazil (-0.064) and Philippines (-0.032) (Colli et al., 2018).

Using a subset of 10,821 SNPs that were informative in both the river and swamp buffaloes from 90K Axiom® Buffalo Genotyping Array, Lu et al. (2020) got the results that the average H_o and H_e among river buffaloes in China were 0.418 and 0.422, respectively, and the average H_o and H_e among swamp buffaloes in China were 0.344 and 0.356, respectively. The average H_o and H_e among Taiwan swamp buffaloes (0.372 and 0.360) (Table 6) were higher than those in the swamp buffaloes in China, but lower than those in the river buffaloes in China (Lu et al., 2020).

The polymorphic SNPs obtained from 90K Axiom® Buffalo Genotyping Array after QC were much more in Iranian river buffaloes: 64,866 (Mokhber et al., 2018), 58,588 to 63,824 (Mokhber et al., 2019), and 60,140 (Davoudi et al., 2020) than that in the Taiwan swamp buffalo (14,456) in this study. The average H_o among Iranian river buffaloes (0.386) (Davoudi et al., 2020) was slightly more than that of the Taiwan swamp buffaloes (0.372) (Table 6) in this study. Likely, the SNP number after QC and merge was 57,455 from 90K Axiom® Buffalo Genotyping Array among the river buffaloes in Iran, Turkey, Pakistan, and Egypt (Rahimadar et al., 2021), which was

much more than that in the Taiwan swamp buffalo (14,456) in this study.

Thakor et al. (2021) analyzed genetic variability and population structure of seven Indian river buffalo breeds with 90K Axiom® Buffalo Genotyping Array. The polymorphic SNPs used for further analysis after QC was 75,704, which was much more than that of the Taiwan swamp buffalo (14,456) in this study. The average H_o among the seven Indian river buffalo breeds was from 0.3719 to 0.3864, and the average H_e was from 0.3643 to 0.3846. The average H_o and H_e among Taiwan swamp buffaloes (0.372 and 0.360, respectively) (Table 6) in this study were similar but slightly less than those of the Indian river buffaloes. As for the inbreeding degree, the average F_{IS} among Taiwan swamp buffaloes in this study was -0.029 (Table 6), which was between that of the Indian river buffaloes (-0.0046 to -0.0314) (Thakor et al., 2021).

Noce et al. (2021) explored the genetic diversity of river buffaloes in Germany, Bulgaria, Romania, and Hungary with a total of 36,014 SNPs from 90K Axiom® Buffalo Genotyping Array. The average H_o among Taiwan swamp buffaloes in this study was 0.372 (Table 6), which was less than those in the river buffalo populations in Germany (0.38 to 0.40), Romania (0.38), and Bulgaria (0.41), but slightly more than that in Hungary (0.35 to 0.37). Similarly, the average H_e among Taiwan swamp buffaloes in this study was 0.360 (Table 6), which was less than those in the river buffalo populations in Germany (0.35 to 0.39), Romania (0.36 to 0.37), and Bulgaria (0.40), but slightly more than that in Hungary (0.32 to 0.35) (Noce et al., 2021).

In brief, the polymorphic SNPs detected in Taiwan swamp buffaloes (14,456) in this study were generally less than other swamp buffaloes worldwide, but the average H_o (0.372) and H_e (0.360) were higher than many of the other swamp buffalo populations. In addition, the degree of inbreeding of Taiwan swamp buffaloes in this study was relatively milder compared with swamp buffaloes in other research. On the

other hand, compared with river buffalo populations, the polymorphic SNPs detected in Taiwan swamp buffaloes in this study were much less, but the average H_o and H_e were slightly less in general. The results corresponded to the description that many SNPs in the river buffalo are monomorphic in the swamp buffalo, and many loci in the 90K Axiom® Buffalo Genotyping Array are not informative for the swamp buffalo (Iamartino et al., 2017).

4.1.3 Comparison between microsatellite markers and HD SNP genotyping array analysis

The average H_o (0.372), H_e (0.360), and PIC (0.282) obtained from the 14,456 SNPs (Table 6) were all lower than those from the 12 microsatellite markers (0.584, 0.581, and 0.521, respectively) (Table 5), indicating medium polymorphism in the 94 Taiwan swamp buffaloes in HAPS by the 14,456 SNPs, but high polymorphism by the 12 microsatellite markers in this study. The same observation was found in the study of Sturm et al. (2020) that the mean H_o and H_e calculated from 9 microsatellite markers were higher across all populations than 9,000 SNPs. The fundamental reason should be that the microsatellite markers were multiallelic, while the SNPs were biallelic. The utmost N_a that could be detected by the SNPs was 2, and the maximum value of the H_e and PIC of the SNPs were 0.5 (Singh et al., 2013; Mourad et al., 2020; Zimmerman et al., 2020). However, the number of the SNPs (14,456) used in this study should be sufficient and could even perform better for the population genetic analysis compared with that of the 14 microsatellite markers (Kruglyak, 1997; Glaubitz et al., 2003; Flanagan and Jones, 2019; Weng et al., 2021). The average F_{IS} among the 14,456 SNPs was negative (-0.029) (Table 6), indicating no serious inbreeding problem among the 94 Taiwan swamp buffaloes. This result corresponded to the results of the microsatellite

markers ($F_{IS} = -0.008$) after removing the two markers that might contain null alleles.

The phylogenetic trees based on the two methods, 14 microsatellite markers (Figure 9) and 14,456 SNPs (Figure 13), seemed to be quite similar. Three subpopulations were identified in both of the results. The clustering of the individuals in the two methods was highly similar, but not exactly the same. For example, the 16 white Taiwan swamp buffaloes were all classified into the same subpopulation in the phylogenetic trees based on the 14,456 SNPs, while four of the white swamp buffaloes were clustered into a different subpopulation in the phylogenetic trees based on the 14 microsatellite markers. In the research of Singh et al. (2013) on 375 Indian rice varieties, the neighbor-joining trees constructed using 36 microsatellite markers and 36 SNP markers both grouped the rice varieties into three major clusters, but the numbers of varieties grouped into the clusters were different. This observation was similar with the results in this study.

The numbers on the nodes of the phylogenetic trees indicated the percentage bootstrap values generated from 1,000 times of resampling (Figure 10 and Figure 14). The average bootstrap value in the results of the 14,456 SNPs (72.11) was much higher than that of the 14 microsatellite markers (15.09). Therefore, it could be inferred that the repeatability and the reliability of the phylogenetic trees drawn with the 14,456 SNPs were greater than that drawn with the 14 microsatellite markers. Similar results were found in the study of Hillel et al. (2007) when assessing biodiversity of various breeds of chicken. The average bootstrap value of the neighbor-joining phylogenetic tree based on 29 microsatellites (47.4) was relatively lower than that based on the 145 SNPs (75.7).

The STRUCTURE cluster analysis plots based on the two methods, 14 microsatellite markers (Figure 11A) and 14,456 SNPs (Figure 15), had similar results

when the K value was three. They both showed that among the 94 Taiwan swamp buffaloes in HAPS, all of the 16 white buffaloes could be clustered into one subpopulation with some gray buffaloes, and the remaining gray buffaloes could be divided into the other two subpopulations. In addition, in both of the results, three white swamp buffaloes (W464, W789 and W799) tended to be classified into a different cluster from the other white swamp buffaloes when the K value got greater. It might indicate that these three white swamp buffaloes had some genetic difference compared with the other 13 white swamp buffaloes and were a little more alike to some of the gray buffaloes genetically. Álvarez et al. (2021) also found similar patterns in microsatellite- and SNP-based structure analyses when using 33 microsatellites and 543,595 SNPs to estimate 185 cattle in three different West African countries. Similarly, population structure analysis conducted with the 9,000 SNPs were in agreement with STRUCTURE analysis based on 9 microsatellite markers in the study of Sturm et al. (2020).

The most optimal K value was three in the results of the 14 microsatellite markers in this study (Figure 11), which was consistent with the previous literature (Lin et al., 2013). In this study, it was further confirmed that all the white swamp buffaloes from HAPS could be distinguished into one subpopulation in the STRUCTURE analysis. It could be inferred that the genetic structure of the white Taiwan swamp buffalo was different from that of the gray Taiwan swamp buffalo in HAPS. On the other hand, the most optimal K value was six in the results of the 14,456 SNPs. It might be indicated that the larger amount of genetic information obtained from the 14,456 SNPs could divide the 94 Taiwan swamp buffaloes into more detailed subgroups (Figure 15). In the STRUCTURE study of Singh et al. (2013), Indian rice varieties were divided into five clusters using 36 microsatellite markers and 15 clusters using 36 SNPs. As a result, it

was indicated that the population structure of crops could be better explained with SNP markers, which corresponded to the assumption of this study. Similarly, in the study of Laoun et al. (2020), when estimating three pairs of datasets of sheep and cattle, STRUCTURE analyses showed very consistent patterns between the two types of markers (21 to 30 microsatellites markers and 15,560 to 31,184 SNP markers), but it was inferred that the results from microsatellite markers were less accurate.

In conclusion, the genetic parameters estimated by microsatellite markers tend to be higher than SNP markers due to their original characteristics. However, if the number of SNP markers are sufficient ($>1,000$ SNPs) (Sturm et al., 2020), the genetic structure of a population may be better described by SNP markers. With the genotyping array, the large number of SNPs may provide more information and more precise results than 10-20 microsatellite markers in population genetic structure analysis. Furthermore, the genetic information from the genotyping array can be used to conduct other studies, for example, GWAS. However, the higher price of the genotyping array, the computational techniques needed for the large number of SNPs, and whether a commercial genotyping array is available for the target samples should be put into consideration.

4.2 Coat color gene analysis of Taiwan swamp buffalo

Since no mutant allele indicating the existence of the *LINE-1* insertion in the *ASIP* gene was found in the white Taiwan swamp buffaloes from HAPS in this study, the cause of the white coat color of the Taiwan swamp buffalo should be different from what Liang et al. (2021) has discovered. Moreover, according to the pedigree data of the Taiwan swamp buffalo in HAPS (Table 12), two gray buffaloes could give birth to a white calf (Figure 29), while there was no record that parents are both white buffaloes having a gray offspring. It might thus be inferred that the white coat color of the Taiwan swamp buffalo in HAPS should be a recessive trait, which was inconsistent with the statement of Liang et al. (2021) that the white coat color of the swamp buffalo was a Mendelian dominant inheritance.

Table 12. Incidence of the gray and white coat color of the Taiwan swamp buffalo based on the pedigree record of 129 pair combinations in HAPS

Parental coat color pair combination	Coat color of the offspring	Number of the offspring
White ♀ x white ♂ (n=10)	White	10
	Gray	0
White ♀ x gray ♂ (n=9)	White	5
	Gray	4
White ♂ x gray ♀ (n=5)	White	3
	Gray	2
Gray ♀ x gray ♂ (n=105)	White	2
	Gray	103

n: number of pairs



Figure 29. A white buffalo calf (gray ♀ x gray ♂) and its gray buffalo parents in HAPS.

The left one was the gray cow, the middle one was the white calf, and the right one was the gray bull in HAPS.

In fact, the variation *MC1R* c.901C>T detected to be highly associated with the white coat color of the Taiwan swamp buffalo in this study was also discovered in the study of Chuang (2007). However, it was not considered as a variant between the gray and white Taiwan swamp buffaloes, but a variant just between the buffalo and the cattle. Chuang (2007) sequenced the *MC1R* gene of six gray and six white Taiwan swamp buffaloes from HAPS, and the results showed that there was no difference in the *MC1R* gene of them. The reason why Chuang (2007) did not detect the c.901C, but only reported the c.901T was mysterious. It might be possible that all of the gray Taiwan swamp buffaloes sequenced in the study of Chuang (2007) were heterozygous, and the wild-type c.901C was not detected out of some reasons.

The genotyping results of the *MC1R* c.901C>T corresponded to the previous assumption based on the pedigree data (Table 12) that the white coat color of the Taiwan swamp buffalo should be a recessive trait. However, in spite of the significant *P*-value of the study, there was still an exception that one white swamp buffalo was heterozygous. It was checked that the white swamp buffalo was recorded as a white buffalo. Nevertheless, the exact phenotype of the buffalo could not be verified. There

might be a possibility that the gray coat color of the Taiwan swamp buffalo was an incomplete dominance trait, or there should be other genetic variants regulating the coat color of the Taiwan swamp buffalo. In fact, coat color of some of the gray Taiwan swamp buffaloes seemed to be darker and some seemed to be lighter (Figure 30). The way people described the coat color of the gray swamp buffalo was also various. They were called black (Liang et al., 2021), gray (Miao et al., 2010), and dark gray or solid (Yusnizar et al., 2015) swamp buffaloes. However, the degree of the darkness of the coat color of the gray Taiwan swamp buffaloes was not considered in this study. It could not be verified whether the gray Taiwan swamp buffaloes in HAPS with *MC1R* c.901C>T heterozygotes had lighter appearance.



Figure 30. The different degree of the darkness of the coat color among the Taiwan swamp buffaloes in HAPS. From the left to the right, (A) was a white Taiwan swamp buffalo. (B), (C), and (D) were gray Taiwan swamp buffaloes with lighter coat color. (E) was a gray Taiwan swamp buffalo with darker coat color.

Melanocytes are dendritic cells located in the basal layer of skin. Melanocyte synthesizes and stores melanin in melanosomes, which are then transported into keratinocytes (Cichorek et al., 2013). The skin color is determined by the amount, type,

and packaging of melanin. The *MC1R* pathway is a major determinant for the amount and type of melanin synthesized by melanocytes. By enhancing eumelanin synthesis, melanosome transfer, and melanin deposition in keratinocytes, *MC1R* gene signaling regulate both basal pigmentation and the UV induced tanning response (Wolf Horrell et al., 2016). The *MC1R* c.901C>T variation was predicted to cause an amino acid change from arginine to cysteine at MC1R protein position 301 (p.R301C). Since the amino acid biochemical properties changed from basic to polar, the SNP might cause some structural impact on the MC1R protein. In fact, all of the tools in this study predicted the variant to be deleterious. Based on the MC1R structure of the human (García-Borrón et al., 2005) and the alpaca (Chandramohan et al., 2015), it can be inferred that the p.R301C of the buffalo should be at the C-terminus of the MC1R protein, which might be essential for the protein structure functional coupling efficacy (Sánchez-Más et al., 2005). The MC1R p.R301C mutation might lead to an additional acylation of cysteine residues within the lipid bilayer, which could affect the structure of MC1R C-terminus, the normal conformational change, and the interaction with the G-protein.

Interestingly, the MC1R 301 mutation was also found associated with the light coat color of the dog (Ollivier et al., 2013; Anderson et al., 2020), mammoth (Römpler et al., 2006), alpaca (*Lama pacos*) (Powell et al., 2008; Feeley and Munyard, 2009; Chandramohan et al., 2015), Peruvian Alpaca (*Vicugna pacos*) (Guridi et al., 2011), the dromedary (*Camelus dromedarius*) (Alshanbari et al., 2019), and Arabian camel (Almathen et al., 2018) (Table 13). It was indicated that the MC1R p.R301C polymorphism was potentially damaging to MC1R protein structure and function, resulting in decreased ligand-induced cAMP accumulation in the experiment of Feeley (2015). The possible explanations were the disability of the MC1R to be correctly

transported to the cell membrane, leading to a reduction in the density of MC1R on the surface of melanocytes, or the interruption of proper G protein coupling (García-Borrón et al., 2005).



Table 13. MC1R mutations at protein position 301 and their amino acid change, function significance, and its effect found in various species in past literature

Specie	SNP observed	Amino acid change	Function significance	MC1R effect	Reference
Dog	c.901C>T	p.R301C	Amino acid changed from basic to polar	Light fiber and reduced eumelanin pigment	Ollivier et al., 2013; Anderson et al., 2020
Mammoth	NA	p.R301S	Amino acid changed from basic to polar; Reduction in MC1R signaling	Light fiber	Römpler et al., 2006
Alpaca	c.901C>T	p.R301C	Amino acid changed from basic to polar; Reduction in MC1R signaling	White, fawn and brown coat color	Powell et al., 2008; Freely and Munyard, 2009; Guridi et al., 2011; Chandramohan et al., 2015
Dromedary	c.901C>T	p.R301C	Amino acid changed from basic to polar	White and brown coat color	Almathen et al., 2018; Alshanbari et al., 2019
Taiwan swamp buffalo	c.901C>T	p.R301C	Amino acid changed from basic to polar	White coat color	This study

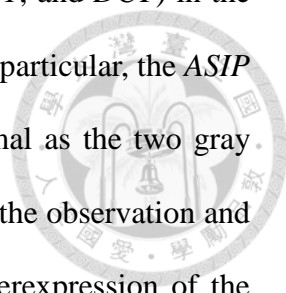
In addition, during our experiments, it was surprising to find that the skin of the ventral side ear and the back of an adult white Taiwan swamp buffalo from HAPS were dark black (Figure 5), but its hair was still white. The pigmented skin might be caused by the UV radiation of the sunlight since the hair of the buffalo was sparse, and its skin

could be exposed to the sunlight easily (Marai and Haebe, 2010). On the other hand, the coat color of the gray Taiwan swamp buffalo calf was brown at birth (Figure 8), and the phenomenon was also mentioned by Ali et al. (2022) in the Azakheli buffalo, a breed of river buffalo in Pakistan. The brown coat color of the Taiwan swamp buffalo calf would turn gray as it aged, but the exact time was not recorded. The reason for the coat color change related to the age of the Taiwan swamp buffalo was not clear.

In the results of the adult white Taiwan swamp buffalo in this study, the gene expression between different parts of skin tissue were different, especially the dorsal and the ventral side ear (Figure 25). Ear skin sample can be accessed more easily compared with other part of body. However, studies in the past (Chuang, 2007; Liang et al., 2021) did not mention if the two sides of the ear skin tissue were separated. From the results of this study, it could be recommended that the two sides of the ear skin tissue should be discussed independently.

On the other hand, the *MC1R* gene expression was higher and the *ASIP* gene expression was lower in the darker color ventral side ear compared with the lighter color dorsal side ear in the adult white Taiwan swamp buffalo in this study. The same results were observed between the darker color back skin and the lighter color abdomen skin. The phenomenon was consistent with the *MC1R* pathway theory mentioned in the literature review. However, the *ASIP* gene seemed to upregulate the *MITF* gene and the *TYR* family genes, which was inconsistent with the theory. Nevertheless, Guibert et al. (2004) also indicated that the pheomelanin coat color dilution in French cattle breeds was not correlated with the *TYR*, *TYRP1*, and *DCT* transcription levels. The relationship between the gene expression in the *MC1R* pathway and the coat color of the cattle and the buffalo should be further clarified.

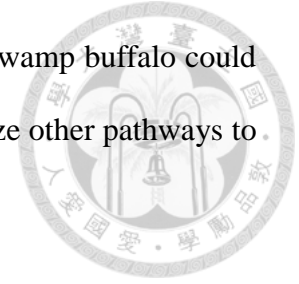
In the results of the gray (brown) and white Taiwan swamp buffalo calves in this



study, the expression of the genes (*MC1R*, *ASIP*, *MITF*, *TYR*, *TYRP1*, and *DCT*) in the *MC1R* pathway had no significant association with the coat color. In particular, the *ASIP* gene expression of the white Taiwan swamp buffalo calf was normal as the two gray (brown) Taiwan swamp buffalo calves, which was inconsistent with the observation and the hypothesis that Liang et al. (2021) has proposed about the overexpression of the *ASIP* gene in the white swamp buffalo. The *MC1R* and *MITF* gene expression levels were not significantly different between the white and gray swamp buffaloes ($P > 0.05$) in the study of Liang et al. (2021), which was consistent to the results in this study between the gray and white Taiwan swamp buffalo. The *TYR* and *TYRP1* gene expression levels were lower in the white swamp buffaloes than in the gray swamp buffaloes ($P < 0.01$) in the study of Liang et al. (2021), but there was no significant difference between the gray and white Taiwan swamp buffalo in this study and in the study of Chuang (2007). Liang et al. (2021) and Chuang (2007) both reported that the *DCT* gene expression levels in the white swamp buffaloes were lower than those in the gray swamp buffaloes ($P < 0.01$ and $P < 0.05$, respectively), while there was no significant difference between the gray and white Taiwan swamp buffalo in this study.

In addition, with the Fontana-Masson staining results, it could be indicated that the skin of the white Taiwan swamp buffalo had less melanin deposition compared with the gray Taiwan swamp buffalo, but the white Taiwan swamp buffalo still had the ability to produce melanin. This finding corresponded with the study of Chuang (2007), but was inconsistent with the results of Liang et al. (2021). Moreover, the skin of the white Taiwan swamp buffalo could accumulate melanin, resulting in the darker color of the ventral side ear and the back skin, probably because of long-term sunlight stimulation (Nguyen and Fisher, 2019). It was indicated that there were many other pathways besides the *MC1R* pathway that could stimulate the *MITF* gene and the *TYR* family

genes and thus lead to melanin production under ultraviolet radiation (Cichorek et al., 2013; Dorgaleleh et al., 2020). The MC1R function of the Taiwan swamp buffalo could be only partially damaged, or the Taiwan swamp buffalo might utilize other pathways to produce melanin.

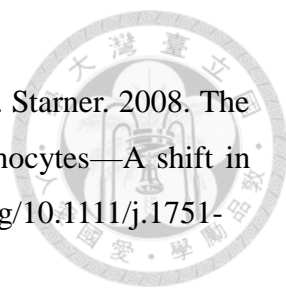


Chapter 5 Conclusion

In this study, the genetic polymorphism of the 94 Taiwan swamp buffaloes in HAPS was high ($PIC > 0.5$) detected by 12 microsatellite markers (0.521), but moderate ($0.25 < PIC < 0.5$) detected by 14,456 SNPs from 90K Axiom® Buffalo Genotyping array (0.282). The degree of inbreeding was not serious based on both of the two genetic markers/methods. The phylogenetic trees drawn by the two methods were roughly the same, but the results obtained with the 14,456 SNPs were more reliable and accurate. The 94 Taiwan swamp buffaloes in HAPS could be divided into three subpopulations. All of the 16 white buffaloes could be clustered into one subgroup with some of the gray buffaloes, while the other gray buffaloes could be divided into two subgroups.

With the results of *ASIP* genotyping, gene expression analysis, and the pedigree data, it could be confirmed that the cause for the white coat color of the Taiwan swamp buffalo should be different from what Liang et al. (2021) discovered. In contrast, with the GWAS, 17 SNPs and 26 genes were discovered to be associated with the coat color of Taiwan swamp buffalo, which have not been reported before. In particular, the *MC1R* c.901C>T (p.R301C) found in this study was a strong candidate that might damage the *MC1R* function, prevent normal melanin synthesis, and thus cause the white coat color of the Taiwan swamp buffalo. The *MC1R*, *ASIP*, *MITF*, *TYR*, *TYRP1*, and *DCT* gene expression between one white calf and two gray (brown) calves had no significant difference. The skin of the white Taiwan swamp buffalo could still produce melanin, but less than the gray Taiwan swamp buffalo. However, the exact mechanism of the candidate variant (*MC1R* c.901C>T) causing the white coat color of Taiwan swamp buffalo remained unclear, and further studies were needed to verify the hypothesis.

REFERENCE

- 
- Abdel-Malek, Z. A., J. Knittel, A. L. Kadekaro, V. B. Swope, and R. Starner. 2008. The melanocortin 1 receptor and the UV response of human melanocytes—A shift in paradigm. *Photochem. Photobiol.* 84:501-508. doi: <https://doi.org/10.1111/j.1751-1097.2008.00294.x>.
- Abdel-Shafy, H., M. A. A. Awad, H. El-Regalaty, S. E. D. El-Assal, and S. Abou-Bakr. 2020. Prospecting genomic regions associated with milk production traits in Egyptian buffalo. *J. Dairy Res.* 87:389-396. doi: <https://doi.org/10.1017/S0022029920000953>.
- Abo Bakr, S., M. A. Ibrahim, Y. Hafez, S. Abdel-Salam, M. Attia, and W. Mekkawy. 2012. Genetic characteristics of Egyptian buffalo using DNA microsatellite markers. *Egypt. J. Anim. Prod.* 49:121-126.
- Acosta, A., O. Uffo, A. Sanz, D. Obregón, R. Ronda, R. Osta, I. Martin-Burriel, C. Rodellar, and P. Zaragoza. 2014. Genetic characterization of the Cuban water buffalo population using microsatellite DNA markers. *Buffalo Bull.* 33:101-106. doi: <http://dx.doi.org/10.14456/ku-bufbu.2014.19>.
- Adamack, A. T., and B. Gruber. 2014. PopGenReport: simplifying basic population genetic analyses in R. *Methods Ecol. Evol.* 5:384-387. doi: <https://doi.org/10.1111/2041-210X.12158>.
- Adzhubei, I. A., S. Schmidt, L. Peshkin, V. E. Ramensky, A. Gerasimova, P. Bork, A. S. Kondrashov, and S. R. Sunyaev. 2010. A method and server for predicting damaging missense mutations. *Nat. Methods* 7:248-249. doi: <https://doi.org/10.1038/nmeth0410-248>.
- Ahmed, S., A. S. Qureshi, M. Usman, S. Rehan, F. Deebea, M. K. Ateeq, M. Younus, M. A. Naeem, Z. Umar, and M. S. A. Taseer. 2023. Seasonal changes in the scrotal skin histology in relation to thermoregulation and testosterone level in camel and buffalo bull. *Anat. Histol. Embryol.* 00:1-10. doi: <https://doi.org/10.1111/ah.12933>.
- Aigner, B., U. Besenfelder, M. Müller, and G. Brem. 2000. Tyrosinase gene variants in different rabbit strains. *Mamm. Genome* 11:700-702. doi: <https://doi.org/10.1007/s00350010120>.
- Ali, S., F. Nabi, M. Awais, S. K. Fareed, J. Hussain, A. C. Adeola, R. Khan, N. Ahmed, and G. Quan. 2022. Genetic diversity relationship in Azakheli buffalo inferred from

mtDNA and MC1R sequences comparison. *Biomed Res. Int.* 2022:5770562. doi: <https://doi.org/10.1155/2022/5770562>.

Almathen, F., H. Elbir, H. Bahbahani, J. Mwacharo, and O. Hanotte. 2018. Polymorphisms in *MC1R* and *ASIP* genes are associated with coat color variation in the Arabian camel. *J. Hered.* 109:700-706. doi: <https://doi.org/10.1093/jhered/esy024>.

Alshanbari, F., C. Castaneda, R. Juras, A. Hillhouse, M. N. Mendoza, G. A. Gutiérrez, F. A. Ponce de León, and T. Raudsepp. 2019. Comparative FISH-mapping of *MC1R*, *ASIP*, and *TYRP1* in new and old world camelids and association analysis with coat color phenotypes in the dromedary (*Camelus dromedarius*). *Front. Genet.* 10:340. doi: <https://doi.org/10.3389/fgene.2019.00340>.

Álvarez, I., I. Fernández, A. Traoré, N. A. Menéndez-Arias, and F. Goyache. 2021. Population structure assessed using microsatellite and SNP data: an empirical comparison in West African cattle. *Animals* 11:151. doi: <https://doi.org/10.3390/ani11010151>.

Anderson, C. A., F. H. Pettersson, J. C. Barrett, J. J. Zhuang, J. Ragoussis, L. R. Cardon, and A. P. Morris. 2008. Evaluating the effects of imputation on the power, coverage, and cost efficiency of genome-wide SNP platforms. *Am. J. Hum. Genet.* 83:112-119. doi: <https://doi.org/10.1016/j.ajhg.2008.06.008>.

Anderson, H., L. Honkanen, P. Ruotanen, J. Mathlin, and J. Donner. 2020. Comprehensive genetic testing combined with citizen science reveals a recently characterized ancient *MC1R* mutation associated with partial recessive red phenotypes in dog. *Canine Med. Genet.* 7:16. doi: <https://doi.org/10.1186/s40575-020-00095-7>.

Ángel-Marín, P. A., H. Cardona, M. Moreno-Ochoa, and M. F. Cerón-Muñoz. 2010. Analysis of genetic diversity in Colombian buffalo herds. *Rev. Colomb. Cienc. Pecu.* 23:411-421.

Animal Genetic Resources Information Network in Taiwan. 2010. Taiwan swamp buffalo breed registration application document. Available online: <https://www.angr.in.tlri.gov.tw/atlas/atlas2006/Buffalo/Buffalo.htm> (accessed on May 26, 2023).

Animal Genetic Resources Information Network in Taiwan. 2015. Taiwan white swamp buffalo breed registration application document. Available online: https://www.angr.in.tlri.gov.tw/NewBreed/2015/WB_data.pdf (accessed on May 26, 2023).

- Arora, R., B. D. Lakhchaura, R. B. Prasad, M. S. Tantia, and R. K. Vijh. 2004. Genetic diversity analysis of two buffalo populations of northern India using microsatellite markers. *J. Anim. Breed. Genet.* 121:111-118. doi: <https://doi.org/10.1111/j.1439-0388.2004.00451.x>.
- Attia, M., S. Abou-Bakr, and Y. Hafez. 2014. Genetic polymorphism of seven microsatellite DNA markers in Egyptian buffalo. *Anim. Biotechnol. (Cattles, Buffalo)* 7:7.
- Babar, M. E., T. Hussain, A. Nadeem, R. Jabeen, and M. Javed. 2009. Genetic characterization of Azakheli buffalo breed of Pakistan using microsatellite DNA markers. *Pak. J. Zool. Suppl. Ser.* 9:361-366.
- Balagué-Dobón, L., A. Cáceres, and J. R. González. 2022. Fully exploiting SNP arrays: a systematic review on the tools to extract underlying genomic structure. *Brief. Bioinform.* 23:1-22. doi: <https://doi.org/10.1093/bib/bbac043>.
- Barbosa, A. J., L. P. Castro, A. Margarida, and M. F. Nogueira. 1984. A simple and economical modification of the Masson-Fontana method for staining melanin granules and enterochromaffin cells. *Stain Technol.* 59:193-196. doi: <https://doi.org/10.3109/10520298409113855>.
- Barbosa, J. D., B. I. O. Possidonio, J. B. Dos Santos, H. Oliveira, A. I. J. Sousa, C. C. Barbosa, E. A. Beuttemuller, N. Silveira, M. F. Brito, and F. M. Salvarani. 2023. Leucoderma in buffaloes (*Bubalus bubalis*) in the Amazon biome. *Animals* 13:1665. doi: <https://doi.org/10.3390/ani13101665>.
- Barker, G. C. 2002. Microsatellite DNA: a tool for population genetic analysis. *Trans. R. Soc. Trop. Med. Hyg.* 96:S21-S24. doi: [https://doi.org/10.1016/S0035-9203\(02\)90047-7](https://doi.org/10.1016/S0035-9203(02)90047-7).
- Barker, J. S. F., S. S. Moore, D. J. S. Hetzel, D. Evans, and K. Byrne. 1997. Genetic diversity of Asian water buffalo (*Bubalus bubalis*): microsatellite variation and a comparison with protein-coding loci. *Anim. Genet.* 28:103-115. doi: <https://doi.org/10.1111/j.1365-2052.1997.00085.x>.
- Bendl, J., J. Stourac, O. Salanda, A. Pavelka, E. D. Wieben, J. Zendulka, J. Brezovsky, and J. Damborsky. 2014. PredictSNP: robust and accurate consensus classifier for prediction of disease-related mutations. *PLoS Comput. Biol.* 10:e1003440. doi: <https://doi.org/10.1371/journal.pcbi.1003440>.
- Berardino, D. D., and L. Iannuzzi. 1981. Chromosome banding homologies in swamp

- and Murrah buffalo. *J. Hered.* 72:183-188. doi: <https://doi.org/10.1093/oxfordjournals.jhered.a109469>.
- Berthouly, C., X. Rognon, T. Nhu Van, A. Berthouly, H. Thanh Hoang, B. Bed'Hom, D. Laloë, C. Vu Chi, E. Verrier, and J.-C. Maillard. 2010. Genetic and morphometric characterization of a local Vietnamese swamp buffalo population. *J. Anim. Breed. Genet.* 127:74-84. doi: <https://doi.org/10.1111/j.1439-0388.2009.00806.x>.
- Bromberg, Y., and B. Rost. 2007. SNAP: predict effect of non-synonymous polymorphisms on function. *Nucleic Acids Res.* 35:3823-3835. doi: <https://doi.org/10.1093/nar/gkm238>.
- Bruford, M. W., and R. K. Wayne. 1993. Microsatellites and their application to population genetic studies. *Curr. Opin. Genet. Dev.* 3:939-943. doi: [https://doi.org/10.1016/0959-437X\(93\)90017-J](https://doi.org/10.1016/0959-437X(93)90017-J).
- Capriotti, E., R. Calabrese, and R. Casadio. 2006. Predicting the insurgence of human genetic diseases associated to single point protein mutations with support vector machines and evolutionary information. *Bioinformatics* 22:2729-2734. doi: <https://doi.org/10.1093/bioinformatics/btl423>.
- Carlsson, J. 2008. Effects of microsatellite null alleles on assignment testing. *J. Hered.* 99:616-623. doi: <https://doi.org/10.1093/jhered/esn048>.
- Chakraborty, R., Y. Zhong, L. Jin, and B. Budowle. 1994. Nondetectability of restriction fragments and independence of DNA fragment sizes within and between loci in RFLP typing of DNA. *Am. J. Hum. Genet.* 55:391-401.
- Chandramohan, B., C. Renieri, V. La Manna, and A. La Terza. 2015. The alpaca *melanocortin 1 receptor*: gene mutations, transcripts, and relative levels of expression in ventral skin biopsies. *Sci. World J.* 2015:265751. doi: <https://doi.org/10.1155/2015/265751>.
- Chen, Y. T., P. H. Chuang, J. C. Chen, and A. K. Su. 2019. Genetic diversity analysis of mitochondrial D-loop region, *Cyt b* and *12S rRNA* genes of Taiwan swamp buffalo (*Bubalus bubalis*). *J. Chin. Soc. Anim. Sci.* 48:105-118.
- Chuang, P. H. 2007. Genotyping of white coat color in Taiwan water buffalo (*Bubalus bubalis*) (Master's thesis, National Dong Hwa University, Hualien County).
- Cichorek, M., M. Wachulska, A. Stasiewicz, and A. Tymińska. 2013. Skin melanocytes: biology and development. *Postep. Derm. Alergol.* 30:30-41. doi: <https://doi.org/10.5114/pdia.2013.33376>.

- Cieslak, M., M. Reissmann, M. Hofreiter, and A. Ludwig. 2011. Colours of domestication. *Biol. Rev.* 86:885-899. doi: <https://doi.org/10.1111/j.1469-185X.2011.00177.x>.
- Clark, L. V., and M. Jasieniuk. 2011. POLYSAT: an R package for polyploid microsatellite analysis. *Mol. Ecol. Resour.* 11:562-566. doi: <https://doi.org/10.1111/j.1755-0998.2011.02985.x>.
- Clark, L. V., and A. D. Schreier. 2017. Resolving microsatellite genotype ambiguity in populations of allopolyploid and diploidized autopolyploid organisms using negative correlations between allelic variables. *Mol. Ecol. Resour.* 17:1090-1103. doi: <https://doi.org/10.1111/1755-0998.12639>.
- Cockrill, W. R. 1967. The water buffalo. *Sci. Am.* 217:118-126. doi: [https://doi.org/10.1016/s0007-1935\(17\)31782-7](https://doi.org/10.1016/s0007-1935(17)31782-7).
- Cockrill, W. R. 1977. The water buffalo: domestic animal of the future. *Bov. pract.* 92-98. doi: <https://doi.org/10.21423/bovine-vol1977no12p92-98>.
- Cockrill, W. R. 1981. The water buffalo: a review. *Br. Vet. J.* 137:8-16. doi: [https://doi.org/10.1016/S0007-1935\(17\)31782-7](https://doi.org/10.1016/S0007-1935(17)31782-7).
- Colli, L., M. Milanese, E. Vajana, D. Iamartino, L. Bomba, F. Puglisi, M. Del Corvo, E. L. Nicolazzi, S. S. E. Ahmed, J. R. V. Herrera, L. Cruz, S. Zhang, A. Liang, G. Hua, L. Yang, X. Hao, F. Zuo, S. J. Lai, S. Wang, R. Liu, Y. Gong, M. Mokhber, Y. Mao, F. Guan, A. Vlaic, B. Vlaic, L. Ramunno, G. Cosenza, A. Ahmad, I. Soysal, E. Ünal, M. Ketudat-Cairns, J. F. Garcia, Y. T. Utsunomiya, P. S. Baruselli, M. E. J. Amaral, R. Parnpai, M. G. Drummond, P. Galbusera, J. Burton, E. Hoal, Y. Yusnizar, C. Sumantri, B. Moioli, A. Valentini, A. Stella, J. L. Williams, and P. Ajmone-Marsan. 2018. New insights on water buffalo genomic diversity and post-domestication migration routes from medium density SNP chip data. *Front. Genet.* 9:53. doi: <https://doi.org/10.3389/fgene.2018.00053>.
- Corpet, F. 1988. Multiple sequence alignment with hierarchical clustering. *Nucl. Acids Res.* 16:10881-10890. doi: <https://doi.org/10.1093/nar/16.22.10881>.
- Crossley, B. M., J. Bai, A. Glaser, R. Maes, E. Porter, M. L. Killian, T. Clement, and K. Toohey-Kurth. 2020. Guidelines for Sanger sequencing and molecular assay monitoring. *J. Vet. Diagn. Invest.* 32:767-775. doi: <https://doi.org/10.1177/1040638720905833>.
- da Costa Barros, C., D. J. de Abreu Santos, R. R. Aspilcueta-Borquis, G. M. F. de

- Camargo, F. R. de Araújo Neto, and H. Tonhati. 2018. Use of single-step genome-wide association studies for prospecting genomic regions related to milk production and milk quality of buffalo. *J. Dairy Res.* 85:402-406. doi: <https://doi.org/10.1017/S0022029918000766>.
- da Cruz, V. A. R., J. S. Alves, M. S. Bastos, L. S. M. Oliveira, I. D. P. S. Diaz, L. F. B. Pinto, R. B. Costa, and G. M. F. de Camargo. 2020. *MC1R* gene and coat color in buffaloes. *Anim. Genet.* 51:345-346. doi: <https://doi.org/10.1111/age.12910>.
- Damé, M. C. F., G. M. Xavier, J. P. Oliveira-Filho, A. S. Borges, H. N. Oliveira, F. Riet-Correa, and A. L. Schild. 2012. A nonsense mutation in the tyrosinase gene causes albinism in water buffalo. *BMC Genet.* 13:62. doi: <https://doi.org/10.1186/1471-2156-13-62>.
- Davoudi, P., H. Moradi-Shahrbabak, H. Mehrabani-Yeganeh, S. M. Ghoreishifar, S. Gholami, and R. Abdollahi-Arpanahi. 2020. Exploring the structure of haplotype blocks, runs of homozygosity and effective population size in Khuzestani river buffalo. *Slovak J. Anim. Sci.* 53:67-77.
- de Araujo Neto, F. R., L. Takada, D. J. A. dos Santos, R. R. Aspilcueta-Borquis, D. F. Cardoso, A. V. do Nascimento, K. M. Leão, H. N. de Oliveira, and H. Tonhati. 2020. Identification of genomic regions related to age at first calving and first calving interval in water buffalo using single-step GBLUP. *Reprod. Domest. Anim.* 55:1565-1572. doi: <https://doi.org/10.1111/rda.13811>.
- de Camargo, G. M. F., R. R. Aspilcueta-Borquis, M. R. S. Fortes, R. Porto-Neto, D. F. Cardoso, D. J. A. Santos, S. A. Lehnert, A. Reverter, S. S. Moore, and H. Tonhati. 2015. Prospecting major genes in dairy buffaloes. *BMC Genom.* 16:872. doi: <https://doi.org/10.1186/s12864-015-1986-2>.
- de Oliveira, E. J., V. B. O. Amorim, E. L. S. Matos, J. L. Costa, M. da Silva Castellen, J. G. Pádua, and J. L. L. Dantas. 2010. Polymorphism of microsatellite markers in papaya (*Carica papaya* L.). *Plant Mol. Biol. Report.* 28:519-530. doi: <https://doi.org/10.1007/s11105-010-0180-6>.
- Deng, T., A. Liang, S. Liang, X. Ma, X. Lu, A. Duan, C. Pang, G. Hua, S. Liu, G. Campanile, A. Salzano, B. Gasparini, G. Neglia, X. Liang, and L. Yang. 2019. Integrative analysis of transcriptome and GWAS data to identify the hub genes associated with milk yield trait in buffalo. *Front. Genet.* 10:36. doi: <https://doi.org/10.3389/fgene.2019.00036>.

- Desjardins, P., and D. Conklin. 2010. NanoDrop microvolume quantitation of nucleic acids. *J. Vis. Exp.* e2565. doi: <https://dx.doi.org/10.3791/2565>.
- Dhandapani, S., V. Vohra, M. Mukesh, S. Kumar, K. L. Mehrara, K. P. Singh, N. Kumari, and R. S. Kataria. 2021. Revealing inheritance of white markings in Nili Ravi buffalo. *Indian J. Anim. Sci.* 91:235–238. doi: <https://doi.org/10.56093/ijans.v91i3.114150>.
- Dorgaleleh, S., K. Naghipoor, A. Barahouie, F. Dastaviz, and M. Oladnabi. 2020. Molecular and biochemical mechanisms of human iris color: A comprehensive review. *J. Cell. Physiol.* 235:8972-8982. doi: <https://doi.org/10.1002/jcp.29824>.
- Du, Z., K. Huang, J. Zhao, X. Song, X. Xing, Q. Wu, L. Zhang, and C. Xu. 2017. Comparative transcriptome analysis of raccoon dog skin to determine melanin content in hair and melanin distribution in skin. *Sci. Rep.* 7:40903. doi: <https://doi.org/10.1038/srep40903>.
- Earl, D. A., and B. M. vonHoldt. 2012. STRUCTURE HARVESTER: a website and program for visualizing STRUCTURE output and implementing the Evanno method. *Conserv. Genet. Resour.* 4:359-361. doi: <https://doi.org/10.1007/s12686-011-9548-7>.
- El-Halawany, N., H. Abdel-Shafy, A.-E.-M. A. Shawky, M. A. Abdel-Latif, A. F. M. Al-Tohamy, and O. M. Abd El-Moneim. 2017. Genome-wide association study for milk production in Egyptian buffalo. *Livest. Sci.* 198:10-16. doi: <https://doi.org/10.1016/j.livsci.2017.01.019>.
- El-Kholy, A., H. Z. Hassan, A. Amin, and M. Hassanane. 2007. Genetic diversity in Egyptian buffalo using microsatellite markers. *Arab J. Biotechnol.* 10:219-232.
- Elbeltagy, A. R., S. Galal, A. Z. Abdelsalam, F. E. El Keraby, M. Blasi, and M. M. Mohamed. 2008. Biodiversity in Mediterranean buffalo using two microsatellite multiplexes. *Livest. Sci.* 114:341-346. doi: <https://doi.org/10.1016/j.livsci.2007.10.006>.
- Fan, B., Z.-Q. Du, D. M. Gorbach, and M. F. Rothschild. 2010. Development and application of high-density SNP arrays in genomic studies of domestic animals. *Asian-Australas. J. Anim. Sci.* 23:833-847. doi: <https://doi.org/10.5713/ajas.2010.r03>.
- FAO. 2011. Molecular genetic characterization of animal genetic resources. FAO Animal Production and Health Guidelines. No. 9. Rome.

- FAOSTAT. 2019. Available online: <http://www.fao.org/faostat/en/#data/QA/visualize> (accessed on July 19, 2021).
- Feeley, N., and K. Munyard. 2009. Characterisation of the melanocortin-1 receptor gene in alpaca and identification of possible markers associated with phenotypic variations in colour. *Anim. Prod. Sci.* 49(8):675-681. doi: <https://doi.org/10.1071/A-N09005>.
- Feeley, N. L. 2015. Inheritance of fibre colour in alpacas: identifying the genes involved (Doctoral dissertation, Curtin University, Australia).
- Feeley, N. L., S. Bottomley, and K. A. Munyard. 2011. Three novel mutations in *ASIP* associated with black fibre in alpacas (*Vicugna pacos*). *J. Agric. Sci.* 149:529-538. doi: <https://doi.org/10.1017/S0021859610001231>.
- Felsenstein, J. 1985. Confidence limits on phylogenies: an approach using the bootstrap. *Evolution* 39:783-791. doi: <https://doi.org/10.1111/j.1558-5646.1985.tb00420.x>.
- Felsenstein, J. 2002. Phylogeny Inference Package (PHYLIP). Genomes sciences, Department of Genetics, Washington Univ., Seattle, WA. Available online: <http://evolution.gs.washington.edu/phylip.html>.
- Fischer, H., and F. Ulbrich. 1967. Chromosomes of the Murrah buffalo and its crossbreds with the Asiatic swamp buffalo (*Bubalus bubalis*). *J. Anim. Breed. Genet.* 84:110-114. doi: <https://doi.org/10.1111/j.1439-0388.1967.tb01102.x>.
- Flanagan, S. P., and A. G. Jones. 2019. The future of parentage analysis: From microsatellites to SNPs and beyond. *Mol. Ecol.* 28:544-567. doi: <https://doi.org/10.1111/mec.14988>.
- García-Borrón, J. C., B. L. Sánchez-Laorden, and C. Jiménez-Cervantes. 2005. Melanocortin-1 receptor structure and functional regulation. *Pigment Cell Res.* 18:393-410. doi: <https://doi.org/10.1111/j.1600-0749.2005.00278.x>.
- Gargani, M., L. Pariset, M. I. Soysal, E. Ozkan, and A. Valentini. 2010. Genetic variation and relationships among Turkish water buffalo populations. *Anim. Genet.* 41:93-96. doi: <https://doi.org/10.1111/j.1365-2052.2009.01954.x>.
- Ghoreishifar, S. M., H. Moradi-Shahrbabak, M. H. Fallahi, A. Jalil Sarghale, M. Moradi-Shahrbabak, R. Abdollahi-Arpanahi, and M. Khansefid. 2020. Genomic measures of inbreeding coefficients and genome-wide scan for runs of homozygosity islands in Iranian river buffalo, *Bubalus bubalis*. *BMC Genet.* 21:16. doi: <https://doi.org/10.1186/s12863-020-0824-y>.

- Glaubitz, J. C., O. E. Rhodes Jr, and J. A. Dewoody. 2003. Prospects for inferring pairwise relationships with single nucleotide polymorphisms. *Mol. Ecol.* 12:1039-1047. doi: <https://doi.org/10.1046/j.1365-294X.2003.01790.x>.
- Gonzalez Guzman, J. L., S. F. Lázaro, A. V. do Nascimento, D. J. de Abreu Santos, D. F. Cardoso, D. C. Becker Scalez, L. Galvão de Albuquerque, N. A. Hurtado Lugo, and H. Tonhati. 2020. Genome-wide association study applied to type traits related to milk yield in water buffaloes (*Bubalus bubalis*). *J. Dairy Sci.* 103:1642-1650. doi: <https://doi.org/10.3168/jds.2019-16499>.
- Goudet, J. 2005. HIERFSTAT, a package for R to compute and test hierarchical F-statistics. *Mol. Ecol. Notes.* 5:184-186. doi: <https://doi.org/10.1111/j.1471-8286.2004.00828.x>.
- Goujon, M., H. McWilliam, W. Li, F. Valentin, S. Squizzato, J. Paern, and R. Lopez. 2010. A new bioinformatics analysis tools framework at EMBL-EBI. *Nucleic Acids Res.* 38:W695-699. doi: <https://doi.org/10.1093/nar/gkq313>.
- Grønskov, K., J. Ek, and K. Brøndum-Nielsen. 2007. Oculocutaneous albinism. *Orphanet J. Rare Dis.* 2:43. doi: <https://doi.org/10.1186/1750-1172-2-43>.
- Greyling, B. J., P. Kryger, S. Du Plessis, W. Van Hooft, P. Van Helden, W. M. Getz, and A. D. Bastos. 2008. Development of a high-throughput microsatellite typing approach for forensic and population genetic analysis of wild and domestic African Bovini. *Afr. J. Biotechnol.* 7:655-660. doi: <https://doi.org/10.5897/AJB07.391>.
- Grootenhuis, J. G., R. H. Dwinger, R. B. Dolan, S. K. Mooloo, and M. Murray. 1990. Susceptibility of African buffalo and Boran cattle to *Trypanosoma congolense* transmitted by *Glossina morsitans centralis*. *Vet. Parasitol.* 35:219-231. doi: [https://doi.org/10.1016/0304-4017\(90\)90057-I](https://doi.org/10.1016/0304-4017(90)90057-I).
- Gruber, B., and A. T. Adamack. 2015. landgenreport: a new R function to simplify landscape genetic analysis using resistance surface layers. *Mol. Ecol. Resour.* 15:1172-1178. doi: <https://doi.org/10.1111/1755-0998.12381>.
- Gruber, B., P. J. Unmack, O. F. Berry, and A. Georges. 2018. dartr: An R package to facilitate analysis of SNP data generated from reduced representation genome sequencing. *Mol. Ecol. Resour.* 18:691-699. doi: <https://doi.org/10.1111/1755-0998.12745>.
- Guibert, S., M. Girardot, H. Leveziel, R. Julien, and A. Oulmouden. 2004. Pheomelanin coat colour dilution in french cattle breeds is not correlated with the *TYR*, *TYRP1*

- and *DCT* transcription levels. *Pigment Cell Res.* 17:337-345. doi: <https://doi.org/10.1111/j.1600-0749.2004.00152.x>.
- Gurao, A., R. Vasisth, R. Singh, M. S. Dige, V. Vohra, M. Mukesh, S. Kumar, and R. S. Kataria. 2022. Identification of differential methylome signatures of white pigmented skin patches in Nili Ravi buffalo of India. *Environ. Mol. Mutagen.* 63:408-417. doi: <https://doi.org/10.1002/em.22511>.
- Guridi, M., B. Soret, L. Alfonso, and A. Arana. 2011. Single nucleotide polymorphisms in the *Melanocortin 1 Receptor* gene are linked with lightness of fibre colour in Peruvian Alpaca (*Vicugna pacos*). *Anim. Genet.* 42:679-682. doi: <https://doi.org/10.1111/j.1365-2052.2011.02205.x>.
- Ha, N.-T., S. Freytag, and H. Bickeboeller. 2014. Coverage and efficiency in current SNP chips. *Eur. J. Hum. Genet.* 22:1124-1130. doi: <https://doi.org/10.1038/ejhg.2013.304>.
- Haase, B., S. A. Brooks, A. Schlumbaum, P. J. Azor, E. Bailey, F. Alaeddine, M. Mevissen, D. Burger, P.-A. Poncet, S. Rieder, and T. Leeb. 2007. Allelic heterogeneity at the equine *KIT* locus in dominant white (W) horses. *PLoS Genet.* 3:e195. doi: <https://doi.org/10.1371/journal.pgen.0030195>.
- Hashimoto, H., M. Goda, R. Futuhashi, R. N. Kelsh, and T. Akiyama. 2021. Pigments, pigment cells and pigment patterns. Springer Nature Singapore Pte. Ltd., Singapore 57-71. doi: <https://doi.org/10.1007/978-981-16-1490-3>.
- Hassanane, M. S., M. Asland, H. Klungland, and D. I. Våge. 2000. Four bovine microsatellites showing polymorphism in river buffalo (*bubalus bubalis*). *Egypt. J. Anim. Prod.* 37:77-84.
- Hassanane, M. S., A. A. Zaki, S. Abou-Bakr, R. R. Sadek, and A. A. Nigm. 2007. Genetic polymorphism of some microsatellites on chromosome seven in the Egyptian buffalo. *Egypt. J. Anim. Prod.* 44:97-110. doi: <https://dx.doi.org/10.21608/ejap.2007.93155>.
- Helyar, S. J., J. Hemmer-hansen, D. Bekkevold, M. I. Taylor, R. Ogden, M. T. Limborg, A. Cariani, G. E. Maes, E. Diopere, G. R. Carvalho, and E. E. Nielsen. 2011. Application of SNPs for population genetics of nonmodel organisms: new opportunities and challenges. *Mol. Ecol. Resour.* 11:123-136. doi: <https://doi.org/10.1111/j.1755-0998.2010.02943.x>.
- Hida, T., K. Wakamatsu, E. V. Sviderskaya, A. J. Donkin, L. Montoliu, M. Lynn

- Lamoreux, B. Yu, G. L. Millhauser, S. Ito, G. S. Barsh, K. Jimbow, and D. C. Bennett. 2009. Agouti protein, mahogunin, and attractin in pheomelanogenesis and melanoblast-like alteration of melanocytes: a cAMP-independent pathway. *Pigment Cell Melanoma Res.* 22:623-634. doi: <https://doi.org/10.1111/j.1755-148X.2009.00582.x>.
- Hillel, J., Z. Granevitze, T. Twito, D. Ben-Avraham, S. Blum, U. Lavi, L. David, M. W. Feldman, H. Cheng, and S. Weigend. 2007. Molecular markers for the assessment of chicken biodiversity. *World's Poult. Sci. J.* 63:33-45. doi: <https://doi.org/10.1017/S0043933907001250>.
- Holland, P. W., C. A. Gill, A. D. Herring, J. O. Sanders, and D. G. Riley. 2016. Identification of regions of the bovine genome associated with gray coat color in a Nellore_Angus cross population. *J. Anim. Sci.* 94:5-5. doi: <https://doi.org/10.2527/ssasas2015-009>.
- Huang, Y. L. 2000. Studies on blood types of Taiwan buffalo (Master's thesis, National Taiwan University, Taipei).
- Hussain, T., M. Ellahi Babar, A. Ali, A. Nadeem, Z. U. Rehman, M. M. Musthafa, and F. M. Marikar. 2017. Microsatellite based genetic variation among the buffalo breed populations in Pakistan. *J. Vet. Res.* 61:535-542. doi: <https://doi.org/10.1515/jvetres-2017-0057>.
- Iamartino, D., E. L. Nicolazzi, C. P. Van Tassell, J. M. Reecy, E. R. Fritz-Waters, J. E. Koltcs, S. Biffani, T. S. Sonstegard, S. G. Schroeder, P. Ajmone-Marsan, R. Negrini, R. Pasquariello, P. Ramelli, A. Coletta, J. F. Garcia, A. Ali, L. Ramunno, G. Cosenza, D. A. A. de Oliveira, M. G. Drummond, E. Bastianetto, A. Davassi, A. Pirani, F. Brew, and J. L. Williams. 2017. Design and validation of a 90K SNP genotyping assay for the water buffalo (*Bubalus bubalis*). *PLoS One* 12:e0185220. doi: <https://doi.org/10.1371/journal.pone.0185220>.
- Ibrahim, R. S., and A. M. Hussin. 2018. Comparative histological study of the integument in buffalo and cow. *Diyala Agric. Sci. J.* 10:24-34.
- Imes, D. L., L. A. Geary, R. A. Grahn, and L. A. Lyons. 2006. Albinism in the domestic cat (*Felis catus*) is associated with a tyrosinase (*TYR*) mutation. *Anim. Genet.* 37:175-178. doi: <https://doi.org/10.1111/j.1365-2052.2005.01409.x>.
- Joly-Tonetti, N., J. I. D. Wibawa, M. Bell, and D. Tobin. 2016. Melanin fate in the human epidermis: a reassessment of how best to detect and analyse histologically.

- Exp. Dermatol. 25:501-504. doi: <https://doi.org/10.1111/exd.13016>.
- Jombart, T. 2008. adegenet: a R package for the multivariate analysis of genetic markers. *Bioinformatics* 24:1403-1405. doi: <https://doi.org/10.1093/bioinformatics/btn129>.
- Jombart, T., and I. Ahmed. 2011. adegenet 1.3-1: new tools for the analysis of genome-wide SNP data. *Bioinformatics* 27:3070-3071. doi: <https://doi.org/10.1093/bioinformatics/btr521>.
- Kalinowski, S. T. 2002. How many alleles per locus should be used to estimate genetic distances? *Heredity* 88:62-65. doi: <https://doi.org/10.1038/sj.hdy.6800009>.
- Kamara, D., K. B. Gyenai, T. Geng, H. Hammade, and E. J. Smith. 2007. Microsatellite marker-based genetic analysis of relatedness between commercial and heritage turkeys (*Meleagris gallopavo*). *Poultry Science* 86:46-49. doi: <https://doi.org/10.1093/ps/86.1.46>.
- Kamvar, Z. N., J. C. Brooks, and N. J. Grünwald. 2015. Novel R tools for analysis of genome-wide population genetic data with emphasis on clonality. *Front. Genet.* 6:208. doi: <https://doi.org/10.3389/fgene.2015.00208>.
- Kamvar, Z. N., J. F. Tabima, and N. J. Grünwald. 2014. Poppr: an R package for genetic analysis of populations with clonal, partially clonal, and/or sexual reproduction. *PeerJ* 2:e281. doi: <https://doi.org/10.7717/peerj.281>.
- Kataria, R. S., S. Sunder, G. Malik, M. Mukesh, P. Kathiravan, and B. P. Mishra. 2009. Genetic diversity and bottleneck analysis of Nagpuri buffalo breed of India based on microsatellite data. *Russ. J. Genet.* 45:941-948. doi: <https://doi.org/10.1134/S1022795409070102>.
- Kawabata, T., M. Ota, and K. Nishikawa. 1999. The protein mutant database. *Nucleic Acids Res.* 27:355-357. doi: <https://doi.org/10.1093/nar/27.1.355>.
- Klungland, H., H. G. Olsen, M. S. Hassanane, K. Mahrous, and D. I. Våge. 2000. Coat colour genes in diversity studies. *J. Anim. Breed. Genet.* 117:217-224. doi: <https://doi.org/10.1111/j.1439-0388.2000.00257.x>.
- Klungland, H., D. I. Vage, L. Gomez-Raya, S. Adalsteinsson, and S. Lien. 1995. The role of melanocyte-stimulating hormone (MSH) receptor in bovine coat color determination. *Mamm. Genome* 6:636-639. doi: <https://doi.org/10.1007/BF00352371>.
- Knaust, J., R. Weikard, E. Albrecht, R. M. Brunner, J. Günther, and C. Kühn. 2020. Indication of premelanosome protein (PMEL) expression outside of pigmented

bovine skin suggests functions beyond eumelanogenesis. *Genes* 11:7 doi: <https://doi.org/10.3390/genes11070788>.

- Kopelman, N. M., J. Mayzel, M. Jakobsson, N. A. Rosenberg, and I. Mayrose. 2015. CLUMPAK: a program for identifying clustering modes and packaging population structure inferences across *K*. *Mol. Ecol. Resour.* 15:1179-1191. doi: <https://doi.org/10.1111/1755-0998.12387>.
- Kruglyak, L. 1997. The use of a genetic map of biallelic markers in linkage studies. *Nat. Genet.* 17:21-24. doi: <https://doi.org/10.1038/ng0997-21>.
- Kumar, S., J. Gupta, N. Kumar, K. Dikshit, N. Navani, P. Jain, and M. Nagarajan. 2006. Genetic variation and relationships among eight Indian riverine buffalo breeds. *Mol. Ecol.* 15:593-600. doi: <https://doi.org/10.1111/j.1365-294X.2006.02837.x>.
- Kumari, N., R. Vasisth, A. Gurao, M. Mukesh, V. Vohra, S. Kumar, and R. S. Kataria. 2023. *ASIP* gene polymorphism associated with black coat and skin color in Murrah buffalo. *Environ. Mol. Mutagen.* 64:309–314. doi: <https://doi.org/10.1002/em.22554>.
- Lamy, P., J. Grove, and C. Wiuf. 2011. A review of software for microarray genotyping. *Hum. Genom.* 5:304-309. doi: <https://doi.org/10.1186/1479-7364-5-4-304>.
- Lao, O., J. M. de Gruijter, K. van Duijn, A. Navarro, and M. Kayser. 2007. Signatures of positive selection in genes associated with human skin pigmentation as revealed from analyses of single nucleotide polymorphisms. *Ann. Hum. Genet.* 71:354-369. doi: <https://doi.org/10.1111/j.1469-1809.2006.00341.x>.
- Laoun, A., S. Harkat, M. Lafri, S. B. S. Gaouar, I. Belabdi, E. Ciani, M. De Groot, V. Blanquet, G. Leroy, X. Rognon, and A. Da Silva. 2020. Inference of breed structure in farm animals: empirical comparison between SNP and microsatellite performance. *Genes* 11:57. doi: <https://doi.org/10.3390/genes11010057>.
- Li, J., J. Liu, G. Campanile, G. Plastow, C. Zhang, Z. Wang, M. Cassandro, B. Gasparrini, A. Salzano, G. Hua, A. Liang, and L. Yang. 2018. Novel insights into the genetic basis of buffalo reproductive performance. *BMC Genom.* 19:814. doi: <https://doi.org/10.1186/s12864-018-5208-6>.
- Li, J., J. Liu, S. Liu, G. Campanile, A. Salzano, B. Gasparrini, G. Plastow, C. Zhang, Z. Wang, A. Liang, and L. Yang. 2020. Genome-wide association study for buffalo mammary gland morphology. *J. Dairy Res.* 87:27-31. doi: <https://doi.org/10.1017/S0022029919000967>.

- Liang, D., P. Zhao, J. Si, L. Fang, E. Pairo-Castineira, X. Hu, Q. Xu, Y. Hou, Y. Gong, Z. Liang, B. Tian, H. Mao, M. Yindee, M. O. Faruque, S. Kongvongxay, S. Khamphoumee, G. E. Liu, D.-D. Wu, J. S. F. Barker, J. Han, and Y. Zhang. 2021. Genomic analysis revealed a convergent evolution of LINE-1 in coat color: A case study in water buffaloes (*Bubalus bubalis*). *Mol. Biol. Evol.* 38:1122-1136. doi: <https://doi.org/10.1093/molbev/msaa279>.
- Lin, D. Y., F. Y. Lai, L. Y. Wei, H. Y. Kuo, P. A. Tu, Y. Y. Lai, M. C. Wu, and P. H. Wang. 2013. Genetic variation analysis of the germplasm population of Taiwan buffalo based on microsatellite markers. *J. Chin. Soc. Anim. Sci.* 42:275-294.
- Liu, J. J., A. X. Liang, G. Campanile, G. Plastow, C. Zhang, Z. Wang, A. Salzano, B. Gasparrini, M. Cassandro, and L. G. Yang. 2018. Genome-wide association studies to identify quantitative trait loci affecting milk production traits in water buffalo. *J. Dairy Sci.* 101:433-444. doi: <https://doi.org/10.3168/jds.2017-13246>.
- Liu, N., L. Chen, S. Wang, C. Oh, and H. Zhao. 2005. Comparison of single-nucleotide polymorphisms and microsatellites in inference of population structure. *BMC Genet.* 6:S26. doi: <https://doi.org/10.1186/1471-2156-6-S1-S26>.
- Livak, K. J., and T. D. Schmittgen. 2001. Analysis of relative gene expression data using real-time quantitative PCR and the 2(-Delta Delta C(T)) method. *Methods* 25:402-408. doi: <https://doi.org/10.1006/meth.2001.1262>.
- Livestock Research Institute. 2015. The main entrance of Hualien Animal Propagation Station. Available online: https://english.tlri.gov.tw/view.php?theme=web_structure&id=82 (accessed on June 15, 2023).
- Lu, X. R., A. Q. Duan, W. Q. Li, H. Abdel-Shafy, H. E. Rushdi, S. S. Liang, X. Y. Ma, X. W. Liang, and T. X. Deng. 2020. Genome-wide analysis reveals genetic diversity, linkage disequilibrium, and selection for milk production traits in Chinese buffalo breeds. *J. Dairy Sci.* 103:4545-4556. doi: <https://doi.org/10.3168/jds.2019-17364>.
- Luo, X., Y. Zhou, B. Zhang, Y. Zhang, X. Wang, T. Feng, Z. Li, K. Cui, Z. Wang, C. Luo, H. Li, Y. Deng, F. Lu, J. Han, Y. Miao, H. Mao, X. Yi, C. Ai, S. Wu, A. Li, Z. Wu, Z. Zhuo, D. Da Giang, B. Mitra, M. F. Vahidi, S. Mansoor, S. A. Al-Bayatti, E. M. Sari, N. A. Gorkhali, S. Prastowo, L. Shafique, G. Ye, Q. Qian, B. Chen, D. Shi, J. Ruan, and Q. Liu. 2020. Understanding divergent domestication traits from the whole-genome sequencing of swamp- and river-buffalo populations. *Natl. Sci. Rev.* 7:686-701. doi: <https://doi.org/10.1093/nsr/nwaa024>.

- Macciotta, N. P. P., L. Colli, A. Cesarani, P. Ajmone-Marsan, W. Y. Low, R. Tearle, and J. L. Williams. 2021. The distribution of runs of homozygosity in the genome of river and swamp buffaloes reveals a history of adaptation, migration and crossbred events. *Genet. Sel. Evol.* 53:20. doi: <https://doi.org/10.1186/s12711-021-00616-3>.
- Madeira, F., M. Pearce, A. R. N. Tivey, P. Basutkar, J. Lee, O. Edbali, N. Madhusoodanan, A. Kolesnikov, and R. Lopez. 2022. Search and sequence analysis tools services from EMBL-EBI in 2022. *Nucleic Acids Res.* 50:W276-W279. doi: <https://doi.org/10.1093/nar/gkac240>.
- Marai, I. F. M., and A. A. M. Haebe. 2010. Buffalo's biological functions as affected by heat stress — A review. *Livest. Sci.* 127:89-109. doi: <https://doi.org/10.1016/j.livsci.2009.08.001>.
- Merdan, S., M. El-Zarei, A. Ghazy, M. Ayoub, Z. Al-Shawa, and S. Mokhtar. 2020. Genetic diversity analysis of five Egyptian buffalo populations using microsatellite markers. *J. Agric. Sci.* 12:271-282. doi: <https://doi.org/10.5539/jas.v12n4p271>.
- Miao, Y. W., G. S. Wu, L. Wang, D. L. Li, S. K. Tang, J. P. Liang, H. R. Mao, H. R. Luo, and Y. P. Zhang. 2010. The role of *MC1R* gene in buffalo coat color. *Sci. China Life Sci.* 53:267-272. doi: <https://doi.org/10.1007/s11427-010-0026-3>.
- Microsoft Corporation. 2019. Microsoft Excel. Available at: <https://office.microsoft.com/excel>.
- Minervino, A. H. H., M. Zava, D. Vecchio, and A. Borghese. 2020. *Bubalus bubalis*: A short story. *Front. Vet. Sci.* 7:570413. doi: <https://doi.org/10.3389/fvets.2020.570413>.
- Mishra, B. P., P. K. Dubey, B. Prakash, P. Kathiravan, S. Goyal, D. K. Sadana, G. C. Das, R. N. Goswami, V. Bhasin, B. K. Joshi, and R. S. Kataria. 2015. Genetic analysis of river, swamp and hybrid buffaloes of north-east India throw new light on phylogeography of water buffalo (*Bubalus bubalis*). *J. Anim. Breed. Genet.* 132:454-466. doi: <https://doi.org/10.1111/jbg.12141>.
- Mishra, B. P., R. S. Kataria, S. S. Bulandi, V. Kumar, and M. Mukesh. 2008. Genetic diversity in river buffalo (*Bubalus bubalis*) breeds of central India using heterologous bovine microsatellite markers. *J. Appl. Anim. Res.* 33:159-163. doi: <https://doi.org/10.1080/09712119.2008.9706919>.
- Mishra, B. P., R. S. Kataria, P. Kathiravan, K. P. Singh, D. K. Sadana, and B. K. Joshi. 2010. Microsatellite based genetic structuring reveals unique identity of Banni

- among river buffaloes of Western India. *Livest. Sci.* 127:257-261. doi: <https://doi.org/10.1016/j.livsci.2009.09.011>.
- Mohammed, E. S. I., F. A. Madkour, M. Zayed, R. Radey, A. Ghallab, and R. Hassan. 2022. Comparative histological analysis of the skin for forensic investigation of some animal species. *EXCLI J.* 21:1286-1298. doi: <https://doi.org/10.17179/excli2022-5335>.
- Moioli, B., A. Georgoudis, F. Napolitano, G. Catillo, E. Giubilei, C. Ligda, and M. Hassanane. 2001. Genetic diversity between Italian, Greek and Egyptian buffalo populations. *Livest. Prod. Sci.* 70:203-211. doi: [https://doi.org/10.1016/S0301-6226\(01\)00175-0](https://doi.org/10.1016/S0301-6226(01)00175-0).
- Mokhber, M., M. Moradi-Shahrbabak, M. Sadeghi, H. Moradi-Shahrbabak, A. Stella, E. Nicolzzi, J. Rahmaninia, and J. L. Williams. 2018. A genome-wide scan for signatures of selection in Azeri and Khuzestani buffalo breeds. *BMC Genom.* 19:449. doi: <https://doi.org/10.1186/s12864-018-4759-x>.
- Mokhber, M., M. M. Shahrbabak, M. Sadeghi, H. M. Shahrbabak, A. Stella, E. Nicolzzi, and J. L. Williams. 2019. Study of whole genome linkage disequilibrium patterns of Iranian water buffalo breeds using the Axiom Buffalo Genotyping 90K Array. *PLoS One* 14:e0217687. doi: <https://doi.org/10.1371/journal.pone.0217687>.
- Moore, S. S., D. Evans, K. Byrne, J. S. F. Barker, S. G. Tan, D. Vankan, and D. J. S. Hetzel. 1995. A set of polymorphic DNA microsatellites useful in swamp and river buffalo (*Bubalus bubalis*). *Anim. Genet.* 26:355-359. doi: <https://doi.org/10.1111/j.1365-2052.1995.tb02674.x>.
- Mourad, A. M. I., V. Belamkar, and P. S. Baenziger. 2020. Molecular genetic analysis of spring wheat core collection using genetic diversity, population structure, and linkage disequilibrium. *BMC Genom.* 21:434. doi: <https://doi.org/10.1186/s12864-020-06835-0>.
- Murisier, F., S. Guichard, and F. Beermann. 2007. The tyrosinase enhancer is activated by Sox10 and Mitf in mouse melanocytes. *Pigment Cell Res.* 20:173-184. doi: <https://doi.org/10.1111/j.1600-0749.2007.00368.x>.
- Nagarajan, M., N. Kumar, G. Nishanth, R. Haribaskar, K. Paranthaman, J. Gupta, M. Mishra, R. Vaidhegi, S. Kumar, A. K. Ranjan, and S. Kumar. 2009. Microsatellite markers of water buffalo, *Bubalus bubalis* - development, characterisation and linkage disequilibrium studies. *BMC Genet.* 10:68. doi: <https://doi.org/10.1186/147>

1-2156-10-68.

- Navani, N., P. K. Jain, S. Gupta, B. S. Sisodia, and S. Kumar. 2002. A set of cattle microsatellite DNA markers for genome analysis of riverine buffalo (*Bubalus bubalis*). *Anim. Genet.* 33:149-154. doi: <https://doi.org/10.1046/j.1365-2052.2002.00823.x>.
- Nei, M. 1972. Genetic Distance between Populations. *Am. Nat.* 106:283-292. doi: <http://www.jstor.org/stable/2459777>.
- Nei, M. 1978. Estimation of average heterozygosity and genetic distance from a small number of individuals. *Genetics* 89:583-590. doi: <https://doi.org/10.1093/genetics/89.3.583>.
- Nei, M., and W. H. Li. 1979. Mathematical model for studying genetic variation in terms of restriction endonucleases. *Proc. Natl. Acad. Sci. (U.S.A.)* 76:5269-5273. doi: <https://doi.org/10.1073/pnas.76.10.5269>.
- Ng, P. C., and S. Henikoff. 2003. SIFT: Predicting amino acid changes that affect protein function. *Nucleic Acids Res.* 31:3812-3814. doi: <https://doi.org/10.1093/nar/gkg509>.
- Nguyen, N. T., and D. E. Fisher. 2019. MITF and UV responses in skin: From pigmentation to addiction. *Pigment Cell Melanoma Res.* 32:224-236. doi: <https://doi.org/10.1111/pcmr.12726>.
- Nicolazzi, E. L., S. Biffani, F. Biscarini, P. Orozco ter Wengel, A. Caprera, N. Nazzicari, and A. Stella. 2015. Software solutions for the livestock genomics SNP array revolution. *Anim. Genet.* 46:343-353. doi: <https://doi.org/10.1111/age.12295>.
- Noce, A., S. Qanbari, R. González-Prendes, J. Brenmoehl, M. G. Luigi-Sierra, M. Theerkorn, M.-A. Fiege, H. Pilz, A. Bota, L. Vidu, C. Horwath, L. Haraszthy, P. Penchev, Y. Ilieva, T. Peeva, W. Lüpcke, R. Krawczynski, K. Wimmers, M. Thiele, and A. Hoeflich. 2021. Genetic diversity of *Bubalus bubalis* in Germany and global relations of its genetic background. *Front. Genet.* 11:610353. doi: <https://doi.org/10.3389/fgene.2020.610353>.
- O'Leary, N. A., M. W. Wright, J. R. Brister, S. Ciufu, D. Haddad, R. McVeigh, B. Rajput, B. Robbertse, B. Smith-White, D. Ako-Adjei, A. Astashyn, A. Badretdin, Y. Bao, O. Blinkova, V. Brover, V. Chetvernin, J. Choi, E. Cox, O. Ermolaeva, C. M. Farrell, T. Goldfarb, T. Gupta, D. Haft, E. Hatcher, W. Hlavina, V. S. Joardar, V. K. Kodali, W. Li, D. Maglott, P. Masterson, K. M. McGarvey, M. R. Murphy, K. O'Neill, S. Pujar,

- S. H. Rangwala, D. Rausch, L. D. Riddick, C. Schoch, A. Shkeda, S. S. Storz, H. Sun, F. Thibaud-Nissen, I. Tolstoy, R. E. Tully, A. R. Vatsan, C. Wallin, D. Webb, W. Wu, M. J. Landrum, A. Kimchi, T. Tatusova, M. DiCuccio, P. Kitts, T. D. Murphy, and K. D. Pruitt. 2016. Reference sequence (RefSeq) database at NCBI: current status, taxonomic expansion, and functional annotation. *Nucleic Acids Res.* 44:D733-745. doi: <https://doi.org/10.1093/nar/gkv1189>.
- Oetting, W. S. 2000. The tyrosinase gene and oculocutaneous albinism type 1 (OCA1): A model for understanding the molecular biology of melanin formation. *Pigment Cell Res.* 13:320-325. doi: <https://doi.org/10.1034/j.1600-0749.2000.130503.x>.
- Ollivier, M., A. Tresset, C. Hitte, C. Petit, S. Hughes, B. Gillet, M. Duffraisse, M. Pionnier-Capitan, L. Lagoutte, R.-M. Arbogast, A. Balasescu, A. Boroneant, M. Mashkour, J.-D. Vigne, and C. Hänni. 2013. Evidence of coat color variation sheds new light on ancient canids. *PLoS One* 8:e75110. doi: <https://doi.org/10.1371/journal.pone.0075110>.
- Özkan Ünal, E., M. İ. Soysal, E. Yüncü, N. D. Dağtaş, and İ. Togan. 2014. Microsatellite based genetic diversity among the three water buffalo (*Bubalus bubalis*) populations in Turkey. *Arch. Anim. Breed.* 57:8. doi: <https://doi.org/10.7482/0003-9438-57-008>.
- Paradis, E. 2010. pegas: an R package for population genetics with an integrated-modular approach. *Bioinformatics* 26:419-420. doi: <https://doi.org/10.1093/bioinformatics/tp696>.
- Pausch, H., X. Wang, S. Jung, D. Krogmeier, C. Edel, R. Emmerling, K.-U. Götz, and R. Fries. 2012. Identification of QTL for UV-protective eye area pigmentation in cattle by progeny phenotyping and genome-wide association analysis. *PloS one* 7:e36346-e36346. doi: <https://doi.org/10.1371/journal.pone.0036346>.
- Pingault, V., D. Ente, F. Dastot-Le Moal, M. Goossens, S. Marlin, and N. Bondurand. 2010. Review and update of mutations causing Waardenburg syndrome. *Hum. Mutat.* 31:391-406. doi: <https://doi.org/10.1002/humu.21211>.
- Powell, A. J., M. J. Moss, L. T. Tree, B. L. Roeder, C. L. Carleton, E. Campbell, and D. L. Kooyman. 2008. Characterization of the effect of Melanocortin 1 Receptor, a member of the hair color genetic locus, in alpaca (*Lama pacos*) fleece color differentiation. *Small Rumin. Res.* 79:183-187. doi: <https://doi.org/10.1016/j.smallrumres.2008.07.025>.

- Pritchard, J. K., M. Stephens, and P. Donnelly. 2000. Inference of population structure using multilocus genotype data. *Genetics* 155:945-959. doi: <https://doi.org/10.1093/genetics/155.2.945>.
- Purcell, S., B. Neale, K. Todd-Brown, L. Thomas, M. A. Ferreira, D. Bender, J. Maller, P. Sklar, P. I. de Bakker, M. J. Daly, and P. C. Sham. 2007. PLINK: a tool set for whole-genome association and population-based linkage analyses. *Am. J. Hum. Genet.* 81:559-575. doi: <https://doi.org/10.1086/519795>.
- R Core Team. 2022. R: a language and environment for statistical computing. R Foundation for Statistical Computing, Vienna, Austria. <https://www.R-project.org/>
- Rahimadar, S., M. Ghaffari, M. Mokhber, and J. L. Williams. 2021. Linkage disequilibrium and effective population size of buffalo populations of Iran, Turkey, Pakistan, and Egypt using a medium density SNP array. *Front. Genet.* 12:608186. doi: <https://doi.org/10.3389/fgene.2021.608186>.
- Raj, A., M. Stephens, and J. K. Pritchard. 2014. fastSTRUCTURE: variational inference of population structure in large SNP data sets. *Genetics* 197:573-589. doi: <https://doi.org/10.1534/genetics.114.164350>.
- Ramasamy, R. K., S. Ramasamy, B. B. Bindroo, and V. G. Naik. 2014. STRUCTURE PLOT: a program for drawing elegant STRUCTURE bar plots in user friendly interface. *SpringerPlus* 3:431. doi: <https://doi.org/10.1186/2193-1801-3-431>.
- Ramensky, V., P. Bork, and S. Sunyaev. 2002. Human non-synonymous SNPs: server and survey. *Nucleic Acids Res.* 30:3894-3900. doi: <https://doi.org/10.1093/nar/gkf493>.
- Rees, J. L. 2003. Genetics of hair and skin color. *Annu. Rev. Genet.* 37:67-90. doi: <https://doi.org/10.1146/annurev.genet.37.110801.143233>.
- Rehman, S. U., F. U. Hassan, X. Luo, Z. Li, and Q. Liu. 2021. Whole-genome sequencing and characterization of buffalo genetic resources: Recent advances and future challenges. *Animals* 11:904. doi: <https://doi.org/10.3390/ani11030904>.
- Rice, P., I. Longden, and A. Bleasby. 2000. EMBOSS: The European Molecular Biology Open Software Suite. *Trends Genet.* 16:276-277. doi: [https://doi.org/10.1016/S0168-9525\(00\)02024-2](https://doi.org/10.1016/S0168-9525(00)02024-2).
- Rieder, S., S. Taourit, D. Mariat, B. Langlois, and G. Guérin. 2001. Mutations in the agouti (*ASIP*), the extension (*MC1R*), and the brown (*TYRP1*) loci and their association to coat color phenotypes in horses (*Equus caballus*). *Mamm. Genome*

- 12:450-455. doi: <https://doi.org/10.1007/s003350020017>.
- Rife, D. C. 1962. Color and horn variations in water buffalo. The inheritance of coat color, eye color and shape of horns. *J. Hered.* 53:239-246. doi: <https://doi.org/10.1093/oxfordjournals.jhered.a107182>.
- Rife, D. C., and P. Buranamas. 1959. Inheritance of white coat color in the water buffalo of Thailand. *J. Hered.* 50:269-272. doi: <https://doi.org/10.1093/oxfordjournals.jhered.a106923>.
- Rogberg Muñoz, A., L. V. Texeira, E. E. Villegas Castagnasso, C. S. Teixeira, P. Peral Garcia, D. Oliveira, and G. Giovambattista. 2011. Brazilian buffalo genetic variability by cross-specific microsatellite set. *J. Agric. Sci. Technol. B* 1:1008-1012.
- Römpler, H., N. Rohland, C. Lalueza-Fox, E. Willerslev, T. Kuznetsova, G. Rabeder, J. Bertranpetit, T. Schöneberg, and M. Hofreiter. 2006. Nuclear gene indicates coat-color polymorphism in mammoths. *Science* 313:62. doi: <https://doi.org/10.1126/science.1128994>.
- Rouzaud, F., A. L. Kadekaro, Z. A. Abdel-Malek, and V. J. Hearing. 2005. MC1R and the response of melanocytes to ultraviolet radiation. *Mutat. Res./Fundam. Mol. Mech. Mutagen.* 571:133-152. doi: <https://doi.org/10.1016/j.mrfmmm.2004.09.014>.
- RStudio Team. 2022. RStudio: Integrated Development Environment for R. RStudio, PBC, Boston, MA, USA. <http://www.rstudio.com/>.
- Saif, R., M. E. Babar, A. R. Awan, A. Nadeem, A. S. Hashmi, and T. Hussain. 2012. DNA fingerprinting of Pakistani buffalo breeds (Nili-Ravi, Kundi) using microsatellite and cytochrome *b* gene markers. *Mol. Biol. Rep.* 39:851-856. doi: <https://doi.org/10.1007/s11033-011-0808-0>.
- Saitou, N., and M. Nei. 1987. The neighbor-joining method: a new method for reconstructing phylogenetic trees. *Mol. Biol. Evol.* 4:406-425. doi: <https://doi.org/10.1093/oxfordjournals.molbev.a040454>.
- Sánchez-Más, J., B. L. Sánchez-Laorden, L. A. Guillo, C. Jiménez-Cervantes, and J. C. García-Borrón. 2005. The melanocortin-1 receptor carboxyl terminal pentapeptide is essential for MC1R function and expression on the cell surface. *Peptides* 26:1848-1857. doi: <https://doi.org/10.1016/j.peptides.2004.11.030>.
- Sanger, F., and A. R. Coulson. 1975. A rapid method for determining sequences in DNA by primed synthesis with DNA polymerase. *J. Mol. Biol.* 94:441-448. doi:

[https://doi.org/10.1016/0022-2836\(75\)90213-2](https://doi.org/10.1016/0022-2836(75)90213-2).

- Saputra, F., J. Jakaria, A. Anggraeni, and C. Sumantri. 2020. Genetic diversity of Indonesian swamp buffalo based on microsatellite markers. *Trop. Anim. Sci. J.* 43:191-196. doi: <https://doi.org/10.5398/tasj.2020.43.3.191>.
- Schiaffino, M. V. 2010. Signaling pathways in melanosome biogenesis and pathology. *Int. J. Biochem. Cell Biol.* 42:1094-1104. doi: <https://doi.org/10.1016/j.biocel.2010.03.023>.
- Schmutz, S. M., T. G. Berryere, D. C. Ciobanu, A. J. Mileham, B. H. Schmitz, and M. Fredholm. 2004. A form of albinism in cattle is caused by a tyrosinase frameshift mutation. *Mamm. Genome* 15:62-67. doi: <https://doi.org/10.1007/s00335-002-2249-5>.
- Schmutz, S. M., and D. L. Dreger. 2013. Interaction of *MC1R* and *PMEL* alleles on solid coat colors in Highland cattle. *Anim. Genet.* 44:9-13. doi: <https://doi.org/10.1111/j.1365-2052.2012.02361.x>.
- Shi, X., J. Wu, X. Lang, C. Wang, Y. Bai, D. G. Riley, L. Liu, and X. Ma. 2021. Comparative transcriptome and histological analyses provide insights into the skin pigmentation in Minxian black fur sheep (*Ovis aries*). *PeerJ* 9:e11122-e11122. doi: <https://doi.org/10.7717/peerj.11122>.
- Shokrollahi, B., C. Amirinia, N. D. Djadid, N. Amirmozaffari, and M. A. Kamali. 2009. Development of polymorphic microsatellite loci for Iranian river buffalo (*Bubalus bubalis*). *Afr. J. Biotechnol.* 8:6750-6755.
- Simonsen, B. T., H. R. Siegismund, and P. Arctander. 1998. Population structure of African buffalo inferred from mtDNA sequences and microsatellite loci: high variation but low differentiation. *Mol. Ecol.* 7:225-237. doi: <https://doi.org/10.1046/j.1365-294x.1998.00343.x>.
- Singh, K. V., R. Das, M. Sodhi, and R. S. Kataria. 2022. Genetic characterization and diversity assessment in 'Bhangor' indigenous swamp buffalo population using heterologous microsatellite markers. *Anim. Biotechnol.* 1-7. doi: <https://doi.org/10.1080/10495398.2022.2154220>.
- Singh, N., D. R. Choudhury, A. K. Singh, S. Kumar, K. Srinivasan, R. K. Tyagi, N. K. Singh, and R. Singh. 2013. Comparison of SSR and SNP markers in estimation of genetic diversity and population structure of Indian rice varieties. *PLoS One* 8:e84136. doi: <https://doi.org/10.1371/journal.pone.0084136>.

- Singh, V. P., R. K. Motiani, A. Singh, G. Malik, R. Aggarwal, K. Pratap, M. R. Wani, S. B. Gokhale, V. T. Natarajan, and R. S. Gokhale. 2016. Water Buffalo (*Bubalus bubalis*) as a spontaneous animal model of Vitiligo. *Pigment Cell Melanoma Res.* 29:465-469. doi: <https://doi.org/10.1111/pcmr.12485>.
- Sraphet, S., B. Moolmuang, A. Na-Chiangmai, S. Panyim, D. R. Smith, and K. Triwitayakorn. 2008. Use of cattle microsatellite markers to assess genetic diversity of Thai swamp buffalo (*Bubalus bubalis*). *Asian-Australas. J. Anim. Sci.* 21:177-180. doi: <https://doi.org/10.5713/ajas.2008.70327>.
- Stanchina, L., V. Baral, F. Robert, V. Pingault, N. Lemort, V. Pachnis, M. Goossens, and N. Bondurand. 2006. Interactions between *Sox10*, *Edn3* and *Ednrb* during enteric nervous system and melanocyte development. *Dev. Biol.* 295:232-249. doi: <https://doi.org/10.1016/j.ydbio.2006.03.031>.
- Statistic Office of C. O. A. 2022. Yearly Report of Taiwan's Agriculture. Taipei: Council of Agriculture, Executive Yuan; 2021:118. Available online: https://agrstat.coa.gov.tw/sdweb/public/book/Book_File.ashx?chapter_id=1383_11_2 (accessed on May 26, 2023).
- Stone, E. A., and A. Sidow. 2005. Physicochemical constraint violation by missense substitutions mediates impairment of protein function and disease severity. *Genome Res.* 15:978-986. doi: <https://doi.org/10.1101/gr.3804205>.
- Strillacci, M. G., H. Moradi-Shahrbabak, P. Davoudi, S. M. Ghoreishifar, M. Mokhber, A. J. Masroure, and A. Bagnato. 2021. A genome-wide scan of copy number variants in three Iranian indigenous river buffaloes. *BMC Genom.* 22:305. doi: <https://doi.org/10.1186/s12864-021-07604-3>.
- Sturm, A. B., R. J. Eckert, J. G. Méndez, P. González-Díaz, and J. D. Voss. 2020. Population genetic structure of the great star coral, *Montastraea cavernosa*, across the Cuban archipelago with comparisons between microsatellite and SNP markers. *Sci. Rep.* 10:15432. doi: <https://doi.org/10.1038/s41598-020-72112-5>.
- Sukla, S., B. R. Yadav, and T. K. Bhattacharya. 2006. Characterization of Indian riverine buffaloes by microsatellite markers. *Asian-Australas. J. Anim. Sci.* 19:1556-1560. doi: <https://doi.org/10.5713/ajas.2006.1556>.
- Sun, T., J. Shen, A. Achilli, N. Chen, Q. Chen, R. Dang, Z. Zheng, H. Zhang, X. Zhang, S. Wang, T. Zhang, H. Lu, Y. Ma, Y. Jia, M. R. Capodiferro, Y. Huang, X. Lan, H. Chen, Y. Jiang, and C. Lei. 2020. Genomic analyses reveal distinct genetic

- architectures and selective pressures in buffaloes. *GigaScience* 9:1-12. doi: <https://doi.org/10.1093/gigascience/giz166>.
- Sung, Y. Y. 2003. Like cattle, like industrial culture. *Animal Genetic Resources Information Network in Taiwan*. Available online: https://www.angrin.tlri.gov.tw/apec2003/apec2003_C/TW_CULT/TW_CULT.htm (accessed on July 25, 2023).
- Switonski, M., M. Mankowska, and S. Salamon. 2013. Family of melanocortin receptor (*MCR*) genes in mammals—mutations, polymorphisms and phenotypic effects. *J. Appl. Genet.* 54:461-472. doi: <https://doi.org/10.1007/s13353-013-0163-z>.
- Tantia, M. S., R. K. Vijh, B. Mishra, S. T. B. Kumar, and R. Arora. 2006. Multilocus genotyping to study population structure in three buffalo populations of India. *Asian-Australas. J. Anim. Sci.* 19:1071-1078. doi: <https://doi.org/10.5713/ajas.2006.1071>.
- Tautz, D. 1989. Hypervariability of simple sequences as a general source for polymorphic DNA markers. *Nucleic Acids Res.* 17:6463-6471. doi: <https://doi.org/10.1093/nar/17.16.6463>.
- Thakor, P. B., A. T. Hinsu, D. R. Bhatia, T. M. Shah, N. Nayee, A. Sudhakar, D. N. Rank, and C. G. Joshi. 2021. High-throughput genotype-based population structure analysis of selected buffalo breeds. *Transl. Anim. Sci.* 5:txab033. doi: <https://doi.org/10.1093/tas/txab033>.
- Thomas, P. D., and A. Kejariwal. 2004. Coding single-nucleotide polymorphisms associated with complex vs. Mendelian disease: evolutionary evidence for differences in molecular effects. *Proc. Natl. Acad. Sci. (U.S.A.)* 101:15398-15403. doi: <https://doi.org/10.1073/pnas.0404380101>.
- Thomas, P. D., A. Kejariwal, N. Guo, H. Mi, M. J. Campbell, A. Muruganujan, and B. Lazareva-Ulitsky. 2006. Applications for protein sequence-function evolution data: mRNA/protein expression analysis and coding SNP scoring tools. *Nucleic Acids Res.* 34:W645-650. doi: <https://doi.org/10.1093/nar/gkl229>.
- Triwitayakorn, K., B. Moolmuang, S. Sraphet, S. Panyim, A. Na-Chiangmai, and D. R. Smith. 2006. Analysis of genetic diversity of the Thai swamp buffalo (*Bubalus bubalis*) using cattle microsatellite DNA markers. *Asian-Australas. J. Anim. Sci.* 19:617-621. doi: <https://doi.org/10.5713/ajas.2006.617>.
- Turner, S. D. 2014. qqman: an R package for visualizing GWAS results using QQ and manhattan plots. *Biorxiv* 005165. doi: <https://doi.org/10.1101/005165>.

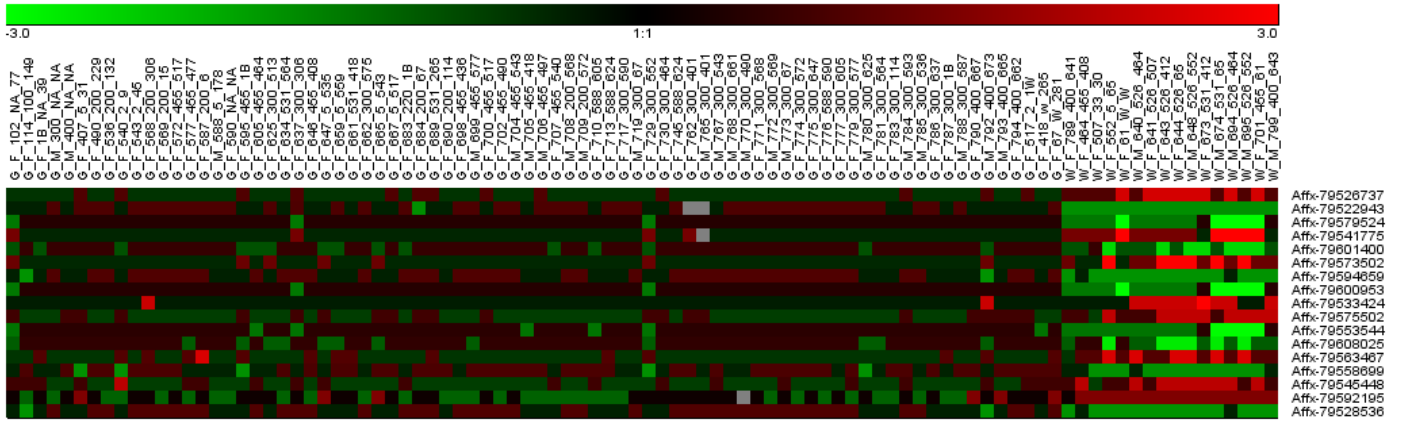
- Turner, S. D. 2018. qqman: an R package for visualizing GWAS results using Q-Q and manhattan plots. *J. Open Source Softw.* 3:731. doi: <https://doi.org/10.21105/joss.00731>.
- Uffelmann, E., Q. Q. Huang, N. S. Munung, J. de Vries, Y. Okada, A. R. Martin, H. C. Martin, T. Lappalainen, and D. Posthuma. 2021. Genome-wide association studies. *Nat. Rev. Methods Primers* 1:59. doi: <https://doi.org/10.1038/s43586-021-00056-9>.
- Uffo, O., N. Martínez, A. Acosta, A. Sanz, I. Martín-Burriel, R. Osta, C. Rodellar, and P. Zaragoza. 2017. Analysis of microsatellite markers in a Cuban water buffalo breed. *J. Dairy Res.* 84:289-292. doi: <https://doi.org/10.1017/S0022029917000425>.
- Ulbrich, F., and H. Fischer. 1966. The chromosomes of the Asiatic buffalo (*Bubalus bubalis*) and the African buffalo (*Cyncerus caffer*). *J. Anim. Breed. Genet.* 83:219-223. doi: <https://doi.org/10.1111/j.1439-0388.1966.tb00865.x>.
- Ünal, E., R. Işık, A. Şen, E. Geyik Kuş, and M. Soysal. 2021. Evaluation of genetic diversity and structure of Turkish water buffalo population by using 20 microsatellite markers. *Animals* 11:1067. doi: <https://doi.org/10.3390/ani11041067>.
- UniProt Consortium. 2012. Reorganizing the protein space at the Universal Protein Resource (UniProt). *Nucleic Acids Res.* 40:D71-75. doi: <https://doi.org/10.1093/nar/gkr981>.
- Van Hooft, W., O. Hanotte, P. Wenink, A. Groen, Y. Sugimoto, H. Prins, and A. Teale. 1999. Applicability of bovine microsatellite markers for population genetic studies on African buffalo (*Syncerus caffer*). *Anim. Genet.* 30:214-220.
- Venturini, G. C., D. F. Cardoso, F. Baldi, A. C. Freitas, R. R. Aspilcueta-Borquis, D. J. Santos, G. M. Camargo, N. B. Stafuzza, L. G. Albuquerque, and H. Tonhati. 2014. Association between single-nucleotide polymorphisms and milk production traits in buffalo. *Genet. Mol. Res.* 13:10256-10268. doi: <https://doi.org/10.4238/2014.December.4.20>.
- Verlouw, J. A. M., E. Clemens, J. H. de Vries, O. Zolk, A. J. M. H. Verkerk, A. am Zehnhoff-Dinnesen, C. Medina-Gomez, C. Lanvers-Kaminsky, F. Rivadeneira, T. Langer, J. B. J. van Meurs, M. M. van den Heuvel-Eibrink, A. G. Uitterlinden, and L. Broer. 2021. A comparison of genotyping arrays. *Eur. J. Hum. Genet.* 29:1611-1624. doi: <https://doi.org/10.1038/s41431-021-00917-7>.
- Vignal, A., D. Milan, M. SanCristobal, and A. Eggen. 2002. A review on SNP and other types of molecular markers and their use in animal genetics. *Genet. Sel. Evol.*

- 34:275. doi: <https://doi.org/10.1186/1297-9686-34-3-275>.
- Vijh, R. K., M. S. Tantia, B. Mishra, and S. T. Bharani Kumar. 2008. Genetic relationship and diversity analysis of Indian water buffalo (*Bubalus bubalis*). *J. Anim. Sci.* 86:1495-1502. doi: <https://doi.org/10.2527/jas.2007-0321>.
- Vohra, V., S. Chhotaray, G. Gowane, R. Alex, A. Mukherjee, A. Verma, and S. M. Deb. 2021a. Genome-wide association studies in Indian buffalo revealed genomic regions for lactation and fertility. *Front. Genet.* 12:696109. doi: <https://doi.org/10.3389/fgene.2021.696109>.
- Vohra, V., N. P. Singh, S. Chhotaray, V. S. Raina, A. Chopra, and R. S. Kataria. 2021b. Morphometric and microsatellite-based comparative genetic diversity analysis in *Bubalus bubalis* from North India. *PeerJ* 9:e11846. doi: <https://doi.org/10.7717/peerj.11846>.
- Wang, L. G., T. T. Lam, S. Xu, Z. Dai, L. Zhou, T. Feng, P. Guo, C. W. Dunn, B. R. Jones, T. Bradley, H. Zhu, Y. Guan, Y. Jiang, and G. Yu. 2019. treeio: An R Package for phylogenetic tree input and output with richly annotated and associated data. *Mol. Biol. Evol.* 37:599-603. doi: <https://doi.org/10.1093/molbev/msz240>.
- Weich, K., V. Affolter, D. York, R. Rebhun, R. Grahn, A. Kallenberg, and D. Bannasch. 2020. Pigment intensity in dogs is associated with a copy number variant upstream of *KITLG*. *Genes* 11:75. doi: <https://doi.org/10.3390/genes11010075>.
- Wen, Y. F., K. Uchiyama, W. J. Han, S. Ueno, W. D. Xie, G. B. Xu, and Y. Tsumura. 2013. Null alleles in microsatellite markers. *Biodiv. Sci.* 21:117-126. doi: <https://doi.org/10.3724/SP.J.1003.2013.10133>.
- Weng, Z., Y. Yang, X. Wang, L. Wu, S. Hua, H. Zhang, and Z. Meng. 2021. Parentage analysis in giant grouper (*Epinephelus lanceolatus*) using microsatellite and SNP markers from genotyping-by-sequencing data. *Genes* 12:1042.
- Wikimedia Commons. 2009. Taiwan ROC political division map. Available online: https://commons.wikimedia.org/wiki/File:Taiwan_ROC_political_divisions_labeled.svg (accessed on June 15, 2023).
- Wolf Horrell, E. M., M. C. Boulanger, and J. A. D'Orazio. 2016. Melanocortin 1 receptor: structure, function, and regulation. *Front. Genet.* 7:95-95. doi: <https://doi.org/10.3389/fgene.2016.00095>.
- Wu, J. J., L. J. Song, F. J. Wu, X. W. Liang, B. Z. Yang, D. C. Wathes, G. E. Pollott, Z. Cheng, D. S. Shi, Q. Y. Liu, L. G. Yang, and S. J. Zhang. 2013. Investigation of

- transferability of BovineSNP50 BeadChip from cattle to water buffalo for genome wide association study. *Mol. Biol. Rep.* 40:743-750. doi: <https://doi.org/10.1007/s11033-012-1932-1>.
- Yajima, I., M. Y. Kumasaka, N. D. Thang, Y. Goto, K. Takeda, M. Iida, N. Ohgami, H. Tamura, O. Yamanoshita, Y. Kawamoto, K. Furukawa, and M. Kato. 2011. Molecular network associated with MITF in skin melanoma development and progression. *J. Skin Cancer* 2011:730170. doi: <https://doi.org/10.1155/2011/730170>.
- Yang, W. C., K. Q. Tang, J. Mei, W. B. Zeng, and L. G. Yang. 2011. Genetic diversity analysis of an indigenous Chinese buffalo breed and hybrids based on microsatellite data. *Genet. Mol. Res.* 10:3421-3426. doi: <https://doi.org/10.4238/2011.December.5.1>.
- Ye, J., G. Coulouris, I. Zaretskaya, I. Cutcutache, S. Rozen, and T. L. Madden. 2012. Primer-BLAST: a tool to design target-specific primers for polymerase chain reaction. *BMC Bioinform.* 13:134. doi: <https://doi.org/10.1186/1471-2105-13-134>.
- Yokoyama, T., D. W. Silversides, K. G. Waymire, B. S. Kwon, T. Takeuchi, and P. A. Overbeek. 1990. Conserved cysteine to serine mutation in tyrosinase is responsible for the classical albino mutation in laboratory mice. *Nucleic Acids Res.* 18:7293-7298. doi: <https://doi.org/10.1093/nar/18.24.7293>.
- Yousefi, D. M., A. S.-R. Miraei, and M. Sadeghi. 2019. Study of genetic diversity of Iranian indigenous buffalo populations using microsatellite markers. *Genetika* 51:147-155. doi: <https://doi.org/10.2298/GENSR1901147D>.
- Yu, G. 2020. Using ggtree to visualize data on tree-like structures. *Curr. Protoc. Bioinform.* 69:e96. doi: <https://doi.org/10.1002/cpbi.96>.
- Yu, G., T. T.-Y. Lam, H. Zhu, and Y. Guan. 2018. Two methods for mapping and visualizing associated data on phylogeny using ggtree. *Mol. Biol. Evol.* 35:3041-3043. doi: <https://doi.org/10.1093/molbev/msy194>.
- Yu, G., D. K. Smith, H. Zhu, Y. Guan, and T. T.-Y. Lam. 2017. GGTREE: an R package for visualization and annotation of phylogenetic trees with their covariates and other associated data. *Methods Ecol. Evol.* 8:28-36. doi: <https://doi.org/10.1111/2041-210X.12628>.
- Yusnizar, Y., M. Wilbe, A. O. Herlino, C. Sumantri, R. R. Noor, A. Boediono, L. Andersson, and G. Andersson. 2015. *Microphthalmia-associated transcription factor* mutations are associated with white-spotted coat color in swamp buffalo.

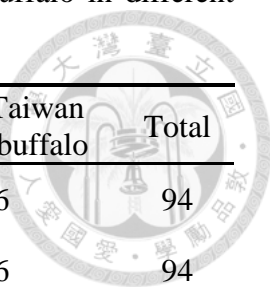
- Anim. Genet. 46:676-682. doi: <https://doi.org/10.1111/age.12334>.
- Zhang, Y., L. Colli, and J. S. F. Barker. 2020. Asian water buffalo: domestication, history and genetics. Anim. Genet. 51:177-191. doi: <https://doi.org/10.1111/age.12911>.
- Zhang, Y., Y. Lu, M. Yindee, K.-Y. Li, H.-Y. Kuo, Y.-T. Ju, S. Ye, M. O. Faruque, Q. Li, Y. Wang, V. C. Cuong, L. D. Pham, B. Bouahom, B. Yang, X. Liang, Z. Cai, D. Vankan, W. Manatchaiworakul, N. Kowlim, S. Duangchantrasiri, W. Wajjwalku, B. Colenbrander, Y. Zhang, P. Beerli, J. A. Lenstra, and J. S. F. Barker. 2016. Strong and stable geographic differentiation of swamp buffalo maternal and paternal lineages indicates domestication in the China/Indochina border region. Mol. Ecol. 25:1530-1550. doi: <https://doi.org/10.1111/mec.13518>.
- Zhang, Y., D. Sun, Y. Yu, and Y. Zhang. 2007. Genetic diversity and differentiation of Chinese domestic buffalo based on 30 microsatellite markers. Anim. Genet. 38:569-575. doi: <https://doi.org/10.1111/j.1365-2052.2007.01648.x>.
- Zhang, Y., D. Sun, Y. Yu, and Y. Zhang. 2008a. Genetic variation and divergence among swamp buffalo, river buffalo and cattle: a microsatellite survey on five populations in China. Asian-Australas. J. Anim. Sci. 21:1238-1243. doi: <https://doi.org/10.5713/ajas.2008.70746>
- Zhang, Y., D. X. Sun, Y. Yu, and Y. Zhang. 2008b. Optimized multiplex PCR sets and genetic polymorphism of 30 microsatellite loci in domestic buffalo. Yi chuan = Hered. 30:59-64. doi: <https://doi.org/10.3724/sp.j.1005.2008.00059>.
- Zhang, Y., D. Vankan, Y. Zhang, and J. S. F. Barker. 2011. Genetic differentiation of water buffalo (*Bubalus bubalis*) populations in China, Nepal and south-east Asia: inferences on the region of domestication of the swamp buffalo. Anim. Genet. 42:366-377. doi: <https://doi.org/10.1111/j.1365-2052.2010.02166.x>.
- Zimmerman, S. J., C. L. Aldridge, and S. J. Oyler-McCance. 2020. An empirical comparison of population genetic analyses using microsatellite and SNP data for a species of conservation concern. BMC Genom. 21:382. doi: <https://doi.org/10.1186/s12864-020-06783-9>.

APPENDIX



Appendix figure 1. Heatmap of the 17 most significant SNPs ($P < 1 \times 10^{-11}$) associated with the white coat color of the Taiwan swamp buffalo in the GWAS. The x-axis represents the 94 Taiwan swamp buffaloes. The y-axis represents the SNPs. The color of the heatmap represents the difference of genotypes.

Appendix table 1. Sample size of gray and white Taiwan swamp buffalo in different experiments in this study



Experiment	Gray Taiwan swamp buffalo	White Taiwan swamp buffalo	Total
Population genetic structure analysis	78	16	94
Genome-wide association study	78	16	94
<i>ASIP</i> genotyping	5	15	20
<i>MC1R</i> sequencing	27	15	42
TaqMan™ SNP Genotyping Assay	115	18	133
Relative gene expression analysis	2	2	4
Histological examination	2	2	4

Appendix table 2. Information of the 94 Taiwan swamp buffaloes analyzed in population genetic structure analysis and GWAS in this study including its father, mother, sex, and coat color

ID	Father	Mother	Sex	Coat color
1B	NA	39	Female	Gray
61	W	w	Female	White
67	W	281	Female	Gray
102	NA	77	Female	Gray
114	100	149	Female	Gray
300	NA	NA	Male	Gray
400	NA	NA	Male	Gray
407	5	31	Female	Gray
418	W	265	Female	Gray
464	455	408	Female	White
490	200	229	Female	Gray
507	33	30	Female	White
517	2	1W	Female	Gray
536	200	132	Female	Gray
540	2	9	Female	Gray
543	2	45	Female	Gray
552	5	65	Female	White
568	200	306	Female	Gray
569	200	15	Female	Gray
572	455	517	Female	Gray
577	455	477	Female	Gray
587	200	6	Female	Gray
588	5	178	Male	Gray
590	NA	NA	Female	Gray
595	455	1B	Female	Gray
605	455	464	Female	Gray
625	300	513	Female	Gray
634	531	564	Female	Gray
637	300	306	Female	Gray
640	526	464	Male	White
641	526	507	Female	White
643	526	412	Female	White
644	526	65	Female	White
646	455	408	Female	Gray
647	5	535	Female	Gray
648	526	552	Male	White
659	5	559	Female	Gray
661	531	418	Female	Gray

NA: not available.

Appendix table 2. Information of the 94 Taiwan swamp buffaloes analyzed in population genetic structure analysis and GWAS in this study including its father, mother, sex, and coat color (continued)

ID	Father	Mother	Sex	Coat color
662	300	575	Female	Gray
665	5	543	Female	Gray
667	5	517	Female	Gray
673	531	412	Female	White
674	531	65	Male	White
683	220	1B	Female	Gray
684	200	67	Female	Gray
689	531	265	Female	Gray
690	200	114	Female	Gray
694	526	464	Male	White
695	526	552	Male	White
698	455	436	Female	Gray
699	455	577	Male	Gray
700	455	517	Female	Gray
701	455	61	Female	White
702	455	490	Female	Gray
704	455	543	Male	Gray
705	455	418	Male	Gray
706	455	497	Male	Gray
707	455	540	Female	Gray
708	200	568	Male	Gray
709	200	572	Male	Gray
710	588	605	Female	Gray
713	588	624	Female	Gray
717	300	590	Female	Gray
719	300	67	Male	Gray
729	300	552	Female	Gray
730	300	464	Female	Gray
745	588	624	Female	Gray
762	300	401	Female	Gray
765	300	401	Male	Gray
767	300	543	Male	Gray
768	300	661	Male	Gray
770	300	490	Male	Gray
771	300	568	Female	Gray
772	300	569	Male	Gray
773	300	67	Male	Gray
774	300	572	Female	Gray
775	300	647	Female	Gray

Appendix table 2. Information of the 94 Taiwan swamp buffaloes analyzed in population genetic structure analysis and GWAS in this study including its father, mother, sex, and coat color (continued)

ID	Father	Mother	Sex	Coat color
776	588	590	Female	Gray
777	300	605	Female	Gray
779	300	577	Female	Gray
780	300	625	Male	Gray
781	300	564	Female	Gray
783	300	114	Female	Gray
784	300	593	Male	Gray
785	300	536	Male	Gray
786	300	637	Female	Gray
787	300	1B	Female	Gray
788	300	587	Male	Gray
789	400	641	Female	White
790	400	667	Female	Gray
792	400	673	Male	Gray
793	400	665	Male	Gray
794	400	662	Female	Gray
799	400	643	Male	White

Appendix table 3. The detected fragment size (bp) of 15 microsatellite markers among 94 Taiwan swamp buffaloes in this study

ID	<i>ILSTS058</i>	<i>INRA128</i>	<i>CSSM022</i>	<i>INRA005</i>	<i>ILSTS059</i>	<i>ETH152</i>	<i>BM1818</i>	<i>ILSTS033</i>	<i>ILSTS029</i>	<i>BM1824</i>	<i>ETH10</i>	<i>CSSM061</i>	<i>CSSM046</i>	<i>CSSM008</i>	<i>TGLA159</i>															
1B	144	144	178	180	223	223	136	148	174	180	206	208	269	286	166	166	171	171	204	206	212	212	131	135	170	170	197	197	247	251
61	144	144	180	180	221	221	140	148	176	180	206	231	269	286	166	166	NA	NA	204	206	212	212	131	135	164	170	197	197	238	247
67	144	151	180	180	221	221	138	142	176	180	206	208	269	286	164	164	171	171	204	206	212	212	121	121	168	168	197	201	238	238
102	144	144	178	178	221	221	132	148	174	180	206	206	269	271	164	166	171	175	206	208	212	212	131	135	170	170	193	203	247	247
114	144	151	180	180	221	221	136	140	174	180	206	223	269	283	164	166	171	171	199	204	212	212	121	121	170	170	193	197	245	247
300	163	163	180	180	219	219	136	138	174	176	206	229	286	286	166	166	171	171	204	204	212	212	121	121	164	164	197	197	247	247
400	144	148	180	187	221	221	132	136	174	176	206	229	286	286	164	164	171	175	204	208	212	212	131	131	164	164	197	197	245	247
407	144	151	178	180	221	221	142	148	174	176	206	208	269	283	164	166	171	171	195	206	212	212	121	131	168	168	197	197	238	243
418	144	163	178	180	221	221	136	140	174	176	206	223	286	286	166	166	171	171	206	206	212	212	121	121	168	168	197	203	247	251
464	144	146	178	178	223	223	136	140	174	180	206	206	269	286	166	166	171	171	204	204	212	212	121	135	170	170	197	197	247	247
490	159	163	178	180	221	221	132	136	174	174	206	208	269	286	166	166	171	171	199	208	212	212	131	131	164	164	193	197	247	247
507	144	144	178	180	221	221	148	148	176	176	206	231	286	286	166	166	171	171	204	206	212	212	121	121	164	170	193	197	247	251
517	144	144	178	180	219	221	138	142	176	176	206	231	269	286	164	164	171	171	204	208	212	212	121	131	170	170	197	197	238	243
536	144	151	178	180	221	221	136	138	174	174	206	208	283	286	164	166	171	171	195	208	212	212	121	131	164	164	193	193	247	247
540	144	144	180	180	221	221	140	142	176	176	206	208	269	286	164	164	171	171	195	204	212	212	135	135	170	170	193	199	247	247
543	144	151	178	183	221	221	136	140	176	176	206	208	286	286	164	166	171	171	204	204	212	212	135	135	164	170	193	197	238	238
552	144	144	178	178	221	221	140	148	176	176	208	223	269	286	166	166	171	171	204	208	212	212	121	135	170	170	193	197	243	247

NA: not available.

Appendix table 3. The detected fragment size (bp) of 15 microsatellite markers among 94 Taiwan swamp buffaloes in this study (continued)

ID	<i>ILSTS058</i>	<i>INRA128</i>	<i>CSSM022</i>		<i>INRA005</i>		<i>ILSTS059</i>		<i>ETH152</i>		<i>BM1818</i>		<i>ILSTS033</i>		<i>ILSTS029</i>		<i>BM1824</i>		<i>ETH10</i>		<i>CSSM061</i>		<i>CSSM046</i>		<i>CSSM008</i>		<i>TGLA159</i>			
568	144	151	178	178	221	221	136	138	176	176	206	206	269	283	164	166	171	171	195	208	212	212	131	135	164	164	193	197	247	251
569	151	163	178	178	221	221	132	138	174	174	206	208	269	283	164	166	171	171	195	199	212	212	121	131	168	168	193	197	238	247
572	144	163	180	180	221	221	140	142	176	176	206	206	269	283	164	164	171	171	204	204	212	212	121	121	170	170	193	197	238	247
577	144	151	178	185	221	221	132	138	174	180	206	208	269	286	164	166	171	171	206	206	212	212	131	131	170	170	197	197	238	247
587	144	144	178	180	221	221	138	148	176	180	206	223	269	286	164	164	171	171	204	208	212	212	121	121	170	170	197	197	238	247
588	159	163	180	180	221	221	136	138	174	180	206	208	283	286	164	166	171	171	204	206	212	212	121	131	164	164	197	197	243	247
590	163	163	178	178	221	221	136	138	174	176	206	208	269	283	166	166	171	171	199	208	212	212	121	121	164	164	193	193	247	247
595	163	163	178	180	221	221	136	142	174	176	208	229	286	286	164	166	171	171	204	204	212	212	121	131	164	164	197	197	247	247
605	144	151	178	180	221	223	132	136	174	180	206	206	283	286	164	166	171	175	206	206	212	212	131	135	170	170	193	197	238	247
625	144	151	178	183	221	221	140	148	176	176	206	208	286	286	164	166	171	171	201	208	212	212	121	135	164	170	193	193	238	247
634	144	144	178	180	221	221	138	148	174	176	206	206	283	283	164	166	171	171	199	199	212	212	121	121	168	170	193	197	238	247
637	144	163	178	180	219	219	138	142	174	180	206	229	269	286	164	166	171	171	204	208	212	212	121	135	164	164	197	197	247	251
640	144	146	178	178	219	219	136	138	174	176	206	208	286	286	164	166	171	171	206	206	212	212	135	135	168	168	197	197	247	247
641	144	144	178	180	219	219	138	148	176	180	206	208	286	286	NA	NA	171	171	204	208	212	212	135	135	164	164	193	197	251	251
643	144	144	178	178	219	221	138	142	176	180	206	206	269	286	164	164	171	171	201	206	212	212	135	135	170	170	197	201	243	247
644	144	144	178	180	219	219	138	140	176	180	208	223	269	286	NA	NA	171	171	201	204	212	212	135	135	164	164	197	197	247	251
646	151	159	178	180	221	221	136	138	174	174	206	206	283	283	166	166	171	171	199	199	212	212	121	121	164	164	193	203	238	247

NA: not available.

Appendix table 3. The detected fragment size (bp) of 15 microsatellite markers among 94 Taiwan swamp buffaloes in this study (continued)

ID	<i>ILSTS058</i>	<i>INRA128</i>	<i>CSSM022</i>	<i>INRA005</i>	<i>ILSTS059</i>	<i>ETH152</i>	<i>BM1818</i>	<i>ILSTS033</i>	<i>ILSTS029</i>	<i>BM1824</i>	<i>ETH10</i>	<i>CSSM061</i>	<i>CSSM046</i>	<i>CSSM008</i>	<i>TGLA159</i>															
647	144	163	178	178	219	219	138	148	176	176	206	223	286	286	164	166	171	171	201	206	212	212	135	135	170	170	197	197	247	247
648	144	144	178	178	219	221	138	148	176	180	208	223	286	286	164	166	171	171	201	208	212	212	135	135	170	170	193	197	247	247
659	144	151	178	178	221	221	138	140	174	176	208	223	269	283	164	166	171	171	195	206	212	212	131	135	170	170	193	197	243	247
661	144	144	178	180	221	221	132	140	174	174	206	223	286	286	164	166	171	171	199	206	212	212	121	131	168	168	193	197	238	251
662	151	163	180	180	219	221	136	138	174	174	206	206	283	286	166	166	171	175	199	204	212	212	121	121	164	164	197	197	247	247
665	144	151	178	183	221	221	136	138	176	176	206	208	269	286	166	166	171	171	201	201	212	212	135	135	164	170	193	193	238	243
667	144	151	178	178	221	221	132	142	174	176	206	206	286	286	164	164	171	171	204	208	212	212	131	131	170	170	193	197	238	247
673	144	144	178	178	219	219	138	142	176	176	206	206	286	286	164	164	171	171	206	206	212	212	135	135	170	170	197	201	243	251
674	144	159	178	178	219	219	138	140	176	180	206	231	269	286	164	166	171	171	204	206	212	212	135	135	170	170	193	197	247	251
683	144	151	178	180	225	225	136	136	174	174	206	208	269	286	166	166	171	171	204	206	212	212	121	131	170	170	193	197	247	247
684	144	163	178	178	219	221	132	148	174	176	206	208	283	286	166	166	171	171	206	208	212	212	121	135	164	164	193	193	238	243
689	144	163	178	180	219	219	136	148	176	176	206	208	286	286	166	166	171	171	201	208	212	212	121	135	164	170	193	197	243	247
690	144	163	178	180	221	221	132	136	174	174	206	223	283	283	166	166	171	171	199	208	212	212	121	121	170	170	193	197	247	247
694	144	144	178	178	221	221	140	148	174	176	206	206	269	286	166	166	171	171	206	208	212	212	121	135	170	170	197	197	247	251
695	144	144	178	178	219	221	148	148	176	180	206	223	269	286	166	166	171	171	208	208	212	212	135	135	168	168	193	197	243	247
698	151	151	180	180	221	221	138	140	174	174	206	208	269	283	164	166	171	171	201	201	212	212	121	131	168	168	193	203	238	238
699	144	151	178	178	221	221	132	138	174	180	206	208	269	283	164	166	171	171	206	206	212	212	131	131	170	170	193	197	238	247

NA: not available.

Appendix table 3. The detected fragment size (bp) of 15 microsatellite markers among 94 Taiwan swamp buffaloes in this study (continued)

ID	<i>ILSTS058</i>	<i>INRA128</i>	<i>CSSM022</i>	<i>INRA005</i>	<i>ILSTS059</i>	<i>ETH152</i>	<i>BM1818</i>	<i>ILSTS033</i>	<i>ILSTS029</i>	<i>BM1824</i>	<i>ETH10</i>	<i>CSSM061</i>	<i>CSSM046</i>	<i>CSSM008</i>	<i>TGLA159</i>															
700	144	151	178	178	221	221	132	138	174	176	206	208	269	286	164	166	171	175	204	208	212	212	131	131	168	168	193	197	238	247
701	144	159	178	180	219	219	148	148	176	180	206	231	269	286	166	166	171	171	204	204	212	212	135	135	164	164	193	197	238	251
702	144	159	178	178	221	221	136	138	174	174	206	206	283	286	NA	NA	171	175	206	208	212	212	131	131	168	168	193	193	247	247
704	144	151	178	178	221	221	132	136	174	176	206	208	283	286	166	166	171	175	204	206	212	212	131	135	164	164	197	197	238	238
705	144	151	178	180	221	221	138	140	174	176	208	223	283	286	164	166	171	171	206	206	212	212	121	131	168	168	193	203	247	251
706	144	151	178	180	221	221	132	148	174	176	208	208	269	286	164	166	171	175	199	199	212	212	131	135	170	170	193	193	238	247
707	144	144	178	180	221	221	132	140	174	176	206	208	286	286	164	166	171	175	195	195	212	212	131	135	170	170	193	199	247	247
708	151	163	178	178	221	221	132	136	174	176	206	206	283	286	166	166	171	171	195	195	212	212	131	135	168	168	193	193	247	247
709	163	163	178	180	221	221	136	140	176	176	206	206	283	286	164	166	171	171	204	204	212	212	121	131	170	170	193	193	247	247
710	144	159	180	180	223	223	132	136	180	180	206	208	283	283	164	166	171	171	204	206	212	212	121	131	168	168	197	197	243	247
713	144	159	178	180	219	219	132	136	174	174	206	208	269	286	166	166	171	171	204	206	212	212	121	135	164	164	193	197	243	247
717	163	163	178	180	221	221	136	138	174	176	206	206	269	286	166	166	171	171	204	204	212	212	121	121	164	164	193	197	247	247
719	151	163	180	180	219	221	138	138	174	180	208	229	286	286	164	166	171	171	204	206	212	212	121	121	164	164	197	197	238	247
729	144	163	178	180	219	219	138	148	174	176	208	229	286	286	166	166	171	171	204	208	212	212	121	135	164	164	193	197	243	247
730	146	163	178	180	219	223	136	138	174	180	206	229	286	286	166	166	171	171	204	206	212	212	121	121	164	164	197	197	247	247
745	144	163	178	180	219	221	132	136	176	176	223	229	269	286	166	166	171	175	204	204	212	212	121	131	164	164	193	197	247	247
762	144	163	178	180	219	219	132	138	174	180	206	206	269	286	164	166	NA	NA	204	206	212	212	121	131	164	164	197	203	247	247

NA: not available.

Appendix table 3. The detected fragment size (bp) of 15 microsatellite markers among 94 Taiwan swamp buffaloes in this study (continued)

ID	<i>ILSTS058</i>	<i>INRA128</i>	<i>CSSM022</i>	<i>INRA005</i>	<i>ILSTS059</i>	<i>ETH152</i>	<i>BM1818</i>	<i>ILSTS033</i>	<i>ILSTS029</i>	<i>BM1824</i>	<i>ETH10</i>	<i>CSSM061</i>	<i>CSSM046</i>	<i>CSSM008</i>	<i>TGLA159</i>															
765	144	163	178	180	219	219	132	138	174	180	206	206	269	286	164	166	171	171	204	206	212	212	121	131	164	164	197	203	247	247
767	144	163	178	180	219	221	136	142	174	176	206	229	286	286	164	166	171	171	204	204	212	212	121	121	164	170	197	197	238	247
768	144	163	178	180	221	221	138	140	176	180	206	206	286	286	164	164	171	171	204	204	212	212	121	133	164	170	193	197	238	243
770	159	163	178	180	219	221	136	138	174	176	208	229	286	286	166	166	171	171	204	208	212	212	121	131	164	164	193	197	247	247
771	144	163	178	180	219	221	136	138	174	176	206	229	283	286	164	166	171	171	204	204	212	212	121	131	164	164	193	197	247	251
772	163	163	178	180	221	221	138	138	174	174	206	229	NA	NA	164	166	171	171	199	204	212	212	121	131	164	164	193	197	247	247
773	151	163	180	180	219	221	138	138	176	180	208	229	286	286	164	166	171	171	204	204	212	212	121	121	164	164	197	201	238	247
774	144	163	180	180	219	219	136	142	174	176	206	206	283	286	164	166	171	171	204	204	212	212	121	121	164	164	197	197	247	247
775	163	163	178	178	219	221	132	148	176	176	206	206	286	286	166	166	171	171	195	201	212	212	121	135	170	170	193	197	247	247
776	163	163	178	180	221	221	136	138	176	176	206	206	283	286	166	166	171	171	204	204	212	212	121	121	164	164	193	197	247	247
777	151	163	178	180	223	223	136	138	176	180	206	206	283	286	166	166	171	175	204	206	212	212	121	131	164	170	NA	NA	247	247
779	151	163	178	180	219	219	136	138	174	180	208	229	269	286	164	166	171	171	204	206	212	212	121	131	164	164	197	197	238	247
780	151	163	178	180	221	221	136	148	174	176	206	208	NA	NA	166	166	171	171	204	208	212	212	121	121	164	170	193	197	247	247
781	144	163	180	180	221	221	136	148	174	176	206	206	286	286	166	166	171	175	204	208	212	212	121	121	164	168	197	197	238	247
783	144	163	180	180	NA	NA	138	140	174	176	206	206	269	286	166	166	171	171	204	204	212	212	121	121	164	170	197	197	247	247
784	144	159	178	180	221	221	138	148	174	176	206	208	269	283	164	164	171	171	206	206	212	212	121	135	170	170	193	197	247	247
785	151	163	180	180	221	221	136	138	174	180	206	208	283	286	164	166	171	171	195	206	212	212	121	131	164	164	193	197	243	247

NA: not available.

Appendix table 3. The detected fragment size (bp) of 15 microsatellite markers among 94 Taiwan swamp buffaloes in this study (continued)

ID	<i>ILSTS058</i>	<i>INRA128</i>	<i>CSSM022</i>	<i>INRA005</i>	<i>ILSTS059</i>	<i>ETH152</i>	<i>BM1818</i>	<i>ILSTS033</i>	<i>ILSTS029</i>	<i>BM1824</i>	<i>ETH10</i>	<i>CSSM061</i>	<i>CSSM046</i>	<i>CSSM008</i>	<i>TGLA159</i>															
786	144	163	178	180	219	219	136	138	180	180	206	206	269	286	166	166	171	171	206	208	212	212	121	131	164	164	197	197	247	247
787	144	163	180	180	219	219	136	138	174	174	206	206	286	286	166	166	171	171	204	204	212	212	121	135	164	164	197	197	247	247
788	163	163	180	180	219	221	136	138	174	174	206	206	283	286	164	166	171	171	201	204	212	212	121	121	164	164	193	197	238	247
789	144	148	180	187	219	219	136	148	174	176	206	229	286	286	164	164	171	175	204	204	212	212	131	135	164	164	197	197	245	251
790	144	151	178	180	221	221	132	132	174	176	206	206	286	286	164	166	171	175	208	208	212	212	131	131	164	170	193	197	238	245
792	144	148	178	187	221	221	136	138	176	176	206	206	286	286	164	164	171	175	204	208	212	212	131	135	164	164	197	201	243	247
793	144	148	178	180	221	221	132	136	176	176	206	206	269	286	NA	NA	171	175	208	208	212	212	131	135	164	164	193	197	238	245
794	144	151	180	180	219	221	136	138	174	176	206	229	286	286	164	166	171	175	204	208	212	212	121	131	164	164	197	197	245	247
799	144	144	178	187	221	221	132	138	176	176	206	206	286	286	164	164	171	175	201	204	212	212	131	135	164	170	197	197	243	245

NA: not available.

Appendix table 4. Mean Ct and delta Ct values in the relative gene expression analysis among different parts of skin tissue of an adult white Taiwan swamp buffalo

Target gene	Values	Sample			
		Ventral side ear	Dorsal side ear	Back	Abdomen
<i>MC1R</i>	<i>MC1R</i> mean Ct	26.68	30.35	28.41	29.88
	<i>18S rRNA</i> mean Ct	19.74	22.75	20.23	20.9
	Δ Ct	6.94	7.6	8.18	8.98
<i>ASIP</i>	<i>ASIP</i> mean Ct	30.27	28.14	28.10	28.39
	<i>18S rRNA</i> mean Ct	19.05	22.05	19.51	20.25
	Δ Ct	11.22	6.09	8.59	8.14
<i>MITF</i>	<i>MITF</i> mean Ct	29.05	28.64	28.30	28.29
	<i>18S rRNA</i> mean Ct	20.05	23.42	20.83	21.34
	Δ Ct	9.00	5.22	7.47	6.95
<i>TYR</i>	<i>TYR</i> mean Ct	30.16	28.26	28.32	28.84
	<i>18S rRNA</i> mean Ct	19.13	21.77	19.69	20.42
	Δ Ct	11.03	6.49	8.63	8.42
<i>TYRP1</i>	<i>TYRP1</i> mean Ct	27.94	26.34	26.72	26.44
	<i>18S rRNA</i> mean Ct	18.62	21.37	19.40	19.40
	Δ Ct	9.31	4.97	7.32	7.04
<i>DCT</i>	<i>DCT</i> mean Ct	30.42	29.02	28.85	29.01
	<i>18S rRNA</i> mean Ct	19.42	22.61	20.44	20.61
	Δ Ct	10.99	6.41	8.41	8.40

Appendix table 5. Mean Ct and delta Ct values in the relative gene expression analysis among ear skin tissue of gray (brown) and white Taiwan swamp buffalo calves

Target gene	Values	Sample					
		Brown(1) Ventral side ear	Brown(1) Dorsal side ear	Brown(2) Ventral side ear	Brown(2) Dorsal side ear	White Ventral side ear	White Dorsal side ear
<i>MC1R</i>	<i>MC1R</i> mean Ct	30.59	29.45	29.65	29.21	29.24	30.40
	<i>18S rRNA</i> mean Ct	20.62	19.38	20.65	19.77	19.61	20.97
	Δ Ct	9.97	10.07	9.00	9.44	9.63	9.43
<i>ASIP</i>	<i>ASIP</i> mean Ct	29.91	28.91	30.52	28.78	29.52	29.89
	<i>18S rRNA</i> mean Ct	19.80	18.99	20.20	18.80	19.06	20.60
	Δ Ct	10.11	9.92	10.32	9.98	10.46	9.29
<i>MITF</i>	<i>MITF</i> mean Ct	29.33	27.50	29.81	28.87	28.17	29.06
	<i>18S rRNA</i> mean Ct	20.76	19.86	20.85	20.69	19.94	21.31
	Δ Ct	8.57	7.63	8.97	8.18	8.23	7.75
<i>TYR</i>	<i>TYR</i> mean Ct	30.50	28.98	30.70	29.48	29.98	30.60
	<i>18S rRNA</i> mean Ct	20.11	18.53	20.07	19.31	18.91	20.47
	Δ Ct	10.39	10.45	10.63	10.17	11.07	10.14
<i>TYRP1</i>	<i>TYRP1</i> mean Ct	28.30	27.67	28.83	27.42	28.24	28.02
	<i>18S rRNA</i> mean Ct	19.15	18.31	19.07	18.33	18.35	19.30
	Δ Ct	9.15	9.36	9.76	9.09	9.88	8.72
<i>DCT</i>	<i>DCT</i> mean Ct	30.39	29.80	30.88	29.79	29.72	30.64
	<i>18S rRNA</i> mean Ct	20.60	19.51	20.15	19.44	19.29	20.81
	Δ Ct	9.79	10.29	10.73	10.35	10.44	9.83